Accurate Boussinesq Oceanic Modeling with a Practical, "Stiffened" Equation of State

Alexander F. Shchepetkin and James C. McWilliams

Institute of Geophysics and Planetary Physics, University of California, Los Angeles, 405 Hilgard Avenue, Los Angeles, CA 90095-1567

e-mail: alex@atmos.ucla.edu jcm@atmos.ucla.edu

Received: 9 August 2008; *received in revised form*: 1 April 2009; 8 March 2010; 25 December 2010; *accepted*: 31 January 2011;

Keywords: Seawater Equation of State; Seawater compressibility; Barotropic-baroclinic mode splitting; Boussinesq and non-Boussinesq modeling; Numerical stability

Published in: *Ocean Modeling*, **Vol. 38**(2011), Issue 1-2, pp. 41-70

doi:10.1016/j.ocemod.2011.01.010

Abstract

The Equation of State of seawater (EOS) relates *in situ* density to temperature, salinity and pressure. Most of the effort in the EOS-related literature is to ensure an accurate fit of density measurements under the conditions of different temperature, salinity, and pressure. *In situ* density is not of interest by itself in oceanic models, but rather plays the role of an intermediate variable linking temperature and salinity fields with the pressure-gradient force in the momentum equations, as well as providing various stability functions needed for parameterization of mixing processes. This shifts the role of EOS away from representation of *in situ* density toward accurate translation of temperature and salinity gradients into adiabatic derivatives of density.

In this study we propose and assess the accuracy of a simplified, computationally-efficient algorithm for EOS suitable for a free-surface, Boussinesq-approximation model. This EOS is optimized to address all the needs of the model: notably, computation of pressure gradient – it is compatible with the monotonized interpolation of density needed for the pressure gradient scheme in sigma-coordinates of Shchepetkin & McWilliams (2003), while more accurately representing the pressure dependency of the thermal expansion and saline contraction coefficients as well as the stability of stratification; it facilitates mixing parameterizations for both vertical and lateral (along neutral surfaces) mixing; and it leads to a simpler, more robust, numerically stable barotropic-baroclinic mode splitting without the need of excessive temporal filtering of fast mode. In doing so we also explore the implications of EOS compressibility for mode splitting in non-Boussinesq free-surface models with with the intent to design a comparatively accurate algorithm applicable there.

1 Role of EOS in oceanic modeling

The Equation of State (EOS) relates the *in situ* density of seawater with its temperature (or potential temperature), salinity, and pressure (Θ, S, P respectively),

$$\rho = \rho_{EOS}(\Theta, S, P)\,. \tag{1.1}$$

In a Boussinesq-approximation oceanic modeling code, *in situ* density does not appear by itself (since it is replaced by a constant reference density). Instead EOS and EOS-related quantities are needed for the following computations:

- Pressure-gradient force (PGF);
- Vertically averaged density $\overline{\rho}$ and the effective dynamic density for the barotropic mode ρ_* (vertically integrated pressure normalized by $gD^2/2$ where g is acceleration of gravity and D is the local column thickness), both of which participate in barotropic–baroclinic mode-splitting algorithm of Shchepetkin & McWilliams (2005, hereafter cited as SM2005);
- Stability of stratification as well as external thermodynamic forcing (surface buoyancy flux) needed for mixing and planetary boundary layer parameterizations;
- Slope of neutral surfaces needed for horizontal (along-isopycnal) mixing (Griffies *et al.*, 1998).

The purpose of this study is to review the present oceanic modeling practices for using EOS in these roles, focusing on the effects associated with seawater compressibility, and it assesses the consequences of the Boussinesq approximation in the context of a realistic EOS. The present study extends the analysis of consequences of Boussinesq approximation from Shchepetkin & McWilliams (2008).

This paper is organized as follows. Sec. 2 makes a overview of the Boussinesq approximation, analyzes the errors associated with using realistic seawater EOS, and introduces stiffening of EOS as a method to reduce these errors. Sec. 3 examines the consequences of finite compressibility of seawater for the four algorithmic roles outlined above, to establish requirements for the most suitable functional form of EOS. Special attention is given to barotropic-baroclinic mode-splitting since this subject is rarely discussed in the literature. Sec. 4 introduces a practical form of EOS and makes estimates of its accuracy. Sec. 5 explores the consequences of eliminating the Boussinesq approximation with the emphasis on accuracy of barotropic-baroclinic mode-splitting algorithm in the context of finite compressibility of seawater. Sec. 6 is the conclusion.

2 Boussinesq approximation and EOS stiffening

The Boussinesq approximation (*e.g.*, Spiegel & Veronis, 1960; Zeytounian, 2003, among others) replaces *in situ* density ρ with a constant reference value ρ_0 in all places where it plays the role of a measure of inertia, *i.e.,* everywhere except where multiplied by the acceleration of gravity g. The velocity field becomes non-divergent (incompressible) because the continuity equation changes its meaning from mass to volume conservation. This reverses the role of EOS from computing specific volume in a mass-conserving model to density ρ in a volume-conserving one. The conservation laws (momentum, energy, tracer content, etc) are changed from mass- to volume-integrated; the thermodynamics is reduced to Lagrangian conservation (advection and diffusion) of Θ and S, while heating/cooling of fluid by adiabatic compression/expansion is neglected (except in the definition of potential temperature itself) and mechanical energy dissipated by viscosity is considered "lost" rather than converted into heat

(Mihaljan, 1962). If EOS is a linear function of Θ and S, mass is conserved (along with volume) as a consequence of, and to the same degree as, the conservation of Θ and S; external heating/cooling produces a decrease/increase in mass, while keeping volume constant; and nonlinear EOS causes a Boussinesq model to conserve only volume, but no longer mass, even in the absence of external forcing.

The Boussinesq approximation brings simplifications by eliminating mass-weighting in a finite-volume code and limiting the role of EOS to the four purposes stated in Sec. 1. Except in the part of pressure-gradient term associated with perturbation of free surface in a free-surface model, ρ itself can be replaced with its perturbation, $\rho' = \rho - \rho_0$, because it appears only inside spatial derivatives (ultimately linked to the gradients of Θ and S) and only in the context of buoyancy commonly defined as $-g\rho'/\rho_0$, *i.e.*, normalized by ρ_0, whereas the equations can always rewritten in such a way that ρ_0 itself appears only in the context of this normalization and nowhere else. The Boussinesq approximation facilitates the barotropic–baroclinic mode-splitting in a pair of vertically-integrated free-surface and momentum equations, effectively uncoupling EOS from the barotropic mode. The incompressibility assumption eliminates acoustic waves regardless of whether the hydrostatic approximation is made.

However, physically important effects associated with seawater – cabbeling and thermobaricity – fundamentally require pressure-dependency in EOS and lead to the common practice of using the full non-approximated EOS, thus retaining its full compressibility even in an otherwise dynamically incompressible Boussinesq model. This obscures the concept of buoyancy because it can no longer be equated to the density (or potential density) anomaly, and can no longer be viewed as a Lagrangianly-conserved properly of the fluid, even thought Θ and S are. A related, frequently used approximation is the replacement of the full *in situ* pressure P in EOS (1.1) with its bulk hydrostatic reference value, $P \rightarrow -\rho_0 g z$, when computing ρ from the model prognostic variables, Θ and S, hence neglecting pressure variation due to baroclinic effects and essentially decoupling EOS pressure from the dynamic.

Under most offshore oceanic conditions ρ varies by $\approx \pm 3\%$ relative to its reference value; this leads to errors associated with the Boussinesq approximation which can be subdivided into two categories:

(*i*) errors relative to not using the Boussinesq approximation including not only quantitative, but conceptual as well, *i.e.*, excluded physical processes and/or missing/altered conservation laws; and

(*ii*) conflicts and internal inconsistencies caused the use of a realistic seawater EOS with full compressibility effects within a Boussinesq oceanic model.

Errors of type (*i*) are widely discussed in the literature (McDougall & Garrett, 1992; Dukowicz, 1997; Lu, 2001; Greatbatch *et al.*, 2001; Huang & Jin, 2002; McDougall *et al.*, 2002; Greatbatch & McDougall, 2003; Losch *et al.*, 2004; Griffies, 2004; Young, 2010; Tailleux, 2009, 2010).

An example of an internal inconsistency of type (*ii*) can be illustrated by considering a barotropic compressible fluid layer whose density is a function of P alone (*i.e.*, because Θ, S are spatially uniform) and in hydrostatic balance,

$$\rho = \rho_{\rm EOS}(P) \qquad \text{and} \qquad \partial_z P = -g\rho\,. \tag{2.1}$$

Integration of (2.1) yields mutually consistent vertical profiles for P and ρ,

$$\left\{ \begin{array}{l} P = \mathcal{P}(\zeta - z) \\ \rho = \mathcal{R}(\zeta - z) \equiv \rho_{\rm EOS}\Big(\mathcal{P}(\zeta - z)\Big) \end{array} \right. \qquad \text{such that} \qquad \left\{ \begin{array}{r} \mathcal{P}'(\zeta - z) = g\mathcal{R}(\zeta - z) \\ \mathcal{P}(0) = P\Big|_{z=\zeta} = 0\,, \end{array} \right. \tag{2.2}$$

where $\mathcal{P}$ and $\mathcal{R}$ are universal functions of a single argument, *i.e.*, their structure depends only one the properties of $\rho_{\rm EOS}(P)$ in (2.1) but not directly on the local dynamical conditions, such as perturbation of the free-surface ζ. $\mathcal{P}'$ denotes derivative of $\mathcal{P}$ with respect to its argument (note that the sign is correct as stated above: both p and ρ increase with increase of $\zeta - z$, meaning increase downward). The condition $\mathcal{P}(0) = 0$ is the free-surface pressure boundary condition (for simplicity the atmospheric pressure is presumed to be constant and subtracted out).

A gradient of ζ induces a pressure gradient,

$$-\nabla_x P = -\mathcal{P}'(\zeta - z) \cdot \nabla_x \zeta \,, \tag{2.3}$$

and creates acceleration

$$-\frac{1}{\rho}\nabla_x P = -\frac{\mathcal{P}'(\zeta - z)}{\mathcal{R}(\zeta - z)} \cdot \nabla_x \zeta \equiv -g\nabla_x \zeta \,, \tag{2.4}$$

independently of vertical coordinate z regardless of the specific functional form $\rho_{\rm EOS}(P)$ in (2.1) and of the magnitude of the density variation within the column. Equation (2.4) is derived without the use of Boussinesq approximation. Its Boussinesq analog is

$$-\frac{1}{\rho_0}\nabla_x P = -g\frac{\mathcal{R}(\zeta - z)}{\rho_0} \cdot \nabla_x \zeta \,. \tag{2.5}$$

The presence of the multiplier $\mathcal{R}/\rho_0$, which increases with depth, is clearly an artifact of the Boussinesq approximation. It results in an unphysical vertical shear in the acceleration, hence a spurious downward intensification of a geostrophically-balanced baroclinic current generated by a $\nabla_x \zeta$. Both these spurious effects are caused by the standard algorithmic chain in a Boussinesq model,

$$\Theta, S \;\rightarrow\; \rho = \rho_{\rm EOS}\Big(\Theta, S, P = \rho_0 g(\zeta - z)\Big) \;\rightarrow\; -\frac{1}{\rho_0}\nabla_x P \,. \tag{2.6}$$

To estimate the significance of this error, consider for simplicity a linear analog of (2.1),

$$\rho_{\rm EOS}(P) = \rho_1 + P/c^2 \,, \tag{2.7}$$

where ρ_1 is the density at $P = 0$ and c is speed of sound. Then the counterpart of (2.2) becomes

$$\begin{aligned} \mathcal{P}(\zeta - z) &= \rho_1 c^2 \left[e^{g(\zeta - z)/c^2} - 1\right] \approx \rho_1 g(\zeta - z) + \frac{\rho_1 g^2}{2c^2}(\zeta - z)^2 + ... \\ \mathcal{R}(\zeta - z) &= \quad \rho_1 e^{g(\zeta - z)/c^2} \quad \approx \rho_1 + \frac{\rho_1 g}{c^2}(\zeta - z) + \frac{\rho_1 g^2}{2c^4}(\zeta - z)^2 + ... \,, \end{aligned} \tag{2.8}$$

hence

$$\frac{\mathcal{R}}{\rho_0} \approx 1 + \frac{\rho_1 - \rho_0}{\rho_0} + \frac{\rho_1}{\rho_0} \cdot \frac{g}{c^2}(\zeta - z) + ... \,. \tag{2.9}$$

Here $\epsilon = g(\zeta - z)/c^2$ plays the role of a small parameter justifying the replacement of ρ with ρ_0. Assuming $c \approx 1500$ m/s and a total depth of 5500 m, we estimate $\epsilon \approx 0.025$, which is a typical level for Boussinesq-approximation errors. This also indicates a strong dominance of the leading-order linear term in Taylor-series expansions over the remaining terms. A comparison of (2.5) with (2.4) suggests that the best choice of Boussinesq reference density is $\rho_0 = \overline{\rho} = \dfrac{1}{D}\displaystyle\int_{-h}^{\zeta} \mathcal{R}(\zeta - z)\,{\rm d}z$, $D = h + \zeta$ to have the vertical integral of (2.5) match its non-Boussinesq counterpart (2.4). In the case of EOS (2.7)

this leads to

$$\overline{\rho} = \rho_1 \cdot \frac{c^2}{gD}\left(e^{gD/c^2} - 1\right) \approx \rho_1 \left(1 + \frac{1}{2} \cdot \frac{gD}{c^2} + ...\right) , \tag{2.10}$$

which makes (2.9) into $(\mathcal{R}/\rho_0) = 1 + g\left(\zeta - z - D/2\right)/c^2$, effectively minimizing its deviation from unity. However, this can not be done universally, since $\overline{\rho}$ changes horizontally mainly due to topography, nor does it eliminate the spurious vertical shear.

The presence of shear in (2.5) depends on whether or not the EOS pressure is computed as *in situ* pressure, which takes place in (2.2), or is approximated by its bulk hydrostatic value proportional to depth, and furthermore, whether the depth is calculated from the dynamic or rest-state free surface, $P_{\rm bulk} = \rho_0 g(\zeta - z)$ or $-\rho_0 g z$,

$$\begin{cases} \rho_{\rm EOS} = \rho_1 + \rho_0 g(\zeta - z)/c^2 \\ -\dfrac{1}{\rho_0}\nabla_x P = -g\left(\dfrac{\rho_1}{\rho_0} + \dfrac{g(\zeta - z)}{c^2}\right)\nabla_x \zeta \end{cases} \quad \text{vs.} \quad \begin{cases} \rho_{\rm EOS} = \rho_1 - \rho_0 g z/c^2 \\ -\dfrac{1}{\rho_0}\nabla_x P = -g\left(\dfrac{\rho_1}{\rho_0} - \dfrac{g\zeta}{c^2}\right)\nabla_x \zeta \, . \end{cases}$$

[vertical shear is present] [no shear]

(2.11)

This sensitivity was noted by Dewar *et al.* (1998) (their Case A), who estimate that the magnitude of the difference in near-bottom geostrophic currents may reach $5\,cm/s$ for Gulf Stream conditions, resulting in an overall difference of about 3 out of 50 Sv for vertically integrated transport. They recommend using full dynamic *in situ* pressure in EOS, which requires simultaneous vertical integration to compute $P_{\rm EOS}$ and ρ. Paradoxically, they do so using Boussinesq approximation, interpreting the difference as the recovered physical effect, rather than a spurious one to be eliminated. Comparison of (2.2)–(2.4) with (2.11) suggests that using the rest-state ($\zeta = 0$) bulk pressure in EOS is more suitable for a Boussinesq model, while a non-Boussinesq model is better using *in situ* pressure. (One can also verify that the opposite combination – bulk rest-state EOS pressure in a non-Boussinesq model – yields a reversal of the spurious shear: it tends to make otherwise barotropic flows decrease with depth.) Another aspect pointed out by Dewar *et al.* (1998) is that in most oceanic situations the baroclinicity naturally tends to cancel the free-surface PGF resulting in weak flows in the abyss. Therefore, it is advantageous to retain baroclinic effects in EOS pressure rather than use $P_{\rm EOS} = \rho_0 g(\zeta - z)$, (*e.g.*, left side of (2.11)) that does not provide such compensation. Using $\rho_0 g(\zeta - z)$ is a common practice in terrain-following-coordinate free-surface models, POM and ROMS, motivated primarily by the convenience: these models do not store the unperturbed geopotential coordinate in a run-time array.

For the situation where the fluid is stratified (*i.e.*, (2.1) is no longer true) but the structure of temperature and salinity fields are such that the resultant isosurfaces of *in situ* density are parallel to the free surface, one can verify that (2.4) still holds and the acceleration generated by a perturbation in ζ does not depend on the vertical coordinate as long as the Boussinesq approximation is not used. Once again, the Boussinesq approximation destroys the true vertical uniformity. The baroclinic PGF – *i.e.*, associated with a physically correct vertical shear – appears only when density isosurfaces become non-parallel to the free surface.

Dukowicz (2001) made a proposal to reduce Boussinesq errors by realizing that the largest ρ vari-

ation is caused by the changes in P rather than in Θ and S. EOS (1.1) may be rewritten as [1]

$$\rho = r(P) \cdot \rho^{\bullet}_{\rm EOS}(\Theta, S, P)\,, \tag{2.12}$$

where the multiplier $r(P)$ is chosen as a universal function that does not depend on local Θ and S. $\rho^{\bullet}_{\rm EOS}(\Theta, S, P)$ is known as thermobaric or "stiffened" density. It only weakly depends on P, thus has much smaller variation than the original *in situ* density. Using (2.12) one can renormalize pressure,

$$\frac{dP^{\bullet}}{dP} = \frac{1}{r(P)}\,, \qquad P^{\bullet}\Big|_{P=0} = 0\,; \tag{2.13}$$

hence the hydrostatic balance and PGF become

$$\frac{\partial P^{\bullet}}{\partial z} = -\rho^{\bullet} g \qquad \text{and} \qquad -\frac{1}{\rho}\nabla_x P = -\frac{1}{\rho^{\bullet}}\nabla_x P^{\bullet}\,. \tag{2.14}$$

These retain the same functional form as in the original non-Boussinesq equations. Because $r(P)$ is a monotone function, (2.13) is invertible, $P = P(P^{\bullet})$, making it possible to rewrite EOS as

$$\rho^{\bullet} = \rho_{\rm EOS}\Big(\Theta, S, P(P^{\bullet})\Big)\Big/\, r\Big(P(P^{\bullet})\Big) = \rho^{\bullet}_{\rm EOS}\Big(\Theta, S, P^{\bullet}\Big)\,. \tag{2.15}$$

The entire set of equations is then expressed in terms of dotted variables, $\rho^{\bullet}$ and $P^{\bullet}$.

A Boussinesq-like approximation is subsequently applied to the renormalized system (2.13)–(2.15) by replacing $\rho^{\bullet} \to \rho^{\bullet}_0$ wherever the replacement $\rho \to \rho_0$ occurs in the standard Boussinesq approximation (*e.g.*, $-(1/\rho^{\bullet})\nabla_x P^{\bullet} \to -(1/\rho^{\bullet}_0)\nabla_x P^{\bullet}$). In addition, one can replace EOS pressure $P^{\bullet}$ in (2.15) with its bulk value, $-\rho^{\bullet}_0 g z$. $\rho^{\bullet}_{\rm EOS}$ is much less sensitive to this replacement than $\rho_{\rm EOS}$ in (1.1), whether the integration of EOS pressure starts from a perturbed or unperturbed free surface (*cf.*, (2.11)) since $\partial\rho^{\bullet}_{\rm EOS}/\partial P^{\bullet}\Big|_{\Theta,S} \ll \partial\rho_{\rm EOS}/\partial P|_{\Theta,S}$ and $P^{\bullet}$ tends to be closer to a linear function of depth than P. The multiplier $r(P)$ does not appear in the momentum equations written in advective form, but it does appears in the non-Boussinesq continuity equation along with $\rho^{\bullet}$. This leads to the two options, either

(*i*) to replace $r(P) \to 1$ along with $\rho^{\bullet} \to \rho^{\bullet}_0$ resulting in a volume-conserving system of Boussinesq-type. In this case EOS stiffening can be viewed just as a measure to remove internal contradiction of using a compressible EOS in a model that already makes the incompressibility assumption; or

(*ii*) keep $r(P)$, while simplifying it by $r(P) \to r\Big(P(P^{\bullet} = -\rho^{\bullet}_0 g z)\Big) = r(z)$, but still replacing $\rho^{\bullet} \to \rho^{\bullet}_0$ in continuity and, in fact, everywhere as it would be in the Boussinesq case.

The latter leads to a model intermediate in its physical approximations between Boussinesq and non-Boussinesq, while maintaining the simplicity of a Boussinesq code. One should note that most oceanic models are discretized using a finite-volume approach with a stretched vertical grid, so they already have an array to compute and store control-volume heights. A non-Boussinesq model uses density weighting over control volumes, resulting in an additional feedback loop arising from the dependency of density on model dynamics by EOS pressure which adds extra complexity. On the other hand, retaining $r(P)$ approximated as $r(z)$ only slightly modifies the procedure of calculating control volumes, while preserving the overall logical flow of a Boussinesq code. This means that the model is

[1] We have changed the original notation of Dukowicz (2001) by replacing his ρ^*, $P^* \to \rho^{\bullet}$, $P^{\bullet}$ to avoid notational conflict with vertically averaged densities $\overline{\rho}$ and ρ_* that appear in (3.19). For the same reason we also changed notation relatively to SM2005, so ρ_* appearing in this article has the same meaning as ρ^* in SM2005.

still volume-conserving, but now control volumes are rescaled to include $r(z)$-weighting that can be viewed just as a *geometrical property of the grid* since it does not depend on model dynamics. In effect, this option approximates *in situ* density as $\rho_0^\bullet \cdot r(z)$ instead of the constant ρ_0 in the standard Boussinesq approximation.

To illustrate the effect of modifying the Boussinesq approximation in this way, we reconsider (2.7)–(2.11). In this case it is natural to chose $\rho_0^\bullet = \rho_1$ and $r(P) = 1 + P/\left(\rho_1 c^2\right)$. Then the stiffened EOS (2.15) becomes $\rho^\bullet = \rho^\bullet_{\mathrm{EOS}}\left(P^\bullet\right) = \rho_1$, which is just a constant value, *i.e.,* $\rho^\bullet_{\mathrm{EOS}}$ becomes infinitely "stiff" and therefore insensitive to how EOS pressure is computed (the opposite of (2.11)). The renormalized pressure is $P^\bullet = g\rho_1(\zeta - z)$, resulting in $-(1/\rho_0^\bullet)\nabla_x P^\bullet = -g\left(\rho_1/\rho_0^\bullet\right)\nabla_x\zeta = -g\nabla_x\zeta$, which coincides with the non-Boussinesq version (2.4) and does not contain any spurious vertical shear. Note that $P(P^\bullet) = \rho_1 c^2\left(e^{P^\bullet/\left(\rho_1 c^2\right)} - 1\right)$ and $r(P^\bullet) = e^{P^\bullet/\left(\rho_1 c^2\right)}$; this translates into $r(z) = e^{g(\zeta - z)/c^2}$.

The preceding example is rather trivial because Θ, S fields are uniform which makes it possible to express the entire density variation in terms of $r(P)$, so the subsequent replacement $\rho^\bullet \to \rho_0^\bullet$ leads to an equivalence of the modified Boussinesq and non-Boussinesq models. In the general case Θ, S are not uniform, and the approximation is not exact. However, (2.12)–(2.15) is still a very effective measure to reduce Boussinesq-approximation errors (by $\sim 90\%$) because for realistic conditions the variations of speed of sound c are relatively small (*i.e.,* $c = 1480 \ldots 1540\, m/s$) and a large portion of that variation is due to changes in pressure alone, which can be excluded from contributing to the errors. EOS in (2.1) is nonlinear with respect to P; however, (2.4) still holds and $r(P)$ can absorb the entire density variation in this case as well. The effectiveness of using (2.12) is facilitated by the fact that variations of Θ, S tend to decrease significantly with depth, where EOS nonlinearities due to P are strongest.

Finally, we should note that McDougall *et al.* (2002) proposed an alternative version of Boussinesq approximation, where they interpret Boussinesq velocity not in its original meaning, but as renormalized mass flux per unit area, $\tilde{\mathbf{u}} = \rho\mathbf{u}/\rho_0$. Their system does not produce non-physical shear in geostrophically-balanced flow in the Boussinesq case (2.6), because now it is $\tilde{\mathbf{u}}$, not $\mathbf{u}$ becomes proportional to vertical density profile, which means that the unscaled velocity in vertically uniform, hence is correct. They concluded that the new Boussinesq makes EOS stiffening of Dukowicz (2001) unnecessary, because it can be avoided by their approach. Unfortunately their system has an undesirable side effect of altering scaling relationship between advection and Coriolis term which makes it impossible to derive a potential vorticity equation for a shallow layer of barotropic compressible fluid, see Appendix A. This puts their system into disadvantage relatively to Boussinesq equations with stiffened EOS, and negates their criticism of Dukowicz (2001).

3 Pressure effects in EOS

In this section we examine the specific requirements on EOS for the purposes listed in Sec. 1 to find a functional form compatible with the PGF calculation in sigma-coordinates, Shchepetkin & McWilliams (2003, hereafter SM2003); re-evaluate the accuracy of the mode-splitting algorithm of SM2005 focusing on compressibility effects; and inspect the EOS needs for subgrid-scale mixing parameterizations.

3.1 Pressure-Gradient Force in sigma-coordinates

Following SM2003, the baroclinic PGF in σ coordinates can be expressed entirely in terms of adiabatic derivatives of *in situ* density: a density-Jacobian scheme is written as

$$\mathscr{J}_{x,s}(\rho, z) = -\alpha \cdot \mathscr{J}_{x,s}(\Theta, z) + \beta \cdot \mathscr{J}_{x,s}(S, z)\,, \tag{3.1}$$

which is then integrated vertically to compute PGF. $\mathscr{J}_{x,s}$ denotes the Jacobian of its two arguments,

$$\mathscr{J}_{x,s}(\rho, z) = \left.\frac{\partial \rho}{\partial x}\right|_s \cdot \frac{\partial z}{\partial s} - \frac{\partial \rho}{\partial s} \cdot \left.\frac{\partial z}{\partial x}\right|_s\,, \tag{3.2}$$

where $s = s(\mathbf{x}, z) \begin{array}{l} \nearrow 0, \quad z \to \zeta \\ \searrow -1, \quad z \to -h \end{array}$; $\quad \dfrac{\partial s}{\partial z} > 0\,,$ s is a generalized sigma-coordinate [2] , and

$$\alpha = \alpha(\Theta, S, P) = -\left.\partial\rho/\partial\Theta\right|_{S,P=\text{const}}\,, \qquad \beta = \beta(\Theta, S, P) = \left.\partial\rho/\partial S\right|_{\Theta,P=\text{const}} \tag{3.3}$$

are thermal expansion and saline contraction coefficients [3] . Geopotential height z in (3.1) is used as a proxy for EOS pressure — replacing it with $-g\rho_0 z$, hence neglecting the non-uniformity of density and the contribution due to $\zeta \neq 0$. This is a common approximation in Boussinesq codes. Eq. (3.1) has as its only EOS requirement on the computation of α and β. Because α and β depend on pressure (depth), the weighting of $\mathscr{J}_{x,s}(\Theta, z)$ and $\mathscr{J}_{x,s}(S, z)$ in the r.h.s. changes with depth as well, so that the same pair of gradients of Θ and S yields differing contributions in PGF with depth (a thermobaric effect).

Eq. (3.1) involves two separate Jacobians for Θ and S. Computing them separately and combining them at the last stage is undesirable because applying discretized monotonicity constraints to Θ and S separately does not guarantee positive stratification of interpolated density, even if the density values corresponding discrete Θ and S are positively stratified. This can lead to large errors and possible numerical instability if the density field is not smooth on the grid scale. Instead, for reasons explained below, the preferred form of EOS is

$$\rho = \rho_1^{(0)} + \rho_1'(\Theta, S) + \sum_{m=1}^{n} \left(q_m^{(0)} + q_m'(\Theta, S)\right) \cdot (-z)^m\,, \tag{3.4}$$

where $\rho_1 = \rho_1^{(0)} + \rho_1'(\Theta, S)$ is density with a given potential temperature and salinity at surface pressure; the compressibility coefficients $q_m = q_m^{(0)} + q_m'(\Theta, S)$ do not depend on z; $\rho_1^{(0)}$, $q_1^{(0)}$, ...,

---

[2] Throughout this study we use s to denote an arbitrary, non-separable, surface- and terrain-following coordinate $z = z(x, y, s)$. In contrast, σ is strictly reserved for the proportional (non-stretched) sigma-coordinate, $\sigma = (z-\zeta)/(h+\zeta)$. However, in any case the displacements of coordinate surfaces caused by free-surface movement are proportional to the distance from the bottom, $\partial_t z|_{s=\text{const}} = \partial_t\zeta \cdot (z+h)/(h+\zeta)$.

[3] In a more standard definition α and β are normalized by density, hence $\alpha = -(1/\rho)\ \partial\rho/\partial\Theta|_{S,P=\text{const}}$ and $\beta = (1/\rho)\ \partial\rho/\partial S|_{\Theta,P=\text{const}}$, where ρ is either *in situ* (non-Boussinesq version), or $\rho = \rho_0$ is Boussinesq reference density (if Boussinesq approximation is used). Since for the purpose of the present study it is important to keep track of the $\rho \to \rho_0$ replacement on every occasion, we chose to exclude $(1/\rho)$ from the definition of α and β.

$q_n^{(0)}$ are constant bulk values chosen in such a way that $\rho_1^{(0)} \gg \rho_1'$, $q_1^{(0)} \gg q_1'$; the absolute depth $(-z)$ serves the role of EOS pressure (when it appears inside EOS it increases downward, counting from either the rest-state free surface $z = 0$, or the actual free surface $z = \zeta$). Then $\mathscr{J}_{x,s}(\rho, z)$ can be computed as

$$\mathscr{J}_{x,s}(\rho, z) = \mathscr{J}_{x,s}(\rho_1', z) + \sum_{m=1}^{n} (-z)^m \cdot \mathscr{J}_{x,s}(q_m', z)\,, \tag{3.5}$$

where $(-z)^m$ are treated as coefficients not subject to differentiation. For this reason this can also be viewed as a form of adiabatic differentiation. The contribution of terms with $\rho_1^{(0)}$, $q_1^{(0)}$, $q_2^{(0)}$..., cancels out identically here; *i.e.*, they are dynamically passive. To ensure that the stratification corresponding to the interpolated density field stays non-negative (non-oscillatory), the algorithm of SM2003 relies on a measure of the smoothness of density field based on the ratio of consecutive adiabatic differences. The scheme is based on cubic polynomial fits and requires evaluation of density derivatives at the same discrete locations as density itself, $\rho_{i,j,k}$, which in its turn needs some kind of averaging of elementary differences over the two adjacent grid intervals. If the two elementary differences are of the same sign, but differ by more than a factor of three, a simple algebraic averaging overestimates the derivative at the location of $\rho_{i,j,k}$ and causes spurious oscillation of the cubic polynomial interpolant. If EOS has no dependency of pressure, a conventional monotonization algorithm for the interpolation of density would suffice, but for a realistic EOS the comparison of elementary differences is meaningful only if they are defined in an adiabatic sense,

$$\Delta\rho_{i+1/2,j,k}^{\prime(\mathrm{ad})} = \rho'_{1\,i+1,j,k} - \rho'_{1\,i,j,k} + \sum_{m=1}^{n} \left(q'_{m\,i+1,j,k} - q'_{m\,i,j,k}\right) \left[-\frac{z_{i+1,j,k} + z_{i,j,k}}{2}\right]^m . \tag{3.6}$$

The two adjacent adiabatic differences are averaged using harmonic mean, and (if needed) the compressible part is computed and added separately,

$$d_{i,j,k} \equiv \left.\frac{\partial\rho}{\partial\xi}\right|_{i,j,k} = \frac{1}{\Delta\xi} \cdot \frac{2\Delta\rho_{i+1/2,j,k}^{\prime(\mathrm{ad})} \cdot \Delta\rho_{i-1/2,j,k}^{\prime(\mathrm{ad})}}{\Delta\rho_{i+1/2,j,k}^{\prime(\mathrm{ad})} + \Delta\rho_{i-1/2,j,k}^{\prime(\mathrm{ad})}} + \left(q'_{1\,i,j,k} + 2q'_{2\,i,j,k} \cdot (-z_{i,j,k}) + ...\right) \left[-\left.\frac{\partial z}{\partial\xi}\right|_{i,j,k}\right], \tag{3.7}$$

which is applicable if $\Delta\rho_{i+1/2,j,k}^{\prime(\mathrm{ad})}$ and $\Delta\rho_{i-1/2,j,k}^{\prime(\mathrm{ad})}$ have the same sign; otherwise the first term in the r.h.s. is replaced with zero. Because the harmonic averaging never exceeds twice the smaller of the two operands, it acts as monotonization algorithm for interpolation. The algorithm (3.6)–(3.7) requires that ρ_1', q_1', q_2'... be available separate from the EOS calculation. This is practical only if (3.4) is restricted to a very few coefficients q_m'. In Sec. 4 we will present a sufficiently accurate approximation to EOS with the functional form of (3.4) that contains only two coefficients, $q_1' = q_1'(\Theta, S)$ and q_2', with the latter being just a constant multiplied by q_1'.

From the above one might get an impression that the passiveness of the bulk terms $\rho_1^{(0)}$, $q_1^{(0)}$, $q_2^{(0)}$... in (3.4) is just a consequence of neglecting the contribution disturbance of ζ in EOS pressure. This is not correct. Including ζ in EOS pressure *would cause* a Boussinesq error of the type (*ii*) in (2.5)–(2.11). Consider an EOS with the form,

$$\rho = \rho_1^{(0)} + \sum_{m=1}^{n} q_m^{(0)} \cdot (\zeta - z)^m + ... \tag{3.8}$$

where ... denotes the primed terms in (3.4) that depend on Θ and S. The contribution of the bulk terms

$$\mathscr{J}_{x,s}(\rho,z)=\sum_{m=1}^{n} q_m^{(0)}\cdot m\cdot(\zeta-z)^{m-1}\cdot\frac{\partial z}{\partial s}\cdot\frac{\partial\zeta}{\partial x}\,, \tag{3.9}$$

leads to

$$\left.\frac{\partial P}{\partial x}\right|_z=g\rho\big|_{z=\zeta}\frac{\partial\zeta}{\partial x}+g\int_s^0\mathscr{J}_{x,s}(\rho,z)\,ds'=g\rho_1^{(0)}\frac{\partial\zeta}{\partial x}+\sum_{m=1}^{n} q_m^{(0)}\cdot(\zeta-z)^m\cdot\frac{\partial\zeta}{\partial x}=g\rho\frac{\partial\zeta}{\partial x}\,. \tag{3.10}$$

In a Boussinesq model the last term in the r.h.s. is divided by ρ_0, which leads to a spurious vertical shear in a purely barotropic flow (*cf.*, (2.5) in Sec. 2). From this point of view, it is desirable to exclude $q_1^{(0)}$, $q_2^{(0)}$... from (3.4):

$$\rho=\rho_0+\rho'\qquad\text{where}\qquad\rho'=\rho_1'(\Theta,S)+\sum_{m=1}^{n} q_m'(\Theta,S)\cdot(-z)^m\,, \tag{3.11}$$

after which using $(-z)$ or $\zeta-z$ no longer makes a noticeable difference SM2003. EOS stiffening of Dukowicz (2001) can be implemented in this context by choosing

$$r(z)=1+\left(1\,\Big/\,\rho_1^{(0)}\right)\sum_{m=1}^{n} q_m^{(0)}\cdot(-z)^m \tag{3.12}$$

and applying it to (3.4). This leads to cancellation of terms containing $q_1^{(0)}, q_2^{(0)}, ...,$ *etc.*, and, after expansion in powers of $(-z)$, the resultant $\rho^{\bullet\prime}$ can be expressed in the same functional form as (3.11), but with a modified set of coefficients: the $q_m'(\Theta,S)$ are slightly reduced to account for $1/r(z)\le 1$. Obviously, $r(z)$ commutes with the Jacobian operator,

$$\mathscr{J}_{x,s}\Big(r(z)\cdot\rho^{\bullet},\,z\Big)=r(z)\cdot\mathscr{J}_{x,s}\Big(\rho^{\bullet},z\Big)\,, \tag{3.13}$$

however, the corresponding discrete relationship holds only within the order of accuracy, not exactly.

The above choice of $r(z)$ is on par with Sun *et al.* (1999); Hallberg (2005), but differs from Dukowicz (2001), who derives it from globally-averaged Θ, S-profiles from observations to make $\rho_0^{\bullet}\cdot r(z)$ as close as possible to *in situ* density: this is incompatible with the algorithm (3.6)–(3.7) for avoiding spurious oscillations in stratification, which leads to the alternative fit in Sec. 4.

In summary we identify the following requirements on EOS for accurate computation of PGF in a sigma-model: accurate dependency of α and β on Θ, S, and pressure (depth); non-appearance of *in situ* density and suppression of the bulk terms $\rho_1^{(0)}$; $q_1^{(0)}$, ..., *etc.*in PGF; and an EOS form that facilitates computation of adiabatic differences in all directions.

3.2 Barotropic-Baroclinic Mode-Splitting

The barotropic-baroclinic mode-splitting algorithm of SM2005 makes the Boussinesq approximation without analyzing its consequences for mode-splitting. It assumes that the fluid is incompressible and that all ρ variations occur due to baroclinicity, which is not the realistic case where most of the ρ

change is caused by P rather than (Θ, S) variation [4]. In this section we provide a detailed analysis of how mode splitting is affected by the compressibility effects.

The purpose of mode-splitting is to take advantage of the difference of time scales between external gravity-wave propagation and other, slower processes. Its key element is expressing the vertically-integrated PGF,

$$\mathscr{F} = -\frac{1}{\rho_0}\int_{-h}^{\zeta} \nabla_\perp P \,\mathrm{d}z \;= \mathscr{F}\Big[\nabla_\perp\zeta,\ \zeta,\ \ \nabla_\perp\rho(\mathbf{x},z),\ \rho(\mathbf{x},z)\Big]\,, \tag{3.14}$$

in two parts: one that can be efficiently computed from only the barotropic variables (*e.g.,* ζ) and another that is independent (or as weakly dependent as possible) on ζ. With $\mathscr{F}$ the vertically integrated momentum equation is rewritten as

$$\partial_t\left(D\overline{\mathbf{u}}\right) + ... = \underbrace{\delta\mathscr{F}}_{\partial(\delta\mathscr{F})/\partial\zeta\neq 0} + \underbrace{\Big[\mathscr{F}-\delta\mathscr{F}\Big]}_{\partial/\partial\zeta\approx 0}\,. \tag{3.15}$$

The first r.h.s. term, $\delta\mathscr{F}$, is identified as the barotropic PGF. In split-explicit time-stepping it is treated as "fast" and recomputed at each barotropic time step. Conversely, the second is "slow" and accordingly kept constant during the barotropic stepping and only updated during the baroclinic step. $\mathscr{F}$ must be computed at every baroclinic step before the barotropic stepping begins. When computing $\mathscr{F}$ by (3.14), there is no other choice than to use the latest available ζ, which at this moment is at the previous time step. Consequently, the residual dependency of $\mathscr{F}-\delta\mathscr{F}$ on ζ results in a r.h.s. term of a hyperbolic nature treated by using an effectively forward-Euler baroclinic time-stepping. This may lead to a numerical instability, imposing an additional non-physical restriction on the baroclinic time-step size or may require extra damping. The difficulty comes from the fact that (3.14) is generally a nonlinear functional, involving products of density and, in principle, dependence of ρ on ζ through EOS compressibility. To address these issues, $\delta\mathscr{F}$ is derived as a variational derivative of $\mathscr{F}$ (SM2005, also Shchepetkin & McWilliams, 2008)

$$\delta\mathscr{F} = \frac{\partial\mathscr{F}}{\partial\left(\nabla_\perp\zeta\right)}\delta\left(\nabla_\perp\zeta\right) + \frac{\partial\mathscr{F}}{\partial\zeta}\delta\zeta\,, \tag{3.16}$$

where ζ and $\nabla_\perp\zeta$ are viewed as independent state variables [5]. The use of (3.16) ensures that when two different time-stepping algorithms are applied separately to the barotropic and baroclinic components, the resultant sum of the updated barotropic PGF (*i.e.,* computed from the new ζ) and the original 3D→2D forcing term $\Big[\mathscr{F}-\delta\mathscr{F}\Big]$ is sufficiently close to the vertically-integrated PGF computed from the new ζ,

$$\delta\mathscr{F}' + \Big[\mathscr{F}-\delta\mathscr{F}\Big] = \mathscr{F} + \frac{\partial\mathscr{F}}{\partial\left(\nabla_\perp\zeta\right)}\nabla_\perp\left(\zeta'-\zeta\right) + \frac{\partial\mathscr{F}}{\partial\zeta}\left(\zeta'-\zeta\right) = \mathscr{F}' + \mathcal{O}\left(\left(\zeta'-\zeta\right)^2\right)\,, \tag{3.17}$$

where $\mathscr{F} = \mathscr{F}\left[\zeta\,,\ \nabla_\perp\zeta\,,\ \nabla_\perp\rho,\ \rho\right]$ and $\mathscr{F}' = \mathscr{F}\left[\zeta'\,,\ \nabla_\perp\zeta'\,,\ \nabla_\perp\rho,\ \rho\right]$ correspond to the old ζ and the updated ζ' each with same density field. The $\mathcal{O}\left(\left(\zeta'-\zeta\right)^2\right)$ estimate of the mismatch between $\mathscr{F}'$ and

[4] This situation is partially addressed by removing the dynamically passive bulk-compressibility terms from EOS in SM2003, but the main motivation was to reduce the PGF error, rather than to improve mode splitting.

[5] A finite-difference version of (3.14) is a function of two adjacent grid-point values, $\zeta_{i,j}$ and $\zeta_{i+1,j}$. Their average and difference are analogous to ζ and $\nabla_\perp\zeta$.

the l.h.s. comes from the fact that (3.17) is essentially a Taylor-series expansion of $\mathscr{F}'$ in powers of $\zeta' - \zeta$. Assuming that ρ does not depend on ζ and remains frozen during barotropic time-stepping [6], (3.16) yields

$$\delta\mathscr{F} = -\frac{g}{\rho_0}\left[h\nabla_\perp\left(\rho_*\zeta\right) + \nabla_\perp\left(\frac{\rho_*\zeta^2}{2}\right) + \left(\rho_* - \overline{\rho}\right)\zeta\nabla_\perp h\right], \tag{3.18}$$

where

$$\overline{\rho}(\mathbf{x}) = \frac{1}{D}\int_{-h}^{\zeta}\rho(\mathbf{x},z)\,\mathrm{d}z \qquad \text{and} \qquad \rho_*(\mathbf{x}) = \frac{1}{D^2/2}\int_{-h}^{\zeta}\left\{\int_z^{\zeta}\rho(\mathbf{x},z')\,\mathrm{d}z'\right\}\mathrm{d}z \tag{3.19}$$

are two-dimensional horizontal (with $\mathbf{x} = (x, y)$) fields kept constant during barotropic time-stepping. This implies that the splitting algorithm relies on the independence of $\overline{\rho}$ and ρ_* from ζ, which in turn relies on the assumption of independence of EOS from ζ.

A property of (3.18) is that if density is uniform, $\rho_* = \overline{\rho} = \rho_0$, $\delta\mathscr{F}$ reverts back to $-gD\nabla_\perp\zeta$ that is used by most of the oceanic models as an approximation for barotropic PGF (Berntsen *et al.*, 1981; Blumberg & Mellor, 1987; Killworth *et al.*, 1991). These are Boussinesq-approximation models that assume the smallness of $\rho(\mathbf{x}, z) - \rho_0$, and their mode-splitting procedures rely on this smallness as well. Isopycnic models tend to be non-Boussinesq and use a different mode-split, essentially linking $\delta\mathscr{F}$ to the bottom pressure of the resting state ($\zeta = 0$) (Bleck & Smith, 1990). Since the bottom pressure is computed by vertical hydrostatic integration, this translates into $\delta\mathscr{F} = -gD\nabla_\perp\left(\overline{\rho}\zeta\right)$, where $\overline{\rho}$ is the vertically-averaged density. (Note that this $\delta\mathscr{F}$ is dimensionally different from the similar term in (3.15) because non-Boussinesq models use density-weighting to compute $\overline{\mathbf{u}}$.) This split is also empirical and approximate. Higdon & de Szoeke (1997) propose a more accurate split for a non-Boussinesq isopycnic model, which replaces $\overline{\rho}$ with a different value computed from the local vertical profile of density (somewhat similar to ρ_*, but expressed in terms of specific volume rather than density). In all cases, with or without the Boussinesq approximation, the fluid was considered as incompressible for the purpose of mode-splitting [7].

The goal of replacing $-gD\nabla_\perp\zeta$ with (3.18)–(3.19) is to achieve mutual consistency between the 3D and 2D parts of the model – mainly in the ability of the split 2D part to yield the same barotropic gravity-wave phase speed $\widetilde{c}$ as the full 3D model. This consistency may or may not provide an improvement in the overall physical accuracy. The sources of mode-splitting error from using $-gD\nabla_\perp\zeta$ as the barotropic PGF are the following:

(*i*) *"Horizontal baroclinicity":* Suppose the fluid is incompressible and there is no vertical stratification, but the density varies horizontally, hence $\rho_* = \overline{\rho} = \overline{\rho}(\mathbf{x})$. Because of the Boussinesq approximation, $\mathscr{F}$ and $\widetilde{c}$ are seen by the 3D part of the model as proportional to $\overline{\rho}/\rho_0$ and $\sqrt{\overline{\rho}/\rho_0}$, respectively. The spatial variation of $\overline{\rho}$ makes it impossible to choose ρ_0 in such a way that the use of the $-gD\nabla_\perp\zeta$-term for the barotropic mode accurately approximates $\mathscr{F}$, especially in a very large basin, thus contributing to mode-splitting error using $-gD\nabla_\perp\zeta$. The small parameter associated with this type of error is $\left(\overline{\rho} - \rho_0\right)/\rho_0$.

[6] More precisely, the density field is "frozen in σ-space" during barotropic time-stepping. This is because the entire vertical coordinate system "breathes" when ζ moves up and down, so each vertical grid box also changes proportional to its height, while the grid-box averaged values of density remain unchanged.

[7] In isopycnic coordinates this approximation is also needed to circumvent a theoretical difficulty with the assumption that potential density is a Lagrangian conserved property, which implies that it can be defined globally relative to a given reference pressure. In fact, the seawater EOS does not have this property (Jackett & McDougall, 1997), allowing only a local definition of potential density with respect to a local reference pressure.

(*ii*) *Vertical stratification:* $\widetilde{c}$ is smaller in a stratified compressible fluid than in a stratified incompressible fluid with the same depth,

$$\widetilde{c}^2 = gh - \hat{c}_1^2 \,, \tag{3.20}$$

where $\hat{c}_1$ is the gravity-wave phase speed of the first baroclinic mode (Appendices C and D). The relevant small parameter for estimating this mode-splitting error is the ratio of the squares of the modal phase speeds, $\widetilde{c}_1^2/(gh)$.

(*iii*) *Seawater compressibility*: In the case of constant bottom topography $\widetilde{c}$ is reduced relative to an incompressible fluid with the same depth by

$$\widetilde{c}^2 = gh\left(1 - \frac{1}{2}\cdot\frac{gh}{c^2} + ...\right) \tag{3.21}$$

(Appendices A and B for non-stratified and stratified cases). The mechanism of this reduction is non-Boussinesq and is associated with the fact that the volumetric divergence of horizontal barotropic velocity causes a smaller response in ζ than in an incompressible fluid. The use of (3.18)–(3.19) qualitatively captures the influence of compressibility – by distinguishing ρ_* and $\overline{\rho}$ with $\rho_* < \overline{\rho}$ in this case – but the analyses below indicate an underestimation of the effect, and therefore a contribution to mode-splitting error with an associated small parameter of gh/c^2. Since both corrections to the barotropic phase speed $\widetilde{c}$, (3.20) and (3.21), are small, they are approximately additive (Appendix C).

(*iv*) *Sea-level contribution to EOS pressure*: In principle, PGF is sensitive to how EOS pressure depends on ζ (*cf.*, (2.11)), hence $\mathscr{F}$, depends on ζ through compressibility in EOS in addition to the explicit dependence from $\nabla_\perp\zeta$. In the case of constant topography the impact on barotropic phase speed $\widetilde{c}$ due to this effect is small relative to that of (*iii*) – $\mathcal{O}\left(g\zeta/c^2\right)$ vs. $\mathcal{O}\left(gh/c^2\right)$ – in fact, it formally vanishes when linearizing with respect to small $\zeta/h \ll 1$ (Appendices A and B). However, since ζ used in EOS pressure is always taken from the previous baroclinic time step and is kept constant during the barotropic time stepping, this leads to the appearance of hyperbolic r.h.s. terms that receive effectively a forward-in-time treatment. This potentially makes it a source of mode-splitting error and even instability. It should also be noted that the effect can be amplified in the presence of steep topography where the last term in (3.18), $\left(\rho_* - \overline{\rho}\right)\zeta\nabla_\perp h$, dominates over $h\nabla_\perp\left(\rho_*\zeta\right)$, even though the influence of ζ into ρ_* and $\overline{\rho}$ via EOS partially cancels due to subtracting one from the other.

The mode-splitting procedure of SM2005 is designed to address items (*i*) and (*ii*) within the Boussinesq approximation, while (*iii*) and (*vi*) are given much less consideration.

Notice that replacing $-gD\nabla_\perp\zeta$ with (3.18)–(3.19) motivated by item (*i*) is an artifact of the Boussinesq approximation. From (2.4) the non-Boussinesq local barotropic phase speed $\sqrt{gh}$ does not depend on local vertically-averaged density $\overline{\rho}$. (The inertial terms in the non-Boussinesq momentum equation use local density rather than ρ_0, resulting in cancellation of density when computing acceleration and phase speed; Appendix B.) Paradoxically, using $-gD\nabla_\perp\zeta$, rather than (3.18)–(3.19) may look more suitable in this case because it yields the correct $\widetilde{c}$. Conversely, the use of (3.18)–(3.19) can be viewed as an introduction of an *a priori* physical distortion into the barotropic mode to match an existing distortion in the 3D $\mathscr{F}$ to minimize mode-splitting error, which is the higher priority. EOS stiffening provides some relief in this conflict by merely transforming $\left(\overline{\rho} - \rho_0\right)/\rho_0 \rightarrow \left(\overline{\rho}^\bullet - \rho_0^\bullet\right)/\rho_0^\bullet$, which is expected to be somewhat smaller; however, practical experience with ROMS SM2005 indicates that the largest deviations of local vertically-averaged density are due to local Θ, S anomalies in shallow marginal seas, often semi-enclosed by topography. Under such conditions the bulk compressibility ef-

fect is not very strong, so stiffening does not make a large difference. Closely related to item (*i*) is the sensitivity of the numerical stability of the code to the choice of ρ_0, and (3.18)–(3.19) eliminates this problem.

The reduction of $\widetilde{c}$ due to stratification, item (*ii*), occurs in both non-Boussinesq and Boussinesq cases, and (3.18)–(3.19) provide an accurate accounting of it (Appendix D). To estimate its importance, note that the ratio of phase speeds also sets the mode-splitting ratio (*i.e.*, the number of barotropic time steps per baroclinic step, typically in the range 30–70 and closer to the upper limit for an open-ocean configuration) [8] . This implies an estimated erroneous reduction of $\widetilde{c}$ by $\sim 10^{-3}$ of its value from (3.20). Although this might seem to too small to be a concern, recall that the phase error due to the slightly different $\widetilde{c}$ values from using $-gD\nabla_\perp\zeta$ is accumulated over many barotropic time steps performed at each baroclinic step, which makes the numerical stability of the code sensitive to whether (3.18)–(3.19) is used or not.

The physical explanation of item (*iii*) is non-Boussinesq in nature: despite the coincidence of (2.4) with the PGF due to the gradient of ζ in a barotropic incompressible flow, the value of $\widetilde{c}$ is smaller in a compressible fluid (*cf.*, (B.6) in Appendix B), where a convergence of horizontal velocity causes a change of both ζ and density with relative proportions of $1-gh/c^2$ and gh/c^2, respectively.

Eqs. (3.18)–(3.19) are derived using the Boussinesq approximation, but nevertheless they also predict a smaller phase speed than with $-gD\nabla_\perp\zeta$. When the density increases with depth, $\rho_* < \overline{\rho}$, so the PGF caused by a given $\nabla_\perp\zeta$ is slightly smaller than in the case of vertically-uniform density with the same water-column mass (*n.b.*, this implies that the choice of $\rho_0 = \overline{\rho}$). Substitution of (2.8) into (3.19) yields

$$\begin{aligned} \overline{\rho} &= \rho_1 \cdot \frac{c^2}{gD}\left(e^{gD/c^2}-1\right) &&\approx \rho_1\left(1+\frac{1}{2}\cdot\frac{gD}{c^2}+...\right) \\ \rho_* &= \rho_1 \cdot \frac{c^2}{gD}\left\{\frac{c^2}{gD}\left(e^{gD/c^2}-1\right)-1\right\} &&\approx \rho_1\left(1+\frac{1}{3}\cdot\frac{gD}{c^2}+...\right) . \end{aligned} \tag{3.22}$$

With a flat bottom this implies $\widetilde{c} = \sqrt{gh\cdot\rho_*/\rho_0}$ instead of just $\sqrt{gh}$. While this qualitatively captures the effect of reducing $\widetilde{c}$ relative to that of an incompressible fluid, even if we make the best possible choice for reference density ($\rho_0 = \overline{\rho}$), the correction is underestimated by a factor of 1.5 relative to its true, non-Boussinesq magnitude in (B.9) in Appendix B. This discrepancy is not surprising since the non-Boussinesq explanation for the reduced phase speed is different than in (3.18).

Equation (3.21) provides an estimate for the barotropic speed reduction due to effect (*iii*) of ∼0.6% of $\sqrt{gh}$ assuming $h = 5500\,m$ and $c = 1500\,m/s$. This is one-and-half orders of magnitude larger than the effect of baroclinicity (*ii*), and therefore it creates a stronger requirement for replacing $-g\nabla_\perp\zeta$ with (3.18)–(3.19) even thought correcting for item (*iii*) was not the initial motivation. EOS stiffening dramatically reduces the difference between $\overline{\rho}$ and ρ_*. This eliminates the non-physical mechanism of reduced barotropic phase speed due to compressibility via (3.22). It also brings the mode-splitting procedure into the realm of assumptions for its original derivation.

The effect of (*iv*) is expected to be much smaller than (*iii*); however, Robertson *et al.* (2001) observed a numerical instability in POM while simulating tides under near-resonant conditions. The source of the instability was traced back to the influence of ζ on EOS pressure through the use of old-time-step ζ due to the specifics of the mode-splitting algorithm. Although they did not classify it

[8] In practice the splitting ratio is adjusted by the ratio of stability limits of the time-stepping algorithms for the 2D and 3D parts. For ROMS the splitting ratio is typically 1.4 times larger than the ratio of phase speeds.

as a mode-splitting instability, the mechanism of its appearance is essentially the same as in (*iv*). They proposed to eliminate the instability by dropping pressure effects in EOS altogether: they split EOS additively as $\rho = \rho_N(\Theta, S) + \rho_p(P)$ (starting with their Eq. (16)), and showed the dynamic passiveness of ρ_p, which they subsequently excluded. This leads to complete loss of the thermobaric effect, and that may be not acceptable in many large-scale applications. EOS stiffening of Dukowicz (2001) helps to reduce (but not to eliminate entirely) the splitting error while keeping thermobaricity intact.

3.3 Vertical mixing parameterization

The vertical mixing parameterizations are based on the stratification stability, expressed as the Brundt–Väisälä Frequency $N(\mathbf{x}, z, t)$, and the translation of surface heat and freshwater fluxes into a buoyancy flux. Both steps use the $\alpha(\Theta, S, P)$ and $\beta(\Theta, S, P)$ coefficients from EOS,

$$N^2 = g\left[\alpha \cdot \partial_z \Theta - \beta \cdot \partial S_z\right] . \tag{3.23}$$

Thus, the requirement for EOS is to accurately reproduce α and β, but now with a shifted emphasis on accurate computation of their ratio, α/β. The primary sensitivity here comes from detecting when stratification and/or buoyancy forcing change sign, because this corresponds to a drastic transition from one stable to convective mixing regime. The Boussinesq — non-Boussinesq and EOS stiffening issues are not a concern here because both α and β are normalized by the same density – whether *in situ* or replaced by ρ_0 or $\rho_0^\bullet$,

$$\alpha = -\frac{1}{\rho}\left.\frac{\partial \rho}{\partial \Theta}\right|_{S,P} \to -\frac{1}{\rho_0^\bullet}\left.\frac{\partial \rho^\bullet}{\partial \Theta}\right|_{S,P} , \qquad \beta = \frac{1}{\rho}\left.\frac{\partial \rho}{\partial S}\right|_{\Theta,P} \to \frac{1}{\rho_0^\bullet}\left.\frac{\partial \rho^\bullet}{\partial S}\right|_{\Theta,P} , \tag{3.24}$$

hence their ratio is not affected. Because negative stratification is intolerable in a hydrostatic model and parameterized vertical mixing is the only mechanism that prevents it (by entrainment of water from adjacent positively stratified layers above or below), it is desirable that the procedure for detecting negative stratification in the mixing scheme be consistent with the monotonized adiabatic differencing in the PGF algorithm (3.6)-(3.7). In particular, the stratification may change abruptly near the interior edge of the top and bottom boundary layers. Accurate determination of the layer thickness requires density interpolation where it is often non-smooth on the vertical grid-scale; this leads to similar requirements on EOS as for PGF.

3.4 Neutral surfaces

The definition of potential density depends a reference pressure, and for a realistic EOS it cannot be defined globally in the sense of a scalar function of local Θ, S, P with spatial derivatives equivalent to adiabatic derivatives of *in situ* density (Jackett & McDougall, 1995). Instead, one should either construct a neutral density (Jackett & McDougall, 1997), which is inherently nonlocal, or, alternatively, one could use a local procedure relying on $\alpha-$, and β-weighting of temperature and salinity gradients (see Eqs. (31)–(32) in Sec. 5 in Griffies *et al.* (1998)). EOS in the form (3.4) and the associated adiabatic differencing (3.6) allow direct computation of the local slopes of neutral surfaces.

4 A practical "stiffened" EOS

The seawater EOS of Jackett & McDougall (1995) has the form,

$$\rho(\Theta, S, \hat{\mathsf{z}}) = \frac{\rho_1(\Theta, S)}{1 - 0.1 \cdot \hat{\mathsf{z}} \,/[K_{00} + K_0(\Theta, S) + K_1(\Theta, S) \cdot \hat{\mathsf{z}} + K_2(\Theta, S) \cdot \hat{\mathsf{z}}^2]}\,, \tag{4.1}$$

where Θ is potential temperature; S salinity; $\rho_1(\Theta, S)$ is the density at a surface pressure of $1\,atm$, fit by a 15-term polynomial containing various products of powers of Θ^n, $n = 1, ..., 5$, and S^m, $m = 1,\ 3/2,\ 2$ (not in all permutations). The divisor $K = K_{00} + K_0(\Theta, S) + ...$ has $K_{00} = \text{const}$, and the remaining three coefficients K_0, K_1 K_2 depend on Θ and S with similar polynomial fits with powers of Θ,..., Θ^4, and S, $S^{3/2}$ that add up to a 26-term polynomial for K. The UNESCO EOS has the same functional form, but it is expressed in terms of *in situ* temperature; hence ρ_1 is identically the same, but the coefficients for K_0, K_1, K_2 are different. In addition, EOS pressure in (4.1) is remapped into depth $\hat{\mathsf{z}}$ [9] . The complexity of the functional form of UNESCO EOS motivates oceanic modelers to derive simplified versions for more efficient calculation (Mellor, 1991; Wright, 1997; Brydon *et al.*, 1999; McDougall *et al.*, 2003 ; Jackett *et al.*, 2006).

Dukowicz (2001) chooses the multiplier $r(P)$ to fit an *in situ* density profile computed from the globally horizontally averaged temperature and salinity profiles based on Levitus WOA94 data [an updated version of which is available today as Locarnini *et al.* (2006); Antonov *et al.* (2006)]. Although this approach yields the minimum possible range of variation for $\rho^\bullet$, and thus has the maximum effect in reducing the Boussinesq–approximation errors, it interferes with the ability to monitor stratification smoothness by (3.6)–(3.7) because the spatial differences of $\rho^\bullet$ constructed this way unavoidably contain a contribution associated with the selected mean density profile as long as the direction of differencing is not strictly horizontal (unlike the horizontal differencing in z-coordinate models, for which the method of Dukowicz (2001) was originally intended). As a result, a change in sign for the differences no longer corresponds to the change from positive to negative physical stratification. This also alters the ratios of consecutive differences in (3.7) ultimately negating its monotonization properties. Therefore we alternatively choose constant reference values, $\Theta^{\rm ref}$ and $S^{\rm ref}$, that are representative of the abyssal part of the ocean, and then construct a multiplier $r(\hat{\mathsf{z}})$ as

$$r(\hat{\mathsf{z}}) = \frac{1}{1 - 0.1\,\hat{\mathsf{z}}/K^{\rm ref}(\hat{\mathsf{z}})}\,, \qquad \text{where} \qquad K^{\rm ref}(\hat{\mathsf{z}}) = K_{00} + K_0^{\rm ref} + K_1^{\rm ref}\hat{\mathsf{z}} + K_2^{\rm ref}\hat{\mathsf{z}}^2\,, \tag{4.2}$$

with $K_0^{\rm ref} = K_0\left(\Theta^{\rm ref}, S^{\rm ref}\right)$, $K_1^{\rm ref} = K_1\left(\Theta^{\rm ref}, S^{\rm ref}\right)$, and $K_2^{\rm ref} = K_2\left(\Theta^{\rm ref}, S^{\rm ref}\right)$. In the results presented here we choose $\Theta^{\rm ref} = 3.5^0C$ and $S = 34.5{}^0\!/_{00}$, which imply $K_0^{\rm ref} = 2924.921$, $K_1^{\rm ref} = 0.34846939$, $K_2^{\rm ref} = 0.145612 \times 10^{-5}$, and $\rho_1\left(\Theta^{\rm ref}, S^{\rm ref}\right) = 1027.43879$. The stiffened EOS (2.15) with this Boussinesq-approximation $r(\hat{\mathsf{z}})$ becomes

$$\rho^{\bullet\prime}(\Theta, S, \hat{\mathsf{z}}) = [\rho_0^\bullet + \rho_1'(\Theta, S)] \cdot \frac{1 - 0.1\,\hat{\mathsf{z}}/K^{\rm ref}(\hat{\mathsf{z}})}{1 - 0.1\,\hat{\mathsf{z}}/K(\Theta, S, \hat{\mathsf{z}})} - \rho_0^\bullet\,. \tag{4.3}$$

$\rho^{\bullet\prime}$ is the perturbation of $\rho^\bullet$ relative to a constant reference value $\rho_0^\bullet$, which is naturally chosen as $\rho_0^\bullet = \rho_1\left(\Theta^{\rm ref}, S^{\rm ref}\right)$. After cancellation of the large terms, the stiffened EOS is rewritten as

[9] Throughout this section we adopt the convention that $\hat{\mathsf{z}}$ increases downward, the same way as hydrostatic pressure. We use notation $\hat{\mathsf{z}}$ to distinguish it from z (increasing upward) as it is used elsewhere in this article.

$$\begin{aligned}\rho^{\bullet\prime}(\Theta,S,\hat{\mathsf{z}}) &= \rho_1'(\Theta,S) + 0.1\,\hat{\mathsf{z}}\cdot\frac{\rho_0^{\bullet}+\rho_1'(\Theta,S)}{K_{00}+K_0^{\rm ref}+K_1^{\rm ref}\hat{\mathsf{z}}+K_2^{\rm ref}\hat{\mathsf{z}}^2}\times \\ &\quad\times\frac{K_0^{\rm ref}-K_0(\Theta,S)+\Big(K_1^{\rm ref}-K_1(\Theta,S)\Big)\cdot\hat{\mathsf{z}}+\Big(K_2^{\rm ref}-K_2(\Theta,S)\Big)\cdot\hat{\mathsf{z}}^2}{K_{00}+K_0(\Theta,S)+(K_1(\Theta,S)-0.1)\,\hat{\mathsf{z}}+K_2(\Theta,S)\hat{\mathsf{z}}^2} \\ &\equiv \rho_1(\Theta,S)+\hat{q}'(\Theta,S,\hat{\mathsf{z}})\cdot\hat{\mathsf{z}}\,,\end{aligned} \tag{4.4}$$

so far without any approximation. This is already close to the desired functional form (3.4); however $\hat{q}'(\Theta,S,\hat{\mathsf{z}})$ still explicitly depends on $\hat{\mathsf{z}}$, although weakly as we show below. Eq. (4.4) implies that

$$\rho^{\bullet\prime}\left(\Theta^{\rm ref},S^{\rm ref},\hat{\mathsf{z}}\right)\equiv 0 \qquad \text{and} \qquad \hat{q}'\left(\Theta^{\rm ref},S^{\rm ref},\hat{\mathsf{z}}\right)\equiv 0 \qquad \text{for all } \hat{\mathsf{z}}\,.$$

This ensures that the range of variation for $\rho^{\bullet\prime}$ is expected to be small in general, and even diminish with depth since variations of Θ and S also diminish.

A Taylor series expansion of (4.4) in powers of $\hat{\mathsf{z}}$ yields

$$\rho^{\bullet\prime}(\Theta,S,\hat{\mathsf{z}}) = \rho_1'(\Theta,S)+q_1'(\Theta,S)\cdot\hat{\mathsf{z}}\,, \tag{4.5}$$

where

$$q_1'(\Theta,S) = 0.1\cdot[\rho_0+\rho_1'(\Theta,S)]\cdot\frac{K_0^{\rm ref}-K_0(\Theta,S)}{\Big(K_{00}+K_0(\Theta,S)\Big)\cdot\Big(K_{00}+K_0^{\rm ref}\Big)}\,. \tag{4.6}$$

This has exactly the functional form of (3.4). It is an approximation to (4.4) where all K_1 and K_2 terms (14 out of 26 coefficients of K) are discarded. In practice we use a slightly modified form,

$$\rho^{\bullet\prime}(\Theta,S,\hat{\mathsf{z}}) = \rho_1'(\Theta,S)+q_1'(\Theta,S)\cdot\hat{\mathsf{z}}\,(1-\gamma\hat{\mathsf{z}})\ , \tag{4.7}$$

with $\gamma = 1.72\times10^{-5}\,m^{-1}$ for the $\Theta^{\rm ref}$ and $S^{\rm ref}$ values listed above. This captures some of the nonlinear dependency of the thermobaric effect without significant increase in complexity, and it also reduces errors relative to (4.5). Consistently with (4.7), the algorithm for computing elementary adiabatic differences (3.6) becomes

$$\Delta\rho^{\bullet\prime({\rm ad})}_{i+\frac{1}{2},j,k} = \rho'_{1\,i+1,j,k}-\rho'_{1\,i,j,k}+\Big(q'_{1\,i+1,j,k}-q'_{1\,i,j,k}\Big)\,\frac{\hat{\mathsf{z}}_{i+1,j,k}+\hat{\mathsf{z}}_{i,j,k}}{2}\left[1-\gamma\frac{\hat{\mathsf{z}}_{i+1,j,k}+\hat{\mathsf{z}}_{i,j,k}}{2}\right]. \tag{4.8}$$

Isolines of $\rho^{\bullet\prime}$ from (4.7) are plotted in the left column of Fig. 1 for five different depths: 0, 200, 1000, 2500, and 5000 m. The shading in Figs. 1–2 indicates the global distribution of hydrographic data values (Levitus WOA data, Antonov *et al.*, 2006; Locarnini *et al.*, 2006). At each depth the data samples are combined into $\Delta\Theta\times\Delta S = 0.25^0C\times0.25^0/_{00}$ bins to compute the probability distribution. This is shown by the three hues of shading: the lightest indicates that this pair of Θ,S values is observed at least once in the dataset, the medium shading contains 99% of the observed data at that depth, and the darkest contains 90%. There is a significant reduction of variation of the observed Θ,S with depth as manifested by the shrinking of the shaded area, which was utilized by McDougall *et al.* (2003) and SM2003 to simplify treatment compressibility effects in EOS (note that only a very little seasonal variation of Θ,S remains at the depths of $\hat{\mathsf{z}}=200\,m$, which is illustrated by a rather narrow strip shaded area, with the lightest shade becomes indistinguishable). Furthermore, as highlighted by McDougall & Jackett (2007), there is a strong tendency for the probability distribution to align itself with the isolines density at each depth – which they call "thinness in $S-\Theta-P$ space".

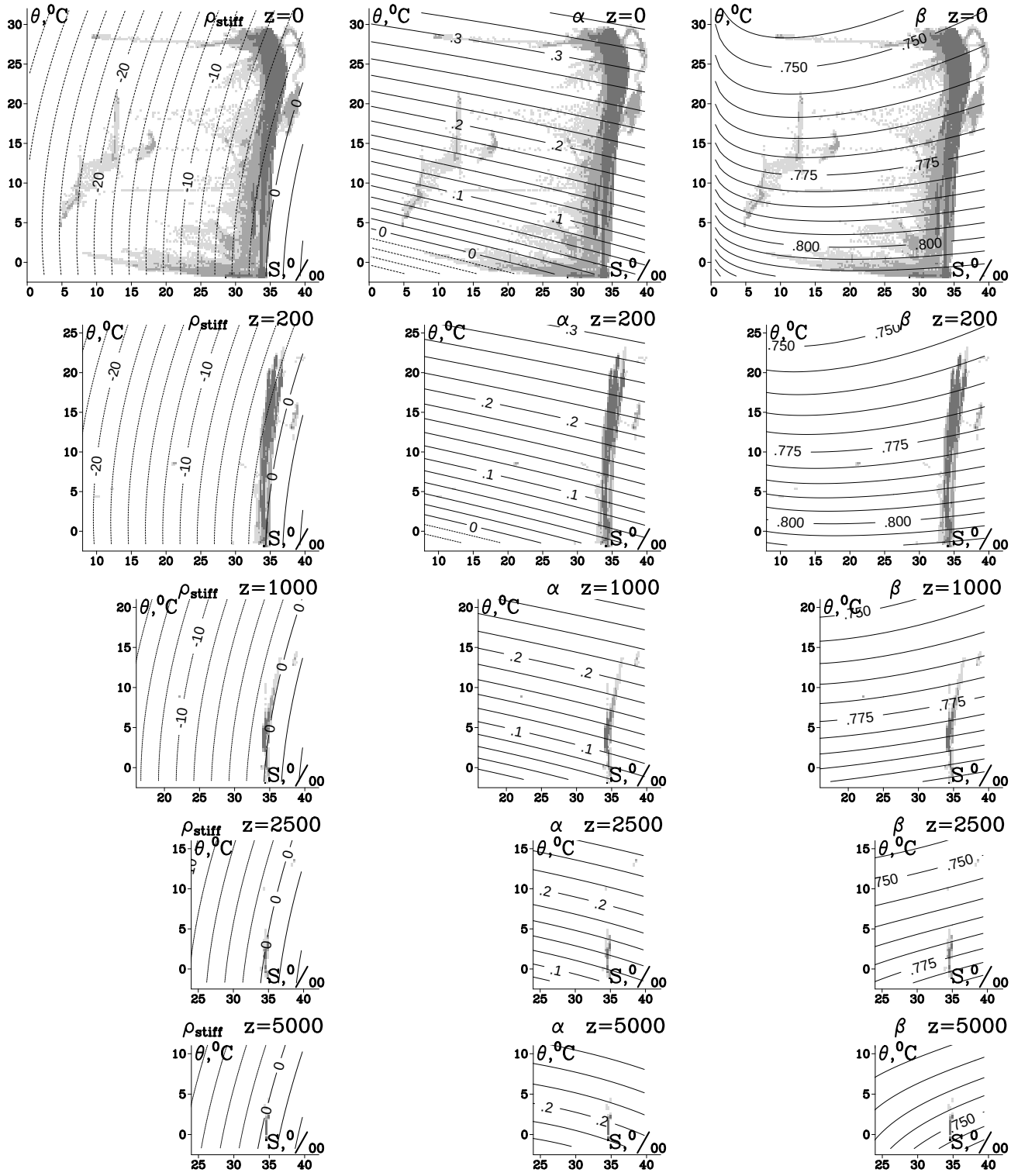

Fig. 1. "Stiffened" density perturbation $\rho^{\bullet\prime}$ defined by (4.7) **(left)**; the corresponding thermal expansion, α **(middle)**, and saline contraction, β **(right)**, coefficients as functions of potential temperature Θ and salinity S at five different depths $\hat{\mathrm{z}} = 0,\ 200,\ 1000,\ 2500$ and $5000m$. The units are kg/m^3, $(kg/m^3)/{}^0C$, and $(kg/m^3)/\left({}^0/_{00}\right)$ respectively (note that here $\alpha = -\partial\rho/\partial_\Theta\big|_{S,P=\mathrm{const}}$ and $\beta = +\partial\rho/\partial_S\big|_{\Theta,P=\mathrm{const}}$ without the usual division by ρ). Shading indicates the distribution of observed (Θ, S) values (see text). (The overall format is similar to Fig. 19 in SM2003.)

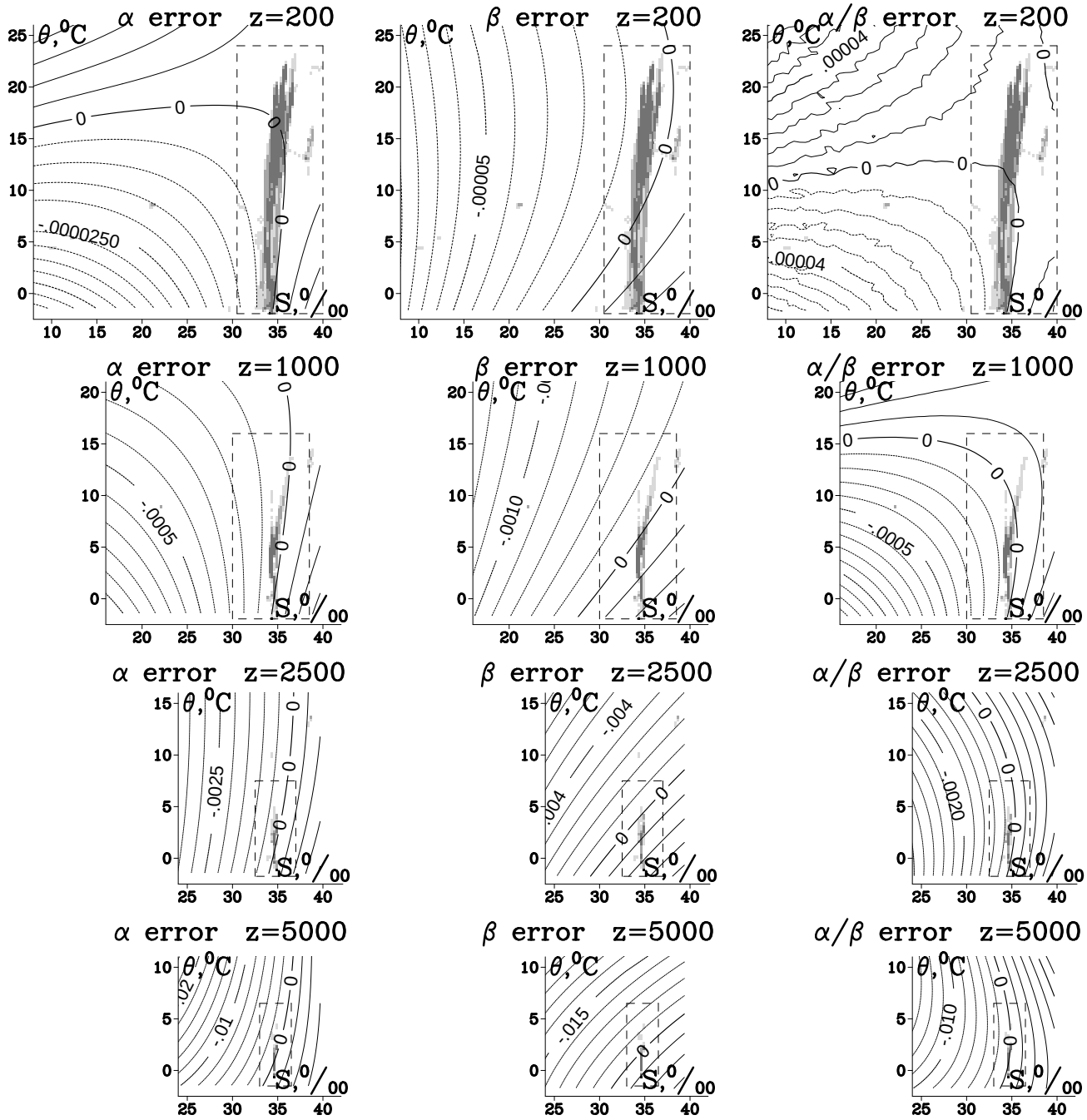

Fig. 2. Errors in α **(left)**, β **(middle)**, and their ratio, α/β **(right)** due to the approximate EOS (4.7) compared to the complete EOS (4.4) at four different depths: $\hat{z} = 200,\ 1000,\ 2500$, and $5000m$. The shading is the same as in Fig. 1, and the dashed box surrounds the domain of interest. (The format is similar to Fig. 20 in SM2003.)

Isolines of $\rho^{\bullet\prime}$ in the (Θ, S)-plane tend to rotate counterclockwise with increasing depth (thermobaric effect) and exhibit a gentle curvature (cabelling). However, as assured by the construction of EOS, the $\rho^{\bullet\prime}$ does not have tendency to increase with depth. The density range for observed (Θ, S) is much reduced; *e.g.*, at $\hat{z} = 5000\,m$, $\Theta \approx 3.5^0$, $S = 34.5^0/_{00}$, and $\rho^{\bullet\prime}$ stays close to zero, in contrast with $\rho_{in\ situ} \approx 1050\,kg/m^3$ (see Fig. 19, left column, in SM2003; note that field plotted there is $\rho_{in\ situ} - 1000$).

The coefficients α and β are plotted in the center and right columns of Fig. 1. α shows a significant

increase with depth, while β decreases slightly. One notices some differences in values and in patterns compared to Fig. 19 in SM2003, especially for β. For example, at $\hat{\mathsf{z}} = 5000\,m$, $\Theta \approx 3.5^0$ C and $S = 35\,{}^0/_{00}$ $\beta = 0.760$ in that Fig. 19, while here $\beta = 0.745$ in Fig. 1. The difference of $\approx 2\%$ is explained by $r(\hat{\mathsf{z}})$, which is responsible for the density difference between $\rho_{in\,situ} \approx 1050$ vs. $\rho_0^\bullet \approx 1027.4$ here, so that β[Fig. 19]$/\rho_{in\,situ} \approx \beta$[Fig. 1]$/\rho_0^\bullet$. Similar adjustment occurs for α, and, as the result, adiabatic differences of stiffened density normalized by $\rho_0^\bullet$ (using Boussinesq-like rules) are now close to that computed from a full EOS (4.1), but normalized by $\rho_{in\,situ}$ (non-Boussinesq rules).

As shown in Sec. 2, the most important requirement for EOS is to accurately reproduce α and β as functions of depth within the subspace of naturally occurring Θ and S values. Furthermore, because hydrostatic models are especially sensitive to the occurrence of negative stratification, the accuracy of representation of the ratio of α/β is even more valuable than the accuracy of α and β taken separately (*e.g.,* this occurs in southern part of Atlantic Ocean characterized by the fresh, but cold near-surface layer on top of warmer, but more saline deeper water, resulting in a thermodynamically delicate situation with very week overall stratification, and the possibility of cabbeling and thermobaric instabilities, Paluszkiewicz *et al.*, 1994; McPhee, 2000). This is also true for modeling deep currents in the presence of Θ and S anomalies, which tends to cancel effects of each other, *e.g.,* Mediterranean outflow. Therefore, we evaluate the differences between α, β, and α/β computed using (4.6)–(4.7) against its prototype (4.4), which is the unapproximated stiffened EOS (Fig. 2). On each panel we indicate the domain of interest with a dashed-line box surrounding observed (Θ, S) values. The error in computing α within the domain of interest can be estimated as ± 0.0001 at $\hat{\mathsf{z}} = 1000\,m$; ± 0.0005 at $\hat{\mathsf{z}} = 2500\,m$; and ± 0.002 at $\hat{\mathsf{z}} = 5000\,m$. For β similar errors are ± 0.0004 at $\hat{\mathsf{z}} = 1000\,m$; ± 0.001 at $\hat{\mathsf{z}} = 2500\,m$; and ± 0.005 at $\hat{\mathsf{z}} = 5000\,m$. These error estimates are conservative because the observed (Θ, S) areas (shaded) occupy only a fraction of the domains of interest we have defined. Normalized by the relevant values of α and β, the relative errors for both quantities stay within $\pm 0.5\%$. This is substantially more accurate than in Fig. 20 of SM2003, and what is essentially new here is that zero-error line is always placed close to the middle of the shaded area. The computation of α/β a better alignment of the zero-error line with the shaded area. This is a somewhat unexpected benefit of EOS stiffening: the multipliers $r(\hat{\mathsf{z}})$ essentially plays the role of a preconditioner to EOS of Jackett & McDougall (1995) by removing most of the nonlinear dependency from depth (pressure). The remaining $\rho^\bullet$ can be more accurately fit by the simple function in (4.7). (Note that the for small depth, $\hat{\mathsf{z}} = 200\,m$, the error pattern of α/β-ratio has a saddle point in the vicinity of observed data, which makes a second-order smallness of error as Θ, S depart from it.)

5 Does Boussinesq approximation still offer any simplification?

During the review process we were challenged why a Boussinesq code should still be used, given the recent theoretical enthusiasm and advocacy for the non-Boussinesq alternative (McDougall *et al.*, 2002; Greatbatch & McDougall, 2003; Marshall *et al.*, 2004; Griffies, 2004). While we acknowledge that some aspects of oceanic modeling become more natural in the non-Boussinesq framework, notably the response to thermodynamic forcing (Mellor & Ezer, 1995; Huang & Jin, 2002), the value of Boussinesq approximation is due to accuracy and dynamical parsimony in retaining the important behaviors in oceanic circulation while excluding extraneous effects (*e.g.,* acoustic waves) that can be computationally difficult (Spiegel & Veronis, 1960; Mihaljan, 1962; Zeytounian, 2003). The non-Boussinesq generalization does not bring in any important additional circulation behaviors (Great-

batch, 1994; Dukowicz, 1997) and *a posteriori* comparison between Boussinesq and non-Boussinesq results has shown that other aspects of the modeling codes (specifics of initialization, version of EOS, etc) produce comparable or even greater sensitivities (Losch *et al.*, 2004).

If one seeks a non-hydrostatic generalization of an oceanic simulation code for smaller, faster dynamical phenomena, the Boussinesq approximation offers a major simplification by excluding dynamic pressure from EOS, which allows a decomposition of pressure into hydrostatic free-surface, hydrostatic baroclinic, and non-hydrostatic components that then can be treated in quasi-independent ways (*e.g.*, Kanarska *et al.*, 2007). For hydrostatic codes, the simplifications due to Boussinesq approximation are somewhat less pronounced (besides the logistical efficiency of not having to compute ρ-weighted control volumes) which leads to the conclusion that Boussinesq approximation is not useful at all, because one can solve an non-approximated system instead (*e.g.*, de Szoeke & Samelson, 2002; Marshall *et al.*, 2004). Still, there are fewer feedback loops and interdependencies among the the model equations in the Boussinesq case, and accordingly, fewer decisions about numerical splittings are to be made. In this and previous studies we have described generally successful treatment of computationally delicate couplings between mode-splitting, time-stepping, and realistic EOS algorithms in a Boussinesq code with accurate, numerically stable and efficient mode-splitting procedure without the necessity of excessive time filtering, with tracer conservation and constancy preservation and with acceptable EOS-related errors in the PGF. In this section we examine how these coupling issues are manifested in a non-Boussinesq algorithm like the ones presently used (*e.g.*, in MOM4; Griffies, 2004) and suggest some directions for further non-Boussinesq model improvements.

Realistic oceanic simulation brings two particular issues that are outside the standard consideration of the Boussinesq approximation: the free surface ζ and the necessity to reintroduce compressibility and pressure into EOS in order to obtain a correct description of the thermobaric effect and other EOS-related nonlinearities. These issues raise subtle questions, most importantly whether to use the full dynamic pressure P in EOS or approximate it with, *e.g.*, the reference value $P_0 = -\rho_0 g z$; the classical Boussinesq does not offer any guideline. Dewar *et al.* (1998) found that there is a quantitatively significant sensitivity to this choice and advocated the use of full dynamic pressure in EOS computed self-consistently between ρ and P related by hydrostatic balance. Dukowicz (2001) pointed out the error discovered by Dewar *et al.* (1998) is self-canceling in a non-Boussinesq model, because the pressure gradient and density are essentially multiplied by a common multiplier, and the modification proposed by Dewar *et al.* (1998) actually *brings error* into the Boussinesq code they used [10] [see also Sec. 2 following (2.11)]. Dukowicz (2001) proposed to correct the PGF error while keeping both the Boussinesq approximation and the the use of reference pressure in EOS by stiffening the latter [11]. However, his approach received limited support. At first, because of the alternative proposal to reinterpret Boussinesq velocity as normalized mass flux per unit area $\rho \mathbf{u}/\rho_0$ as described by McDougall *et al.* (2002) [12] They advocate full P in EOS and demonstrated that no EOS stiffening is required

[10] Although Dewar *et al.* (1998) did not explicitly identify in their formulas that they used a Boussinesq code, this choice is evident from their Footnote 2, which discusses non-existence of sound waves and the absence of a time derivative in the continuity equation, as well as from the general context of the MOM2 code available at that time, which they used.

[11] Note that while Dukowicz (2001) suggests using *both* reference pressure $P_0 = -\rho_0 g z$ in EOS and stiffening of EOS at the same time, *either* measure taken alone is sufficient to solve the Case A dilemma of Dewar *et al.* (1998) in a Boussinesq model, *cf.*, (2.11). However both measures are needed in the more general baroclinic case.

[12] It is interesting to note that the idea of increasing/decreasing velocities depending on local density to elimi-

to obtain correct geostrophically-balanced flow. A side effect of their approach is that it disturbs the relationship between Coriolis and advection terms, which interferes with the derivation potential vorticity conservation even in the simplest case of barotropic, but slightly compressible fluid with free surface (Appendix A). Secondly, by noting that in a hydrostatic model it is actually not very difficult to compute density via EOS using *in situ* pressure self-consistent with the density being computed [13], therefore negating one of the starting arguments of Dukowicz (2001). The third reason for little interest in Dukowicz (2001) comes from the realization that a free-surface, hydrostatic oceanic code can be relatively easy converted from Boussinesq to non-Boussinesq by replacing the discretized vertical volume factor $\rho_0 \Delta z$ to $\rho \Delta z$ (Greatbatch *et al.*, 2001), or by noting that non-Boussinesq equations can be transformed into pressure coordinates where they resemble Boussinesq written in z-coordinates (de Szoeke & Samelson, 2002; Huang & Jin, 2002; Losch *et al.*, 2004; Marshall *et al.*, 2004). Non-Boussinesq model requires the use of full dynamic P in the fully compressible, realistic EOS: otherwise it would reintroduce the error pointed out by Dewar *et al.* (1998). This is natural and requires no extra effort in pressure coordinates (in fact, it is impossible to separate "coordinate" pressure, which is also dynamic pressure from EOS pressure), but a special effort should be taken if using approach of Greatbatch *et al.* (2001). The use of dynamic P does not reintroduce acoustic waves because they are excluded by the hydrostatic approximation alone.

What remains somewhat unsettled in the literature is that the choice of using reference $-\rho_0 g z$ vs. full pressure P in EOS is not arbitrary, but should be tied to whether the model is Boussinesq or not. Thus, following the advice of Dewar *et al.* (1998), Losch *et al.* (2004, Sec. 2*a. Initialization*) advocate the use of P in EOS for *both* Boussinesq and non-Boussinesq versions of MITgcm they have compared and criticize Huang & Jin (2002) for doing it otherwise (P for non-Boussinesq and z for Boussinesq) which is actually a better choice. Similarly, P-dependent EOS appears in Boussinesq equations of Marshall *et al.* (2004), even thought it clearly breaks the completeness of non-Boussinesq-P- – Boussinesq-z-coordinate isomorphism, and changing to z-dependent EOS repairs this without causing any downstream contradiction (*i.e.*, EOS depends on *coordinate* in both cases). The same applies to de Szoeke & Samelson (2002) who in their remark in Sec. 3, p. 2197, left column, indicated Dewar *et al.* (1998) as the reason for this choice. Furthermore, the classical Boussinesq (with pressure-independent EOS) equations have proper potential-to-kinetic energy conversion resulting in total energy conservation. This property is lost if a nonlinear pressure-dependent EOS is introduced into Boussinesq (or anelastic) equations, *cf.,* Ingersoll (2005). Recently Young (2010) showed that to maintain the energetic consistency in the case of non-linear EOS the dynamic part of pressure in EOS *must be excluded*, providing yet another argument for using $-\rho_0 g z$ in EOS in Boussinesq models.

Once this correspondence is respected, the only surviving arguments for EOS stiffening in Boussinesq model are:

- conceptually it brings the model closer to the original Boussinesq physical framework where the only density variations which matter are the ones which contribute to *buoyancy* variations (Oberbeck, 1879, 1888; Boussinesq, 1903, see p. VII, pp. 154-161, and pp. 172-176 there; Mihaljan, 1962). Bulk compressibility does not translate into buoyancy and therefore must be excluded. Ther-

---

nate approximation errors can be traced back to Oberbeck (1888, Sec. II, paragraph (5)) who was interested in explaining steady motions in the atmosphere.

[13] This requires knowledge of the state of free-surface (or bottom pressure in a non-Boussinesq code) which becomes available only *after* the advance of barotropic mode is complete. This obstacle is typically addressed by one-time-step lag of the pressure field in EOS, *e.g.*, Griffies & Adcroft (2008, see Sec. 11.4 there).

mobaric EOS pressure dependency does, hence is to be kept. EOS pressure is decoupled from the dynamic, and becomes basically a function of location (in the classical Boussinesq EOS pressure is constant or not needed at all).

While these guidelines help to simplify theoretical interpretations, they actually have very little practical consequences in the hydrostatic models, and mostly related to the treatment of free surface. This is not surprising, given that in a Boussinesq model the absolute density (as opposite to density perturbation) appears only in the context of free-surface part of pressure gradient term. Our analysis reveals that while bulk compressibility is mainly dynamically passive (Secs. 3.1, 3.3, and 3.4), its re-introduction into a Boussinesq code brings changes which cannot be interpreted as correct physical effects (***e.g.,*** proper decrease of barotropic wave phase speed if compressibility is taken into account; also the appearance artificial multipliers ρ/ρ_0), are dependent on subtle code decisions (***e.g.,*** $\rho_{\mathrm{EOS}}(\Theta, S, -z)$ vs. $\rho_{\mathrm{EOS}}(\Theta, S, \zeta - z)$) and, not surprisingly again, are associated with the barotropic mode (Sec. 3.2). In a nonhydrostatic code these guidelines bring a substantial simplification by allowing decoupling of the non-hydrostatic pressure from buoyant, and treating the former one as Lagrange multiplier to enforce nondivergence;

- as pointed out by Dukowicz (2001), because of nonlinearity of EOS pressure-dependency (only bulk $r(P)$ nonlinearity is of concern for this purpose), remapping $P = P(P^{\bullet})$ via (2.15) results in a more accurate referencing of bulk pressure in comparison with just approximating it with $-\rho_0 g z$. In practice this translates into re-tuning of pressure-related coefficients in z-dependent EOS if they are originally tuned for using *in situ* pressure, but no extra computational cost;
- if, due to specific needs of a particular ocean model, there is a preferred functional form of EOS different from the available standard EOS. Separating the bulk pressure effect from EOS "preconditions" it to the extent that it can be fitted more easily or more accurately with the desired form. Similarly, after identifying that bulk compressibility is dynamically passive, excluding it before computing pressure-gradient terms is preferable over relying on numerical cancellation within the PGF scheme in a sigma-model; and
- all existing mode-splitting algorithms in split-explicit models can be subdivided into two categories:

(*i*) *a-priori* "physicist's" splitting by extracting a shallow-water like "fast" term (for Boussinesq models this is typically, $-gD\nabla_{\perp}\zeta$ or $-(gD/\rho_0)\nabla_{\perp}(\rho_{\mathrm{surf}}\zeta)$, where ρ_{surf} is surface density at surface; and for non-Boussinesq $-(g/\rho_0)p_b\nabla_{\perp}p'_b$ where p_b and p'_b are bottom pressure and its perturbation relatively to static reference) from the vertically-integrated PGF, while the remainder is treated as slow-time "forcing" (***e.g.,*** Berntsen ***et al.,*** 1981; Blumberg & Mellor, 1987; Bleck & Smith, 1990; Killworth ***et al.,*** 1991, see also Sec. 7.7 in Griffies, 2009, for an overview). In this approach no effort is made to take into account the influence of stratification within the terms recomputed during fast-time stepping [14]; and

(*ii*) "mathematical" splittings motivated by the operator-splitting theory, where the fast-time pressure-gradient terms are designed to capture as close as possible (subject to practicality of implementation and cost) the time tendencies of the non-split 3D system. In practice this translates in introduction of a special density-weighting into "fast" terms. The residual "forcing" terms have very minor dependency on the state of free surface field. Higdon & de Szoeke (1997); Hallberg (1997), and SM2005 belong to this category.

Both techniques rely on essentially the same small parameters, notably separation of time scales between the baroclinic and barotropic processes which is ultimately linked to the smallness of density

[14] This influence was noticed and suspected to be the cause of numerical instability by Killworth ***et al.*** (1991, see Eq. (31) and the discussion in Sec. 3 *c. Coupling between modes* there).

perturbations, however the second captures the leading-order corrections due to non-uniform density and treats them as "fast", while the first one keeps them within "forcing". Naturally, algorithms from the second category produce more accurate splitting (second- vs. first-order errors with respect to the associated small parameters) and require less fast-time filtering for the numerical stability. However, they are also tend to be more code-specific, and, more importantly, none of the available to date is designed to be compatible with fully-compressible EOS [15]. For Boussinesq model like ROMS it is acceptable, if EOS is stiffened. Conversely, re-introduction of bulk compressibility depletes its order of accuracy from the second to the first, thus negating the advantage in splitting accuracy relatively to the first group.

For non-Boussinesq models with fully compressible EOS a splitting algorithm comparable in accuracy with that of Higdon & de Szoeke (1997) or SM2005 is yet to be designed: using dynamic P is EOS also means that ζ influences EOS via P, which means that dependency must be somehow reflected within the "fast" terms. Parameter estimate in Sec. 3.2 suggests that the influence of compressibility on barotropic phase speed is at least as large as the influence of stratification, thus neglecting the former would negate any accuracy advantage of Higdon & de Szoeke (1997) or SM2005 in comparison with simple splitting, if fully compressible EOS is used.

5.1 Comparison of discrete time stepping in Boussinesq and non-Boussinesq models

The ROMS time-stepping algorithm guarantees that the following semi-discretized equations hold exactly:

$$\Delta z_k^{n+1} = \Delta z_k^n - \Delta t \cdot \left[\nabla_\perp(\Delta z_k \mathbf{u}_k) + w_{k+1/2} - w_{k-1/2}\right]^{n+1/2} \tag{5.1}$$

$$\Delta z_k^{n+1} = \Delta z_k\left(\Delta z_k^{(0)}, \langle\zeta\rangle^{n+1}\right) = \Delta z_k^{(0)}\left(1 + \langle\zeta\rangle^{n+1}/h\right) \tag{5.2}$$

$$\langle\zeta\rangle^{n+1} = \langle\zeta\rangle^n - \Delta t \cdot \nabla_\perp \left\langle\!\!\left\langle \overline{\mathbf{U}} \right\rangle\!\!\right\rangle^{n+1/2} \tag{5.3}$$

$$\sum_{k=1}^{N} \Delta z_k = h + \zeta \qquad \text{and} \qquad \left\langle\!\!\left\langle \overline{\mathbf{U}} \right\rangle\!\!\right\rangle^{n+1/2} \equiv \left\langle\!\!\left\langle \overline{U}, \overline{V} \right\rangle\!\!\right\rangle^{n+1/2} = \left\{\sum_{k=1}^{N} \Delta z_k u_k\,,\ \sum_{k=1}^{N} \Delta z_k v_k\right\}^{n+1/2} \tag{5.4}$$

$$\Delta z_k^{n+1} q_k^{n+1} = \Delta z_k^n q_k^n - \Delta t \cdot \left[\nabla_\perp\left(q_k \Delta z_k \mathbf{u}_k\right) + q_{k+1/2} w_{k+1/2} - q_{k-1/2} w_{k-1/2}\right]^{n+1/2}, \tag{5.5}$$

where for symbolic simplicity we omit horizontal indices, tracer diffusion terms, and heat and freshwater fluxes at the ocean surface. Δt is the "slow"-time step (for the 3D "baroclinic" mode); time indices n and $n+1$ correspond to slow-time as well; $\nabla_\perp$ is the two-dimensional, horizontal-coordinate divergence operator; Δz_k are the vertical grid-box heights which depend on ζ and are therefore time-dependent and also depend on the horizontal coordinates through ζ and topography; and $q \in \{\Theta, S, ...\}$ is material concentration (tracer). Eq. (5.2) states that Δz_k are computed by perturbing $\Delta z_k^{(0)}$ which correspond to $\zeta = 0$. ROMS uses the specific way of perturbing them given by the rightmost part of (5.2), but in principle it may be by any other choice that satisfies the left condition (5.4) [*e.g.*, the rescaled-height version of the MITgcm (Adcroft & Campin, 2004); an implementation of the coastal coordinate of Stacey *et al.* (1995); and models that allow only the uppermost grid-box to change with

[15] Here we emphasize that although Higdon & de Szoeke (1997) is formally non-Boussinesq, one of their starting assumptions is that barotropic changes in free surface (or bottom pressure) cause proportional changes in thicknesses of each layer. This assumption breaks down if the fluid is compressible.

ζ while keeping all others fixed, as in MOM/POP (Griffies, 2004) and TRIM (Casulli & Cheng, 1992; Rueda *et al.*, 2007)].

In ROMS the barotropic mode is integrated forward explicitly in "fast"-time using much smaller time steps than the rest of the system. A special fast-time-averaging procedure is employed to ensure that the averaged $\langle\zeta\rangle$ and $\left\langle\!\left\langle \overline{\mathbf{U}} \right\rangle\!\right\rangle$ are exactly matched to satisfy the slow-time free-surface equation (5.3). This can be, in principle, replaced with an implicit free-surface algorithm using special precautions (Campin *et al.*, 2004) to ensure that (5.3) is still respected. In either case, once ζ^{n+1} is known, all grid-box heights Δz_k^{n+1} within each vertical column ($k = 1, ..., N$) are slaved to it. This leaves the slow-time continuity equation (5.1) no other role than computing vertical velocity $w_{k+1/2}$, which in this context has the meaning of finite-volume fluxes across the interfaces between vertically-adjacent grid boxes moving with ζ. The compatibility conditions (5.4) ensure that the bottom and top kinematic boundary conditions for vertical velocity computed are satisfied. while there is some freedom in choosing how to compute the flux-variables with time index $n + 1/2$ (***n.b.***, multiple variants of ROMS code exist), two important properties of (5.1)–(5.5) must always be respected: formally substituting $q_k \equiv 1$ into (5.5) turns it into (5.1), and vertical summation of (5.1) results in (5.3). These guarantee that the tracer equations (5.5) have simultaneous conservation and constancy-preservation properties. Eqs. (5.1)-(5.5) are solved explicitly and sequentially (non-iteratively) as described in SM2005: compute r.h.s. terms for the 3D momentum equation; compute forcing (coupling) terms for the barotropic mode; update barotropic variables and their fast-time-averaged values $\langle\zeta, \overline{U}, \overline{V}\rangle$ and $\left\langle\!\left\langle \overline{U}, \overline{V} \right\rangle\!\right\rangle$; update 3D momentum equations and enforce the compatibility conditions (5.4); advance tracer concentrations with (5.5); then roll the procedure over to the next time step. Notice that EOS does not participate anywhere in (5.1)-(5.5); it is needed only at the stage of computing the PGF for the momentum equation. We refer this type of algorithm as a logically-Boussinesq, hydrostatic, free-surface code.

Next, consider the non-Boussinesq version of (5.1)-(5.5):

$$\rho_k^{n+1} \Delta z_k^{n+1} = \rho_k^n \Delta z_k^n - \Delta t \cdot \Big[\nabla_\perp \left(\rho_k \Delta z_k \mathbf{u}_k \right) + \rho_{k+1/2} w_{k+1/2} - \rho_{k-1/2} w_{k-1/2} \Big]^{n+1/2} \tag{5.6}$$

$$\Delta z_k = \Delta z_k \left(\Delta z_k^{(0)}, \zeta \right) \qquad \text{(unchanged)} \tag{5.7}$$

$$\overline{\rho}^{n+1} \left(h + \zeta^{n+1} \right) = \overline{\rho}^n \left(h + \zeta^n \right) - \Delta t \cdot \nabla_\perp \left\langle\!\left\langle \overline{\rho} \overline{\mathbf{U}} \right\rangle\!\right\rangle^{n+1/2} \tag{5.8}$$

where

$$\overline{\rho} = \frac{1}{h+\zeta} \cdot \sum_{k=1}^{N} \Delta z_k \rho_k \qquad \text{and} \quad \sum_{k=1}^{N} \Delta z_k = h + \zeta \tag{5.9}$$

$$\left\langle\!\left\langle \overline{\rho} \overline{\mathbf{U}} \right\rangle\!\right\rangle^{n+1/2} \equiv \left\langle\!\left\langle \overline{\rho} \overline{U},\, \overline{\rho} \overline{V} \right\rangle\!\right\rangle^{n+1/2} = \left\{ \sum_{k=1}^{N} \rho_k \Delta z_k u_k \,,\; \sum_{k=1}^{N} \rho_k \Delta z_k v_k \right\}^{n+1/2} \tag{5.10}$$

$$\begin{aligned} \rho_k^{n+1} \Delta z_k^{n+1} q_k^{n+1} = \rho_k^n \Delta z_k^n q_k^n - \Delta t \cdot \Big[& \nabla_\perp \left(q_k \cdot \rho_k \Delta z_k \mathbf{u}_k \right) + q_{k+1/2} \cdot \rho_{k+1/2} w_{k+1/2} \\ & - q_{k-1/2} \cdot \rho_{k-1/2} w_{k-1/2} \Big]^{n+1/2} \end{aligned} \tag{5.11}$$

$$\rho_k = \rho_{\mathrm{EOS}}(\Theta_k, S_k, P_k) \qquad \text{where} \quad P_k = g \sum_{k'=k+1}^{N} \rho_{k'} \Delta z_{k'} + \frac{1}{2} g \rho_k \Delta z_k \,. \tag{5.12}$$

All vertical integrations are now done with density weighting. Nevertheless, similarly to (5.1)-(5.5), substitution of $q_k \equiv 1$ into (5.11) turns it into (5.6), and the non-Boussinesq free-surface equation (5.8) is derived by vertical summation of (5.1). Because of this, the system conserves mass and the integral

content and constancy for each tracer. In comparison with its Boussinesq counterpart, the new system exhibits a more sophisticated coupling among the equations. The major difficulty is associated with the free-surface equation (5.8): one needs to know $\overline{\rho}^{n+1}$ in advance in order to solve it. But knowing $\overline{\rho}^{n+1}$, hence ρ_k^{n+1}, also requires Θ_k^{n+1} and S_k^{n+1} because ρ_k^{n+1} is related to them through EOS (5.12). Ultimately this precludes a sequential algorithm comparable to that for (5.1)-(5.5).

There are two known approaches to address this dilemma. The first one is by Greatbatch *et al.* (2001) who proposed to break the cyclic dependency by replacing ρ_k^{n+1} and ρ_k^n with their forward-extrapolated values,

$$\rho^{(e)}{}_k^{n+1} = 2\rho_k^n - \rho_k^{n-1} \qquad \text{and, similarly} \quad \rho^{(e)}{}_k^{n} = 2\rho_k^{n-1} - \rho_k^{n-2}\,, \tag{5.13}$$

everywhere throughout (5.6)–(5.12) where they appear in the control volumes. Subsequently this approach was adopted in MOM4 (Griffies, 2004). A similar extrapolation was applied to convert a sigma-coordinate model (Mellor & Ezer, 1995, with credit given to then unpublished work by Greatbatch and Lu). Despite the fact that ρ_k^n is available before the update of (5.6)-(5.12) begins, it cannot be used in $\Delta z_k^n \rho_k^n$, because doing so implies that during the next time step $\rho^{(e)}{}_k^{n+1}$ will be replaced with ρ_k^{n+1} when it becomes available;because $\rho^{(e)}{}_k^{n+1} \neq \rho_k^{n+1}$, this results in loss of mass conservation. With this precaution taken, however, the discrete mass and tracer conservation properties exist in form of

$$\sum_{i,j,k} \Delta\mathscr{A}_{i,j}\Delta z_{i,j,k}^n \left(2\rho_{i,j,k}^{n-1} - \rho_{i,j,k}^{n-2}\right) = \text{const} \qquad \sum_{i,j,k} \Delta\mathscr{A}_{i,j}\Delta z_{i,j,k}^n q_{i,j,k}^n \left(2\rho_{i,j,k}^{n-1} - \rho_{i,j,k}^{n-2}\right) = \text{const}\,, \tag{5.14}$$

where $\Delta\mathscr{A}_{i,j}$ is the horizontal area of grid element i,j. This is not as accurate as mass, heat, and salt content conservation expressed in terms of simultaneous variables (*i.e.*, computed as $\sum \Delta\mathscr{A}_{i,j}\Delta z_{i,j,k}^n q_{i,j,k}^n \rho_{i,j,k}^n$ with $\rho_{i,j,k}^n$ and $q_{i,j,k}^n = (\Theta, S)_{i,j,k}^n$ related by EOS). However (5.14) still guarantees that the associated errors are bounded with no tendency of accumulation with time. Additionally, extrapolation with some weights being negative, as in (5.13), is undesirable if monotonicity properties are required (*e.g.*, near sharp fronts or extreme salinity anomalies associated with river outflows); and, as we will show in the next section, extrapolation (5.13) is a source of mode-splitting error and may cause numerical instability.

The second, and actually more promising approach to address the solvability of (5.6)–(5.12) in the case of a hydrostatic model is to convert them into pressure coordinates, (de Szoeke & Samelson, 2002; Marshall *et al.*, 2004). The principal idea is to note that $\rho_k \Delta z_k$ can be interpreted as vertical pressure increment over grid box Δz_k, hence

$$\rho_k^n \Delta z_k^n = (1/g)\Delta p_k^n \qquad \text{and} \quad \rho_k^{n+1}\Delta z_k^{n+1} = (1/g)\Delta p_k^{n+1}\,, \tag{5.15}$$

after which (5.6)–(5.11) can be rewritten as

$$\Delta p_k^{n+1} = \Delta p_k^n - \Delta t \cdot \left[\nabla_\perp \left(\Delta p_k \mathbf{u}_k\right) + \widetilde{\omega}_{k+1/2} - \widetilde{\omega}_{k-1/2}\right]^{n+1/2} \tag{5.16}$$

$$\Delta p_k = \Delta p_k \left(\Delta p_k^{(0)}, p_b\right) \tag{5.17}$$

$$p_b^{n+1} = p_b^n - \Delta t \cdot \nabla_\perp \langle\langle p_b \overline{\mathbf{u}} \rangle\rangle^{n+1/2} \tag{5.18}$$

where

$$p_b = \sum_{k=1}^{N} \Delta p_k \tag{5.19}$$

$$\langle\!\langle p_b\overline{\mathbf{u}}\rangle\!\rangle^{n+1/2} \equiv \langle\!\langle p_b\overline{u},\, p_b\overline{v}\rangle\!\rangle^{n+1/2} = \left\{\sum_{k=1}^{N} \Delta p_k u_k\,,\ \sum_{k=1}^{N} \Delta p_k v_k\right\}^{n+1/2} \tag{5.20}$$

$$\Delta p_k^{n+1} q_k^{n+1} = \Delta p_k^n q_k^n - \Delta t \cdot \left[\nabla_\perp\left(q_k \Delta p_k \mathbf{u}_k\right) + q_{k+1/2}\widetilde{\omega}_{k+1/2} - q_{k-1/2}\widetilde{\omega}_{k-1/2}\right]^{n+1/2} \tag{5.21}$$

which are isomorphic to their Boussinesq counterparts (5.1)-(5.5) subject to the correspondence between the variables,

$$\begin{aligned} \Delta p_k &\leftrightarrow \Delta z_k \\ p_b &\leftrightarrow D = h + \zeta \\ \widetilde{\omega}_{k+1/2} &\leftrightarrow w_{k+1/2} \end{aligned} \tag{5.22}$$

where p_b is identified as "bottom pressure" – the total weight of water column. Vertical velocity $\widetilde{\omega}_{k+1/2}$ computed from (5.16) has the meaning of mass flux per-unit-area through, generally speaking, moving pressure surface. The kinematic boundary conditions at the bottom and free surface ($\widetilde{\omega} = 0$ at both) are respected automatically because vertical summation of (5.16) yields (5.18). All other variables, $\mathbf{u}_k$, $\overline{\mathbf{u}}$, $q_k = \{\Theta_k, S_k, ...\}$, remain the same in both systems. Neither density ρ_k, nor grid-box heights Δz_k appear anywhere in (5.16)–(5.21), while substitution of $q = const$ into (5.21) converts it into (5.16) which means that simultaneous constancy and conservation of tracers (now in mass-weighted sense) can be achieved independently from EOS as long as the compatibility conditions (5.18)–(5.20) are respected. Another similarity between the non-Boussinesq pressure-coordinate system and its Boussinesq counterpart is that EOS is involved only in computation of horizontal pressure-gradient terms (also stratification and isopycnic slopes for the purpose of subgrid-scale mixing parameterization), but not for density weighting of grid-box heights like in (5.6)–(5.12). However, the role of EOS is reversed: now it is needed to compute grid-box heights, geopotentials $\Phi_{k+1/2}$, and, ultimately, free surface,

$$\Delta z_k = \frac{\Delta p_k}{g} \cdot \alpha_{\rm EOS}(\Theta_k, S_k, P_k)\,, \qquad \Phi_{k+1/2} = g\sum_{k'=1}^{k} \Delta z_{k'} - gh\,, \quad \text{and} \quad \zeta = \frac{\Phi_{N+1/2}}{g}\,. \tag{5.23}$$

The pressure increments Δp_k and EOS pressures P_k above are known as long as p_b is known,

$$\Delta p_k = p_b \cdot \Delta z_k^{(0)}/h \qquad \text{where} \quad \Delta z_k^{(0)} = \Delta z^{(0)}(x,y) = z_{k+1/2}^{(0)}(x,y) - z_{k-1/2}^{(0)}(x,y)\,, \tag{5.24}$$

after which

$$P_k = \frac{P_{k+1/2} + P_{k-1/2}}{2} \quad \text{and} \quad P_{k-1/2} = \sum_{k'=k}^{N} \Delta p_{k'}\,. \tag{5.25}$$

Above $z_{k+1/2}^{(0)} = z_{k+1/2}^{(0)}(x,y)$, $k = 0, 1, ..., N$, such that $z_{1/2}^{(0)} = -h$ and $z_{N+1/2}^{(0)} = 0$ is an *a priori* defined generalized terrain-following coordinate mapping function (*cf.*, Eq. (1.8) from SM2005. Note that in the case of uniform density $\rho = \rho_0$ hence $p_b = \rho_0 g(h + \zeta)$, the generalized pressure-sigma coordinate reverts back to the original z-sigma, Eqs. (1.9)–(1.10) from SM2005).

In summary, the principal distinction between the Boussinesq and non-Boussinesq cases is that the Boussinesq free-surface equation (5.3) entirely belongs to the barotropic mode (hence does not require any mode-splitting decision about which terms are fast and which are slow), while all EOS-related computations occur entirely within the slow mode. This is no longer the case in (5.8) as it appears in the approach of Greatbatch *et al.* (2001). In the pressure-coordinate aproach of de Szoeke & Samelson (2002) the equation for "bottom pressure" p_b, Eq. (5.18) is entirely "fast", however, despite the terminology, the vertically-integrated pressure gradient term cannot be computed from p_b

alone, but requires the knowledge of geopotential heights and free-surface, which in their turn require the use of EOS (5.23). Because EOS is pressure dependent, and pressure-coordinate levels are scaled by p_b (which brings "fast" dependency in EOS), the barotropic system is closed via EOS, which means that in order to develop an efficient and accurate solver mode-splitting unavoidably involves splitting of EOS as well. This is inherently related to the incompleteness of isomorphism associated with free surface: the complete similarity between z-coordinate Boussinesq and pressure-coordinate non-Boussinesq system would be only if both are rigid-lid (de Szoeke & Samelson, 2002, see their Sec. 4), which, in fact, decouples barotropic (i.e., rigid lid) pressure from EOS. In the remainder of Sec. 5 we re-examine known mode-splitting techniques in order to explore the implication for splitting non-Boussinesq ocean models with fully-compressible EOS, while avoiding introduction of additional splitting errors.

5.2 Stability analysis of mode splitting algorithm in Greatbatch et al. (2001)

Using the identity,

$$\overline{\rho}^{n+1}\left(h+\zeta^{n+1}\right)-\overline{\rho}^{n}\left(h+\zeta^{n}\right)\equiv\frac{\overline{\rho}^{n+1}+\overline{\rho}^{n}}{2}\left(\zeta^{n+1}-\zeta^{n}\right)+\left(\overline{\rho}^{n+1}-\overline{\rho}^{n}\right)\left(h+\frac{\zeta^{n+1}+\zeta^{n}}{2}\right),$$

one can introduce fast-and-slow splitting into (5.8) as follows (*cf.*, Eq. (12.56) in Griffies, 2004 [16]):

$$\frac{\overline{\rho^{(e)}}^{n+1}+\overline{\rho^{(e)}}^{n}}{2}\cdot\frac{\partial\zeta}{\partial t}+\frac{\overline{\rho^{(e)}}^{n+1}-\overline{\rho^{(e)}}^{n}}{\Delta t}\cdot(h+\zeta)+\nabla_{\perp}\left(\frac{\overline{\rho^{(e)}}^{n+1}+\overline{\rho^{(e)}}^{n}}{2}\cdot(h+\zeta)\,\overline{\mathbf{u}}\right)=0\,, \quad (5.26)$$

where $\overline{\rho^{(e)}}$ is vertically averaged density computed from (5.13). For the purpose of the subsequent analysis, we discretize the slow-time, but keep fast-time continuous (*i.e.*, assume that barotropic time steps are sufficiently small that the associated discretization errors are negligible in slow-time). Suppose density is computed using the non-approximated EOS with full P. In this case ρ depends on ζ through hydrostatic pressure. This dependency is taken into account within the slow-mode when computing terms containing $\overline{\rho^{(e)}}$, but these terms are kept constant during the barotropic time-stepping.

For further simplicity of analysis, we now restrict ourselves to the situation where density depends on pressure alone (Appendix B). In this case EOS is $\rho=\rho_1+P/c^2$, where $\rho_1=const$ is density at the surface atmospheric pressure, and c is speed of sound. This translates into the vertical profile $\rho=\rho_1 e^{g(\zeta-z)/c^2}$ and

$$\overline{\rho}=\rho_1\left[e^{g(h+\zeta)/c^2}-1\right]\Big/\left[g(h+\zeta)/c^2\right]\approx\rho_1\left[1+g(h+\zeta)/\left(2c^2\right)+...\right]. \quad (5.27)$$

Substituting this into (5.26), assuming a flat bottom at $z=-h=const$, linearizing about the rest state, and using the extrapolation rule (5.13), we obtain

$$\frac{\partial\zeta}{\partial t}+h\nabla_{\perp}\overline{\mathbf{u}}=-\frac{1}{2}\cdot\frac{gh}{c^2}\cdot\frac{{\zeta^{(e)}}^{n+1}-{\zeta^{(e)}}^{n}}{\Delta t}=-\frac{1}{2}\cdot\frac{gh}{c^2}\cdot\frac{2\zeta^{n}-3\zeta^{n-1}+\zeta^{n-2}}{\Delta t}\,. \quad (5.28)$$

[16] The original code of Greatbatch *et al.* (2001) uses leap-frog stepping; later a more advanced, staggered time placement of tracers and momenta was introduced in MOM4. In this approach stepping of tracers and free surface is from n to $(n+1)$th baroclinic step.

This and the barotropic momentum equation (Appendix B),

$$\partial_t \overline{\mathbf{u}} + g\nabla_\perp \zeta = 0\,, \tag{5.29}$$

comprise the barotropic mode. Unlike the more usual situation with splitting in a stratified Boussinesq model, now it is the free-surface equation (5.28) that receives r.h.s. the forcing term from the slow mode, while there is no slow r.h.s. in the momentum equation. Density ρ is still allowed to change due to compressibility, and (5.29) does not imply smallness of density variation in vertical direction.

The solution procedure for (5.28)-(5.29) uses values of ζ at the previous time steps (up to n) to compute the r.h.s. term. (In an oceanic code this happens through EOS.) Using ζ^n and $\overline{u}^n$ at time $t = t_n$ as the initial conditions, advance them using fast-time stepping to $t = t_n + \Delta t$. The final values are accepted as ζ^{n+1} and $\overline{u}^{n+1}$, and the r.h.s. is recomputed in proceeding to the next baroclinic step.

We now demonstrate that this procedure is computationally unstable unless some temporal filtering is employed. Without loss of generality consider a one-dimensional analog of (5.28)-(5.29), which makes it possible to obtain the solution as a sum of left- and right-traveling Riemann invariants:

$$\partial_t \mathfrak{R}^\pm \pm \sqrt{gh}\cdot\partial_x \mathfrak{R}^\pm = \frac{\partial}{\partial t}\left(\zeta \pm \sqrt{\frac{h}{g}}\overline{u}\right) \pm \sqrt{gh}\cdot\frac{\partial}{\partial x}\left(\zeta \pm \sqrt{\frac{h}{g}}\overline{u}\right) = -\frac{1}{2}\cdot\frac{gh}{c^2}\cdot\frac{2\zeta^n - 3\zeta^{n-1} + \zeta^{n-2}}{\Delta t}\,. \tag{5.30}$$

This is just a linear combination of one-dimensional versions of (5.28)-(5.29). $\mathfrak{R}^+$ and $\mathfrak{R}^-$ can be solved for separately as $\mathfrak{R}^+(t_n+\Delta t, x) = \mathfrak{R}^+(t_n, x-\Delta t\sqrt{gh}) + Q^+(t_n+\Delta t, x)$ and $\mathfrak{R}^-(t_n+\Delta t, x) = \mathfrak{R}^-(t_n, x+\Delta t\sqrt{gh}) + Q^-(t_n+\Delta t, x)$, where $Q^\pm(t,x)$ are responses to the r.h.s. forcing in (5.30) with $Q^\pm(t_n, x) = 0$. Consider a Fourier component, $\begin{pmatrix}\zeta\\ \overline{u}\end{pmatrix}^n = (\lambda)^n \begin{pmatrix}\hat\zeta\\ \hat u\end{pmatrix} e^{ikx}$ where the step multiplier λ is not yet known. Ideally, without the errors introduced but numerical discretization, its values should be $\lambda_\pm = e^{\pm ic\Delta t\sqrt{1-e^{-gh/c^2}}}$, hence $|\lambda| = 1$, which corresponds to the finite-time-step phase increments for non-damped left- and right-traveling waves (*cf.*, (B.8) in Appendix B). The phase speed is slightly smaller than that for incompressible fluid. The actual solution of (5.30) is

$$\mathfrak{R}^\pm(t,x) = \lambda^n\left(\hat\zeta \pm \sqrt{\frac{h}{g}}\hat u\right) e^{ik\left(x\mp(t-t_n)\sqrt{gh}\right)} - \frac{1}{2}\frac{gh}{c^2}\hat\zeta\left(2\lambda^n - 3\lambda^{n-1} + \lambda^{n-2}\right)e^{ikx}\cdot\frac{e^{\mp ik(t-t_n)\sqrt{gh}} - 1}{\mp ik(t-t_n)\sqrt{gh}}\,,$$

which after reaching $t = t_{n+1} = t_n + \Delta t$ becomes

$$\mathfrak{R}^\pm(t+\Delta t, x) = \lambda^n\left(\hat\zeta \pm \sqrt{\frac{h}{g}}\hat u\right) e^{ikx}e^{\mp i\alpha} - \frac{1}{2}\epsilon\hat\zeta\left(2\lambda^n - 3\lambda^{n-1} + \lambda^{n-2}\right)e^{ikx}\cdot\frac{e^{\mp i\alpha} - 1}{\mp i\alpha}\,.$$

The quantities $\alpha = k\Delta t\sqrt{gh}$ and $\epsilon = gh/c^2$ have the same meaning as in Appendix B.

Since $\mathfrak{R}^\pm(t+\Delta t, x) = \lambda^{n+1}\left(\hat\zeta \pm \sqrt{\frac{h}{g}}\hat u\right)e^{ikx}$,

$$\lambda\left(\hat\zeta \pm \sqrt{\frac{h}{g}}\hat u\right) = \left(\hat\zeta \pm \sqrt{\frac{h}{g}}\hat u\right)e^{\mp i\alpha} - \frac{1}{2}\epsilon\hat\zeta\left(2 - 3\lambda^{-1} + \lambda^{-2}\right)\cdot\frac{e^{\mp i\alpha} - 1}{\mp i\alpha}\,. \tag{5.31}$$

This pair of equations is homogeneous for $\{\hat\zeta, \hat u\}$, which means that it admits non-trivial solutions only

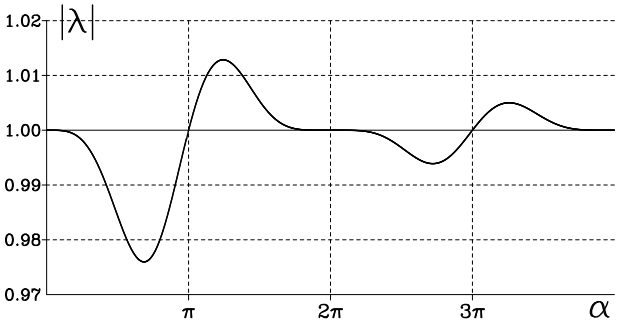

Fig. 3. Absolute value of characteristic roots of (5.32) corresponding to the physical modes as a function of α for $\epsilon = 0.025$, corresponding to $h = 5500$ m and $c = 1500$ ms^{-1}. Because the mode-splitting ratio $\Delta t/\Delta t_{\rm fast}$ is expected to be significantly larger than unity, α is allowed to exceed π, hence entering the range, where barotropic motions are aliased, if sampled with the baroclinic time steps, t_n, t_{n+1}.... Only two periods are shown; the continuation in α is nearly periodic with damping toward $|\lambda| = 1$; $|\lambda| > 1$ means numerical instability.

for the specific values of λ determined by the characteristic equation,

$$\lambda^2 - 2\lambda\cos\alpha + 1 + \frac{1}{2}\epsilon\left(2 - 3\lambda^{-1} + \lambda^{-2}\right)\frac{\sin\alpha}{\alpha} = 0\,. \tag{5.32}$$

The limit of $\epsilon \to 0$ recovers $\lambda = e^{\pm i\alpha}$, and one can also verify that $\lambda \approx e^{\pm i\alpha(1-\epsilon/4)}$ for $\alpha, \epsilon \ll 1$, which matches (B.9) in Appendix B. For large α but still small ϵ, the splitting procedure distorts the amplitude, resulting in a possible numerical instability, $|\lambda| > 1$ (Fig. 3). This mechanism is generic to mode-splitting instability, and it is associated with phase-delay of the slow-time r.h.s. terms — computed only once at the beginning of the fast-time-stepping and kept constant thereafter — relative to the more rapidly changing phase of fast-time terms. Because α has the meaning of phase increment for the barotropic wave during one baroclinic step Δt, α may exceed $\pm\pi$ by several multiples, depending on the mode-splitting ratio. The instability occurs even if the fast- and slow-time algorithms are both stable if taken separately, and even if there is numerical dissipation within the slow-mode algorithm.

The remedy for instability is a more accurate splitting; *i.e.,* eliminate or reduce the ϵ-terms, or to introduce artificial damping in the fast-time-stepping, essentially preventing it from entering into the aliasing range $|\alpha| > \pi$ while still maintaining $|\lambda|$ near unity. In the MOM4 code this is achieved by uniform averaging of both ζ and $\overline{u}$ over a $2\Delta t$ interval, or $1\Delta t$ in the case of staggered time-stepping (Sec. 12.5 of Griffies, 2004). This introduces damping comparable to that of a backward-Euler implicit step and reduces the temporal accuracy to first-order. A gentler fast-time-averaging should take into account this instability mechanism, which is comparable in its strength with that associated with the splitting of PGF terms (items (*iii*) and (*iv*) in Sec. 3.2). Furthermore, because of its specific form of fast-time averaging, MOM4 does not have exact discrete consistency between the averaged free surface and averaged volume or mass fluxes (for the Boussinesq or non-Boussinesq variants) in the slow-time step. Thus, the content conservation or constancy preservation properties for tracer advection cannot be maintained simultaneously, and one must chose between them. The selected choice is constancy, implemented by an auxiliary slow-time step for ζ in Eq. (12.95) of Griffies (2004)). This ζ is then used to compute new-time-step control-volumes for the tracer update but thereafter discarded. The loss of content conservation comes from the fact that the ζ updated this way is not equivalent to that obtained from the barotropic mode, resulting in a difference in control volumes. (Another source of non-conservation is the Robert-Asselin filter needed in the case of leap-frog time-stepping.) The choice of vertical grid that allows a change of only the top-most grid-box height with ζ only (while all others are fixed) results in a slight redistribution of discrete values of density within the vertical column in the case of purely barotropic motions. The existing non-Boussinesq splitting algorithms neglect this effect, which leads to some non-conservation of mass.

Dukowicz' idea factoring of EOS provides a guideline to improve stability and splitting accuracy in (5.26) by moving most of ζ dependency in EOS into the fast mode. Without any approximation EOS can be rewrittem as

$$\rho = r \cdot (\rho_0^\bullet + \rho^{\bullet\prime}) \ , \tag{5.33}$$

where $r = r(\zeta - z)$ chosen to absorb most of the EOS compressibility, but is also simple to compute; $\rho_0^\bullet = const$ is chosen in such that $\rho^{\bullet\prime} \ll \rho_0^\bullet$, and $\rho^{\bullet\prime}$ is only weakly dependent on ζ. With (5.33) only the second parenthetical factor need be extrapolated in time. Then

$$\frac{\partial}{\partial t}\int_{-h}^{\zeta} \rho \, \mathrm{d}z = \frac{\partial}{\partial t}\int_{-1}^{0} \rho \cdot (h+\zeta)\mathrm{d}\sigma = \frac{\partial \zeta}{\partial t}\int_{-1}^{0} (\rho_0^\bullet + \rho^{\bullet\prime}) \left[r + (h+\zeta)\frac{\partial r}{\partial \zeta} \right] \mathrm{d}\sigma + \int_{-1}^{0} r \frac{\partial \rho^{\bullet\prime}}{\partial t}(h+\zeta)\mathrm{d}\sigma \, . \tag{5.34}$$

Choosing $r = e^{g(\zeta - z)/c^2}$ (which in σ-coordinate becomes $r = e^{-\sigma g(h+\zeta)/c^2} = e^{-\sigma\epsilon}$, where c is a representative constant value for speed of sound) converts the above into

$$\underbrace{\frac{\partial \zeta}{\partial t} \cdot \left[\rho_0^\bullet (1+\epsilon) + \int_{-1}^{0} \rho^{\bullet\prime}(1 - 2\sigma\epsilon)\mathrm{d}\sigma \right]}_{\text{“fast”}} + \underbrace{(h+\zeta) \cdot \int_{-1}^{0} \frac{\partial \rho^{\bullet\prime}}{\partial t}(1-\sigma\epsilon)\mathrm{d}\sigma}_{\text{“mostly slow”}} \tag{5.35}$$

where we have expanded $r = e^{-\sigma\epsilon} \approx 1 - \sigma\epsilon + ...$ for $\epsilon \ll 1$.

Even in the simplest case of barotropic compressible fluid, $\rho = \rho_1 + P/c^2$ (hence $\rho_0^\bullet = \rho_1$ and $\rho^{\bullet\prime} \equiv 0$) the expression inside $[...]$ in the "fast" term is not equivalent to vertically averaged density $\overline{\rho}$ – as follows from (5.27) $\overline{\rho} = \rho_1(1+\epsilon/2)$ in this case instead of $\rho_1(1+\epsilon)$. This non-equivalence leads to the replacement of (5.28) with

$$(1+\epsilon)\, \partial_t \zeta + (1+\epsilon/2)\ h\, \nabla_\perp \overline{\mathbf{u}} = 0 \, , \tag{5.36}$$

which in combination with (5.29) yields the correct barotropic phase speed in agreement with (B.9). Unlike (5.28) the above does not have any r.h.s. at all, hence produces no splitting error.

In the general case of $\rho^{\bullet\prime} \neq 0$, splitting (5.35) requires forward extrapolation of $\rho^{\bullet\prime}$ as in (5.13) with subsequent computation of the two-dimensional fields,

$$\overline{\rho^{\bullet\prime}} = \int_{-1}^{0} \rho^{\bullet\prime}\mathrm{d}\sigma \quad \text{and} \quad \widehat{\rho^{\bullet\prime}} = -2\int_{-1}^{0} \rho^{\bullet\prime}\sigma \, \mathrm{d}\sigma \, , \tag{5.37}$$

with their discretized formulas [17] ,

$$D = \sum_{k=1}^{N} \Delta z_k \, , \quad \overline{\rho^{\bullet\prime}} = \frac{1}{D}\sum_{k=1}^{N} \Delta z_k \rho_k^{\bullet\prime} \, , \qquad \widehat{\rho^{\bullet\prime}} = \frac{2}{D^2}\sum_{k=1}^{N} \left\{ \Delta z_k \left(\frac{\Delta z_k}{2} + \sum_{k'=k+1}^{N} \Delta z_k' \right) \rho_k^{\bullet\prime} \right\} \, . \tag{5.38}$$

With (5.35), the non-Boussinesq nonlinear free-surface equation is

[17] These sums do not rely on a particular structure of the vertical coordinate and are self-normalizing in the sense that substituting $\rho_k^{\bullet\prime} \equiv 1$ yields $\overline{\rho^{\bullet\prime}} = \widehat{\rho^{\bullet\prime}} = 1$. Even though Δz_k depends on ζ, the resulting $\overline{\rho^{\bullet\prime}}$ and $\widehat{\rho^{\bullet\prime}}$ are only weakly dependent through EOS pressure, but the ζ-dependency through Δz_k cancels out (*cf.*, Eq. (3.23) in SM2005). This makes it possible to use the most recently available Δz_k to compute $\overline{\rho^{\bullet\prime}}$ and $\widehat{\rho^{\bullet\prime}}$.

$$\left[\rho_0^\bullet + \overline{\rho^{\bullet\prime}} + \left(\rho_0^\bullet + \widehat{\rho^{\bullet\prime}}\right) g\frac{h+\zeta}{c^2}\right] \cdot \frac{\partial \zeta}{\partial t} + \nabla_\perp \left[\left(\rho_0^\bullet + \overline{\rho^{\bullet\prime}} + \left(\rho_0^\bullet + \widehat{\rho^{\bullet\prime}}\right) g\frac{h+\zeta}{2c^2}\right)(h+\zeta)\overline{\mathbf{u}}\right] = -(h+\zeta)\left[\frac{\partial \overline{\rho^{\bullet\prime}}}{\partial t} + \frac{\partial \widehat{\rho^{\bullet\prime}}}{\partial t} g\frac{h+\zeta}{2c^2}\right], \tag{5.39}$$

where we back-substituted $\epsilon = g(h+\zeta)/c^2$ to expose all ζ dependencies. The most accurate (but also the most complicated) time-splitting procedure precomputes the r.h.s. time derivatives of $\overline{\rho^{\bullet\prime}}$ and $\widehat{\rho^{\bullet\prime}}$ using slow-time variables, and keeps them constant during barotropic time-stepping, while all ζ-terms, including the ones in $g(h+\zeta)/c^2$ in both l.h.s. and r.h.s., are allowed to change at every barotropic step. The splitting error of this algorithm can be estimated as $\mathcal{O}\left(\epsilon^2\right)$ and $\mathcal{O}\left(\epsilon \cdot \Delta\left(c^2\right)/c^2\right)$. It does not rely on the smallness of $\rho^{\bullet\prime}/\rho_0^\bullet$. This algorithm replaces (5.14) with

$$\begin{aligned}
&\sum_{i,j,k} \Delta\mathscr{A}_{i,j} \Delta z^n_{i,j,k} r^n_{i,j,k} \left(\rho_0^\bullet + 2\rho^{\bullet\prime n-1}_{i,j,k} - \rho^{\bullet\prime n-2}_{i,j,k}\right) = \text{const} \\
&\sum_{i,j,k} \Delta\mathscr{A}_{i,j} \Delta z^n_{i,j,k} q^n_{i,j,k} r^n_{i,j,k} \left(\rho_0^\bullet + 2\rho^{\bullet\prime n-1}_{i,j,k} - \rho^{\bullet\prime n-2}_{i,j,k}\right) = \text{const}\,.
\end{aligned} \tag{5.40}$$

These are closer to the simultaneous-field conservation laws since $r^n_{i,j,k}$ is computed using the same ζ as used to compute $\Delta z^n_{i,j,k}$ and all ζ-terms in (5.39) evolve in fast-time with r evolving synchronously with ζ without any splitting.

A simplified, but slightly less accurate procedure for (5.39) can be devised by precomputing $\widehat{\rho^{\bullet\prime}} g(h+\zeta)/c^2$-terms at the beginning of barotropic stepping using ζ^n and combining them with $\rho_0^\bullet + \overline{\rho^{\bullet\prime}}$. This admits additional $\mathcal{O}\left(\epsilon \cdot \zeta/h \cdot \rho^{\bullet\prime}/\rho_0^\bullet\right) = \mathcal{O}\left(g\zeta/c^2 \cdot \rho^{\bullet\prime}/\rho_0^\bullet\right)$-errors (definitely negligible in any practical case). Finally, precomputing $\rho_0^\bullet g(h+\zeta)/c^2$ using ζ^n brings $\mathcal{O}\left(\epsilon \cdot \zeta/h\right) = \mathcal{O}\left(g\zeta/c^2\right)$ errors. This is only marginally more computationally demanding than the nonlinear analog of (5.28). Even in this case the splitting is more accurate than (5.28), which admits $\mathcal{O}\left(\epsilon\right)$ error. However, these simplifications cause loss of synchronization between $r^n_{i,j,k}$ and $\Delta z^n_{i,j,k}$, resulting in some compromising of the conservation properties (5.40).

Splitting of PGF terms in the non-Boussinesq case follows Sec. 3.2 using EOS (5.33). The multiplier r can be moved outside the pressure gradient operator (2.14) and furthermore can be separated from the influence of ζ via (3.10). This means that ρ_* and $\overline{\rho}$ are now expressed entirely in terms of $\rho_0^\bullet$ and $\overline{\rho^{\bullet\prime}}$, so the difference from the Boussinesq model is in the appearance of r-terms as a multiplier in the PGF when the momentum equations are rewritten in conservation form.

5.4 An overview of mode-splitting algorithms in non-Boussinesq models

Regardless of the type of vertical coordinate, vertical integration of non-Boussinesq momentum and mass-conservation equation yields,

$$\begin{aligned}
&\frac{\partial}{\partial t}\left(\overline{\rho} D \overline{\mathbf{u}}\right) + \underbrace{g\left[\nabla_\perp\left(\frac{\rho_* D^2}{2}\right) - \overline{\rho} D \nabla_\perp h\right]}_{=-\mathscr{F}} = \text{advection, Coriolis, dissipation, forcing terms} \\
&\partial_t\left(\overline{\rho} D\right) + \nabla_\perp\left(\overline{\rho} D \overline{\mathbf{u}}\right) = \text{fresh-water flux}
\end{aligned} \tag{5.41}$$

where $D = h + \zeta\,, \quad \overline{\rho} = \dfrac{1}{D}\int_{-h}^{\zeta} \rho\,\mathrm{d}z\,, \quad \rho_* = \dfrac{2}{D^2}\int_{-h}^{\zeta}\int_{z'}^{\zeta} \rho\,\mathrm{d}z'\mathrm{d}z\,, \quad \overline{\mathbf{u}} = \dfrac{1}{\overline{\rho}D}\int_{-h}^{\zeta} \rho\mathbf{u}\,\mathrm{d}z$ are the total depth of water-column, vertically-averaged density, vertically-averaged "dynamic" density [both are the same as in (3.19)], and vertically-averaged density-weighted velocity, respectively. The derivation of pressure-gradient term in this form can be found in Sec. 3.1 of SM2005, up to Eq. (3.15), with the only difference is that $\overline{\rho} \to \rho_0$ in terms containing time derivatives and in the definition of $\overline{\mathbf{u}}$ if Boussinesq approximation is applied. Analogous derivations, but expressed in terms Montgomery potential can be found in Higdon & de Szoeke (1997, see their Sec. 2.1, note the appearance of triangular sum in the second unnumbered equation following (2.11) there), and also in Hallberg (1997). The above can be rewritten in terms of bottom pressure, $p_b \equiv g\overline{\rho}D$,

$$\begin{aligned} \frac{\partial}{\partial t}\left(p_b\overline{\mathbf{u}}\right) + \underbrace{g\left[\nabla_\perp\left(\frac{\rho_*}{\overline{\rho}}\cdot\frac{p_b(h+\zeta)}{2}\right) - p_b\nabla_\perp h\right]}_{=-\mathscr{F}} &= \ldots \\ \partial_t p_b + \nabla_\perp\left(p_b\overline{\mathbf{u}}\right) &= \ldots \end{aligned} \tag{5.42}$$

where the new prognostic variable p_b is more natural for non-Boussinesq models because it appears as a single prognostic variable under time derivative in the second equation, however, the presence of ζ in PGF terms separately from $\overline{\rho}$ or p_b cannot be eliminated completely. It should be noted that despite the common meaning $\mathscr{F}$'s have different dimensions in (3.14), (5.41) and (5.42) – relatively to (5.41), $\mathscr{F}$ is divided by ρ_0 in (3.14) and is multiplied by an extra g in (5.42). Nevertheless, for notational simplicity we retain the same symbol $\mathscr{F}$ for all versions, and, consistently with SM2005 and with (3.15) in Sec. 3.2, we choose the sign of $\mathscr{F}$ as it appears in the r.h.s. of barotropic momentum equations, hence negative sign in (5.41) and (5.42).

Mode-splitting requires decomposition of vertically integrated PGF into

$$\mathscr{F} = -g\,[\ldots] = \text{"fast"} + \text{"slow"} \tag{5.43}$$

where "fast" term can be efficiently computed from either p_b, $\overline{\rho}D$, or ζ field – whichever plays role of prognostic variable in the barotropic continuity equation, while "slow" must be made as weakly dependent as possible from this variable. The inherent dilemma in (5.41) and (5.42) is that while $\overline{\rho}D$ or p_b/g may be considered as a single variable, in the general case of compressible fluid changes in p_b translate in changes in *both* free surface ζ (hence changing D) and $\overline{\rho}$ (via dependency from pressure through EOS). In pressure-based coordinated, knowing p_b means that the distribution of pressure throughout the water column is known, so one can use EOS to compute specific volumes at each grid box, after which grid-box heights become known as well. Vertical summation of heights yields D, and therefore free surface $\zeta = D - h$. However, this would work only if there is no mode splitting, because it involves using EOS to compute a 3D field, and EOS depends on p_b, which changes in fast time. Therefore a computationally efficient time-split model should employ some sort of approximation to allow computation of ζ via p_b in fast time solely from two-dimensional barotropic fields. The second aspect is that in the presence of stratification and non-uniform topography $\mathscr{F}$ consists parts which tend to cancel each other, so any splitting which disregards this balance is doomed to be inaccurate.

SM2005 (*cf.*, Eq. (3.15) there) addressed the latter issue by canceling the large terms by hand, first

by rewriting the upper equation (5.41) as

$$\partial_t \left(\overline{\rho} D \overline{\mathbf{u}}\right) + gD \left\{ \rho_* \nabla_\perp \zeta + \frac{D}{2} \nabla_\perp \rho_* + \left(\rho_* - \overline{\rho}\right) \nabla_\perp h \right\} = ... \tag{5.44}$$

and, subsequently, substituting $D = h + \zeta$ into $gD\{...\}$ term and separating terms which depend on ζ from those which do not. The resultant ζ-dependent part is given by (3.18) [In SM2005 this is $\mathscr{F} = \mathscr{F}^{(0)} + \mathscr{F}'$ decomposition via Eqs. (3.31)–(3.32) there.] In the Boussinesq case this is all what is needed because ζ is also prognostic variable of the barotropic continuity equation because of the $\overline{\rho} \to \rho_0$ replacement in terms with time derivatives, hence $\partial_t \left(\overline{\rho} D\right) \to \partial_t \left(\rho_0 D\right) = \rho_0 \partial_t \zeta$. In doing so it is also assumed that both $\overline{\rho}$ and ρ_* are independent of ζ, which in its turn imposes two restrictions: (*i*) either exclusion of ζ from EOS pressure, or incompressibility of EOS; and (*ii*) specific functional dependency of how vertical coordinate system is adjusted by changes in free-surface – proportional stretching.

The same two issues must be dealt with in the non-Boussinesq case using bottom pressure instead of free surface. A "physicist's" split extracts the $-g p_b \nabla_\perp \zeta$ term [18] from the PGF term in (5.42),

$$\begin{aligned} \mathscr{F} = -g \left[\nabla_\perp \left(\frac{\rho_*}{\overline{\rho}} \cdot \frac{p_b (h+\zeta)}{2} \right) - p_b \nabla_\perp h \right] = -g p_b \nabla_\perp \zeta - g \nabla_\perp \left[\left(\frac{\rho_*}{\overline{\rho}} - 1 \right) \cdot \frac{p_b (h+\zeta)}{2} \right] \\ - \frac{1}{2} g \Big[p_b \nabla_\perp (h+\zeta) - (h+\zeta) \nabla_\perp p_b \Big] . \end{aligned} \tag{5.45}$$

Then, utilizing the fact density variations are small relative to its mean value, p_b is dominated by bulk part which does not change in time, so it is convenient to split p_b into its reference value and anomaly, which in the simplest case [19] are

$$\begin{aligned} \rho &= \rho_0 + \rho' \qquad & \rho' &\ll \rho_0 \\ p_b &= \rho_0 g h + p'_b \qquad & p'_b &\ll \rho_0 g h \end{aligned} \tag{5.46}$$

after which (5.45) can be rewritten as

$$\begin{aligned} \mathscr{F} = -g p_b \nabla_\perp \zeta \; - \; g \nabla_\perp \left[\left(\frac{\rho_*}{\overline{\rho}} - 1 \right) \cdot \left(\frac{\rho_0 g h^2}{2} + \frac{p'_b + \rho_0 g \zeta}{2} h + \frac{p'_b \rho_0 g \zeta)}{2} \right) \right] \\ - \; \frac{1}{2} g \underbrace{\Big[(p'_b - \rho_0 g \zeta) \nabla_\perp h - h \nabla_\perp (p'_b - \rho_0 g \zeta) + p'_b \nabla_\perp \zeta - \zeta \nabla_\perp p'_b \Big]}_{=0, \quad \text{if} \quad \zeta = p'_b / (\rho_0 g)} \end{aligned} \tag{5.47}$$

so far without any approximation. This still needs a relationship to translate p_b into ζ within the barotropic mode (hence using barotropic variables alone) in order to close the system. In the simplest case it is approximated as

$$\zeta = p'_b / (\rho_0 g) \, , \tag{5.48}$$

[18] This particular form is motivated by the PGF term of a barotropic layer of compressible fluid, see Appendix B, Eq. (B.2), note the mutual placement of p_b and ζ.

[19] A more elaborate decomposition involves using reference profile for density (specific volume) instead of constant value can be found in Appendix B of de Szoeke & Samelson (2002).

which turns (5.42) into

$$\begin{aligned}
&\frac{\partial}{\partial t}\left(p_b\overline{\mathbf{u}}\right)+\underbrace{g\left(\rho_0 gh+p_b'\right)\nabla_\perp\frac{p_b'}{\rho_0 g}}_{\text{“fast”}}=-\underbrace{g\nabla_\perp\left[\left(\frac{\rho_*}{\overline{\rho}}-1\right)\cdot p_b' h\right]}_{\text{“mixed”}}-\underbrace{g\nabla_\perp\left[\left(\frac{\rho_*}{\overline{\rho}}-1\right)\frac{\rho_0 gh^2}{2}\right]}_{\text{baroclinic, “slow”}}+...\\
&\partial_t p_b'+\nabla_\perp\Big(\left(\rho_0 gh+p_b'\right)\overline{\mathbf{u}}\Big)=...\,,
\end{aligned}\tag{5.49}$$

where dots (...) in the first equation indicate other slow terms, such as advection, Coriolis, forcing, viscous dissipation terms, as well as minor 3D correction terms in pressure-gradient associated with the fact that (5.48) is only approximately match the actual free surface as it is computed by the 3D mode using the actual EOS. Typically only the “fast” term is recomputed at every barotropic time step, while all other terms are computed by the 3D mode and play the role of 3D→2D forcing. The particular form of “fast” term as in (5.49) appears in Griffies & Adcroft (2008, see Eqs. (182)-(183)); also Griffies (2009, see Sec. 7.7.4, Eqs. (7.137)-(7.139) there). A similar approach of considering perturbation p_b' relative to a statically-defined rest-state reference field, with subsequent approximate closure to compute geopotential was taken by Marshall *et al.* (2004, see Eq. (27) and the two paragraphs after it, Eqs. (40)-(42), and, finally, $\Phi_l=-b_s r_s$ at the end of Sec. 3a) for an atmospheric model. The actual codes do not compute “slow” and “mixed” terms literally as in (5.49), but instead compute the full baroclinic 3D PGF term using an appropriate scheme and integrate it vertically. Since there is no use for $\overline{\rho}$ and ρ_* within the fast term, there is no need to compute them as well, however we explicitly include all the terms in r.h.s. of (5.49) to facilitate the error analysis.

Neglecting all terms except “fast” yields $\sqrt{gh}$ for the phase speed of external waves. Unlike in the Boussinesq case, it does not depend on the choice of ρ_0 and it should not in non-Boussinesq models. Although this is mainly correct, three effects are not captured: the slowdown of barotropic speed due to bulk compressibility (Appendix B), stratification (Appendices C,D), and topographic coupling between free-surface and stratification if $\nabla_\perp h\neq 0$ (*cf.*, the second line in Eq. (3.32) in SM2005). As all three effects are present in the 3D mode, and are also depend on the fast variables, the differences contribute to mode-splitting error. The “mixed” term is baroclinic because it vanishes if density is uniform due to $\left((\rho_*/\overline{\rho})-1\right)\to 0$, but it also contains p_b' which evolves in fast time. This term is mainly responsible for baroclinic slowdown (recall that $\rho_*<\overline{\rho}$ for positively stratified fluids) and for topographic coupling, if $h\neq const$. It should also be noted that in the case of compressible fluid the ratio $\rho_*/\overline{\rho}$ also depends on on ζ and p_b' due to pressure dependency in EOS, so the “slow” term also contains some traces of p_b'-dependency. The accuracy of this split relies on the following smallnesses:

$$\left|\frac{\rho_*}{\overline{\rho}}-1\right|\ll 1\,,\qquad\qquad \left|\frac{\overline{\rho}-\rho_0}{\overline{\rho}}\cdot\nabla_\perp h\right|\ll 1\,,\qquad\qquad \frac{gh}{c^2}\ll 1 \tag{5.50}$$

and mode-splitting error has terms proportional of each of the three. One of the main difficulties specific to the non-Boussinesq case is the definition of the reference state for p_b: while (5.46) by itself is merely a variable change and does not constitute any approximation, (5.46) in combination with (5.48) is a rather strong assumption: free-surface elevation ζ computed by 3D mode via EOS does not necessarily agree with (5.48),

$$\zeta=D-h=\frac{p_b}{\overline{\rho}g}-h=\underbrace{h\left(\frac{\rho_0}{\overline{\rho}}-1\right)}_{\text{bias}}+\frac{p_b'}{\overline{\rho}g}\qquad\text{vs.}\qquad\zeta=\frac{p_b'}{\rho_0 g}\,. \tag{5.51}$$

In the case of flat bottom the bias mostly differentiates out from the "fast" term $-gp_b\nabla_\perp\zeta$ leaving only a minor error of $\mathcal{O}\left((\overline{\rho}-\rho_0)\nabla_\perp\zeta\right)$, and mostly cancels out from all other terms in (5.47). However, in the case of non-flat topography the bias does affects the split (hence the second parameter in (5.50)) and is not easy to remove by including the "mostly slow" into the terms recomputed during fast-time stepping: if computed as a part of 3D algorithm, it uses the correct values of free surface, but once treated as fast, there is no other choice than to use an approximate ζ form (5.48). For the same reason it is not easy to modify this algorithm to account for the effect of slower barotropic phase speed due to the influence of stratification within the "fast" term [20] . The other aspect specific to non-Boussinesq case is that for a fully compressible EOS it is no longer possible to interpreted the ratio of $\rho_*/\overline{\rho}$ as purely due to stratification: it is affected by bulk compressibility as well. In the next section we will design a more accurate split which avoids the use of a statically defined reference state altogether.

5.5 Mode splitting using incremental variables: The Boussinesq case

Because the theoretical rationale for splitting the total fluid motion into barotropic and baroclinic modes mainly comes from the orthogonality of wave motions in the case of linearized equations over flat bottom, and, accordingly, virtually all theoretical studies about numerical stability of splitting algorithms are done in the flat-bottom framework, the justification of splitting in the presence of bottom topography is more obscure: while the separation of time scales remains well-defined, the orthogonality principle is no longer valid. Nevertheless, the splitting must be dealt with in the general case of non-flat bottom despite the fact that a complete analysis of numerical stability is no longer possible. SM2005 (and even more so in Sec. 3.2 Shchepetkin & McWilliams (2008)) advance the following principle: the modification of vertically-integrated pressure gradient term by advancing the barotropic mode from 3D time step n to $n+1$ should resemble as close as possible the difference between the original and the new vertically-integrated pressure gradient as it would be computed by the 3D mode using the new free-surface field, but the same baroclinic density distribution. The intuitive rationale for this principle is the presumption that if the barotropic mode drives the barotropic fields toward a new equilibrium when advancing from n to $n+1$, that equilibrium should be disturbed as little as possible during the next time step. The resultant form of the barotropic pressure gradient term coincides with that of Higdon & de Szoeke (1997) in the case of flat bottom (subject to non-Boussinesq to Boussinesq translation), but it also leads to specific form of topography-and-free-surface terms, and practical experience of gaining/loosing stability of the model when switching between treating/not-treating these as "fast" terms.

This leads to an equivalent, but alternative to SM2005 interpretation of the splitting procedure if we rewrite (5.41) in terms of *incremental* variables – basically changes caused by the barotropic mode starting from the initial state corresponding to 3D time step n. Thus we introduce $\delta\zeta = \zeta - \langle\zeta\rangle^n$, and, consequently, substitute

$$\zeta \to \zeta + \delta\zeta \equiv \langle\zeta\rangle^n + \delta\zeta \qquad \text{hence} \quad D \to D + \delta\zeta \equiv h + \langle\zeta\rangle^n + \delta\zeta \tag{5.52}$$

[20] This aspect is somewhat parallel to the initialization issues for pressure-coordinate models, Griffies (2009, see Secs. 7.2, 7.3 there, especially the difficulties with the sigma-pressure model, Sec. 7.3.3.7.)

into (5.41) while algebraically separating all terms containing $\delta\zeta$. The Boussinesq version of it becomes

$$\begin{aligned}\frac{\partial}{\partial t}\Big(\rho_0(D+\delta\zeta)\overline{\mathbf{u}}\Big) - \mathscr{F} + g\,(D+\delta\zeta)\,\nabla_\perp\,(\rho_*\delta\zeta) + g\rho_*\delta\zeta\nabla_\perp\zeta \\ -g\frac{\delta\zeta^2}{2}\nabla_\perp\rho_* + g\,(\rho_*-\overline{\rho})\,\delta\zeta\nabla_\perp h = ... \\ \frac{\partial}{\partial t}\delta\zeta + \nabla_\perp\Big((D+\delta\zeta)\overline{\mathbf{u}}\Big) = ...\end{aligned} \tag{5.53}$$

where now only $\delta\zeta$ and $\overline{\mathbf{u}}$ are changing during the barotropic time stepping (***e.g.,*** ζ is kept constant in fast-time in $g\rho_*\delta\zeta\nabla_\perp\zeta$ – the last term in the first line of the first equation).

The solution procedure is therefore as follows: before starting the barotropic mode the full vertically-integrated pressure-gradient term $\mathscr{F} = -g\left[\nabla_\perp\left(\frac{\rho_* D^2}{2}\right) - \overline{\rho}D\nabla_\perp h\right]$ is precomputed via *the actual* pressure gradient scheme of 3D mode using the state of free-surface at time step n and the predicted or extrapolated density field at $n+1/2$. Note, this is *not equivalent* to computing $\overline{\rho}$ and ρ_* first and then computing $\mathscr{F}$ as suggested by this formula using an ad hoc spatial discretization — when considering continuous equations these two forms are equivalent to each other, but discrete forms they are not. In a sigma-model not exercising proper care here would result in an unacceptable pressure gradient error passed into the barotropic mode. Instead, the precomputed $\overline{\rho}$ and ρ_* are to be used *only* in terms containing $\delta\zeta$. Once all preparations are complete, the barotropic variables are advanced and fast-time averaged,

$$\begin{pmatrix}\delta\zeta = 0 \\ \\ \overline{\mathbf{u}} = \langle\overline{\mathbf{u}}\rangle^n\end{pmatrix} \rightarrow \begin{pmatrix}\langle\delta\zeta\rangle^{n+1} \\ \langle(D+\delta\zeta)\overline{\mathbf{u}}\rangle^{n+1} \\ \langle\!\langle(D+\delta\zeta)\overline{\mathbf{u}}\rangle\!\rangle^{n+1/2}\end{pmatrix} \rightarrow \begin{pmatrix}\langle\zeta\rangle^{n+1} = \langle\zeta\rangle^n + \langle\delta\zeta\rangle^{n+1} \\ D^{n+1} = h + \langle\zeta\rangle^{n+1} \\ \langle\overline{\mathbf{u}}\rangle^{n+1} = \dfrac{\langle(D+\delta\zeta)\overline{\mathbf{u}}\rangle^{n+1}}{D+\langle\delta\zeta\rangle^{n+1}}\end{pmatrix} \tag{5.54}$$

where, obviously, the initial state for $\delta\zeta = 0$, and the right-most operations symbolize setting new state of the "slow" variables, which are also used as the initial state for the barotropic mode during the next 3D time step.

In comparison with (3.18) the incremental form (5.53) completely "hides" the baroclinic-topographic hydrostatic balance into the 3D term. Assuming spatially uniform free surface, hence setting $\zeta = const \neq 0$ in (3.18) turns it into $-g\zeta\,[(h+\zeta/2)\nabla_\perp\rho_* + (\rho_*-\overline{\rho})\,\nabla_\perp h]$. It must vanish in the case of horizontally uniform (flat) stratification. However its vanishing requires cancellation of the two terms inside square braces [.] because in the presence of topography flat stratification results in non-uniform $\overline{\rho}$ and ρ_*. The incremental form (5.53) ensures this cancellation for any $\zeta = const$ (not necessarily $\zeta = 0$) as long as the vertically integrated pressure gradient term computed by 3D mode vanishes: recall that 3D computing of pressure gradient term is inherently more accurate that via $\overline{\rho}$ and ρ_*. It should also be noted that smallness of $\delta\zeta/D$ is more justifiable than smallness of ζ/D (or, similarly ζ/h) because in deep areas where phase barotropic speed is large both are small, but comparable, since ζ may change rapidly per time step, if barotropic is running using time step close to the maximum allowed by stability. On the other hand, in shallow areas where free-surface changes may no longer be very small in comparison with depth, the barotropic motions may resolved in 3D time step resulting is smooth changes, hence $\delta\zeta$ is expected to be smaller than ζ. For this reason, if linearization is required, ***e.g.,*** in the case of implicit treatment of free surface using a third-party elliptic solver, the use of $\delta\zeta$ in

(5.53) provides a more natural approach. It should be noted that the most commonly used approach retains only the $gD\nabla_\perp\left(\rho_*\delta\zeta\right)$ term, and usually with ρ_* replaced with ρ_0. Eq. (5.53) suggests two more terms, and notably the very last of the first equation couples stratification with topography and free surface, but still the whole approach yields essentially the same 5-diagonal elliptic equation for $\delta\zeta$.

5.6 Mode splitting using incremental variables: non-Boussinesq case with fully compressible EOS

Another consequence of incremental form (5.53) is that it can be generalized to the case of non-Boussinesq model with compressible EOS. Similarly to (5.52) we introduce incremental variables

$$\begin{aligned}
\overline{\rho}D &\rightarrow \overline{\rho}D + \delta m \\
\zeta \quad &\rightarrow \zeta + \delta\zeta \qquad \text{hence} \quad D \rightarrow D + \delta\zeta \\
\overline{\rho} \quad &\rightarrow \overline{\rho} + \delta\overline{\rho} \\
\rho_* \quad &\rightarrow \rho_* + \delta\rho_*
\end{aligned} \tag{5.55}$$

after which the barotropic continuity equation becomes

$$\frac{\partial}{\partial t}\delta m + \nabla_\perp\Big((\overline{\rho}D + \delta m)\overline{\mathbf{u}}\Big) = ... \tag{5.56}$$

which identifies δm as the natural fast-time prognostic variable.

The incremental form of the non-Boussinesq version of (5.41) can be derived by noting that

$$\begin{aligned}
\nabla_\perp\left(\frac{\rho_* D^2}{2}\right) - \overline{\rho}D\nabla_\perp h \;\equiv\; \nabla_\perp\left(\frac{\rho_*}{\overline{\rho}}\cdot\frac{\overline{\rho}D\cdot D}{2}\right) - \overline{\rho}D\nabla_\perp h \;\rightarrow \\
\rightarrow\; \nabla_\perp\left[\left(\frac{\rho_*}{\overline{\rho}} + \delta\left(\frac{\rho_*}{\overline{\rho}}\right)\right)\cdot\frac{(\overline{\rho}D + \delta m)\cdot(D + \delta\zeta)}{2}\right] - (\overline{\rho}D + \delta m)\,\nabla_\perp h
\end{aligned} \tag{5.57}$$

where, we must provide some the means to compute responses $\delta\zeta$ and $\delta(\rho_*/\overline{\rho})$ to changing δm. Both relationships involve EOS, however they are needed during fast-time stepping, so they must be expressed somehow in terms of 2D fields only.

The principal assumption that at the "slow" time step n the free-surface field ζ and the three-dimensional density are in hydrostatic equilibrium with each other as governed by fully compressible EOS, *e.g.,* given a distribution of masses throughout each vertical column, hydrostatic pressure is computed by integration from surface downward, after which specific volume and height of each grid box is computed via EOS, and vertical summation of grid box heights results in ζ. Once the barotropic mode departs from the state corresponding to time step n, the change in δm results in change of both free surface $\delta\zeta$ and vertically averaged density $\delta\overline{\rho}$ in such a way that the hydrostatic equilibrium is maintained. This means that an increase in δm results in proportional increases in both $\delta\zeta$ and $\delta\overline{\rho}$,

$$\delta\overline{\rho} = \frac{1}{2}\epsilon\cdot\frac{\delta m}{D}\,, \qquad\qquad \delta\zeta = \frac{1 - \dfrac{1}{2}\epsilon}{1 + \dfrac{1}{2}\epsilon\cdot\dfrac{\delta m}{\overline{\rho}D}}\cdot\frac{\delta m}{\overline{\rho}} \approx \left(1 - \frac{1}{2}\epsilon\right)\cdot\frac{\delta m}{\overline{\rho}} \tag{5.58}$$

where the $\frac{1}{2}\epsilon\cdot\frac{\delta m}{\overline{\rho}D}$ term in denominator quadratically small, and is merely to keep

$$\overline{\rho}D+\delta m=(\overline{\rho}+\delta\overline{\rho})(D+\delta\zeta) \tag{5.59}$$

as an exact identity. Above $\epsilon\ll 1$ is effective vertically integrated compressibility parameter computed via EOS. In the simplest case (see Appendix B) $\epsilon=gD/c^2$, where c is speed of sound, resulting in an estimate $\epsilon\approx 0.025$ for deep ocean. In a more general case we assume EOS in form of

$$\rho=r(P)\cdot(\rho_0^\bullet+\rho^{\bullet\prime}(\Theta,S,P)) \tag{5.60}$$

where $\rho_0^\bullet=const$, $\rho^{\bullet\prime}\ll\rho_0^\bullet$, and $\left(\partial\rho^{\bullet\prime}/\partial P\right)\big|_{\Theta,S=const}\ll dr/dP$, so most of pressure effect is absorbed into $r(P)$. Since $\overline{\rho}=\dfrac{1}{D}\displaystyle\int_{-h}^{\zeta}\rho\,\mathrm{d}z=\frac{1}{D}\int_{-h}^{\zeta}r\,(\rho_0^\bullet+\rho^{\bullet\prime})\,\mathrm{d}z=\rho_0^\bullet\cdot\frac{1}{D}\int_{-h}^{\zeta}r\,\mathrm{d}z+\frac{1}{D}\int_{-h}^{\zeta}r\rho^{\bullet\prime}\mathrm{d}z$ it is natural to express

$$\overline{\rho}=\overline{r}\cdot\overline{\rho^\bullet}=\overline{r}\left(\rho_0^\bullet+\overline{\rho^{\bullet\prime}}\right)\qquad\text{where}\qquad\overline{r}=\frac{1}{D}\int_{-h}^{\zeta}r\,\mathrm{d}z\qquad\text{and}\qquad\overline{\rho^{\bullet\prime}}=\frac{1}{\overline{r}D}\int_{-h}^{\zeta}r\rho^{\bullet\prime}\mathrm{d}z\,. \tag{5.61}$$

Change in the total depth of water-column causes proportional stretching of $\rho^\bullet$ profile (hence $\overline{\rho^\bullet}$ is not affected by the change), while in contrast, $r(P)$ profile moves up-and-down with free surface without any stretching at all (since it is function of pressure alone)

$$\delta m=r_{\mathrm{bott}}\rho^\bullet_{\mathrm{bott}}\delta\zeta\approx r_{\mathrm{bott}}\rho_0^\bullet\delta\zeta \tag{5.62}$$

where r_{bott} and $\rho^\bullet_{\mathrm{bott}}$ are bottom values of r and $\rho^\bullet$. On the other hand,

$$\delta m=\left(1-\frac{1}{2}\epsilon\right)\overline{r}\overline{\rho^\bullet}\cdot\delta\zeta\approx\left(1-\frac{1}{2}\epsilon\right)\overline{r}\rho_0^\bullet\cdot\delta\zeta \tag{5.63}$$

which leads to an estimate

$$\epsilon=2\,(1-\overline{r}/r_{\mathrm{bott}})\ . \tag{5.64}$$

In the simplest case of vertically uniform speed of sound r is a linear function of pressure, $\overline{r}=1+\epsilon/2$, *cf.,* (3.22). A more general (5.64) accounts for the nonuniformity of c due to its pressure dependency, leaving aside only the temperature effect in the upper ocean.

The ratio $(\rho_*/\overline{\rho})$ is affected by both compressibility and baroclinicity, so its behavior is controlled by on EOS. Similarly to (5.61),

$$\rho_*=r_*\rho_*^\bullet=r_*\,(\rho_0^\bullet+\rho_*^{\bullet\prime})\ ,\quad\text{where}\quad r_*=\frac{2}{D^2}\int_{-h}^{\zeta}\int_z^{\zeta}r\,\mathrm{d}z'\mathrm{d}z\quad\text{and}\quad\rho_*^{\bullet\prime}=\frac{2}{r_*D^2}\int_{-h}^{\zeta}\int_z^{\zeta}r\rho^{\bullet\prime}\,\mathrm{d}z'\mathrm{d}z\,, \tag{5.65}$$

where r_* can be estimated as $r_*=1+\epsilon/3$ in the case of uniform c, *cf.,* (3.22). Combining the above,

$$\frac{\rho_*}{\overline{\rho}}=\frac{r_*}{\overline{r}}\cdot\frac{\rho_0^\bullet+\rho_*^{\bullet\prime}}{\rho_0^\bullet+\overline{\rho^{\bullet\prime}}}\approx\left(1-\frac{1}{6}\epsilon\right)\cdot\left(1-\frac{\overline{\rho^{\bullet\prime}}-\rho_*^{\bullet\prime}}{\rho_0^\bullet}\right)\,, \tag{5.66}$$

which leads to an estimate of how $(\rho_*/\overline{\rho})$ responds to perturbation in free surface $\delta\zeta$, and δm,

$$\frac{\rho_*}{\overline{\rho}}=\frac{r_*}{\overline{r}}\cdot\frac{\rho_*^\bullet}{\overline{\rho^\bullet}}\ \ \rightarrow\ \ \frac{\rho_*^\bullet}{\overline{\rho^\bullet}}\left(1-\frac{1}{6}\epsilon-\frac{1}{6}\epsilon\cdot\frac{\delta\zeta}{D}\right)\approx\frac{\rho_*^\bullet}{\overline{\rho^\bullet}}\left(1-\frac{1}{6}\epsilon\right)-\frac{1}{6}\epsilon\cdot\frac{\delta m}{\overline{\rho}D} \tag{5.67}$$

where we have neglected quadratically small terms $\mathcal{O}\left(\epsilon^2\right)$ and $\mathcal{O}\left(\epsilon \cdot \dfrac{\overline{\rho^{\bullet\prime}} - \rho_*^{\bullet\prime}}{\rho_0^\bullet}\right)$.

Substitution of (5.58) and (5.67) into r.h.s. of (5.57) turns it into

$$\nabla_\perp \left[\left(\frac{\rho_*^\bullet}{\overline{\rho^\bullet}} \left(1 - \frac{1}{6}\epsilon\right) - \frac{1}{6}\epsilon \frac{\delta m}{\overline{\rho} D} \right) \cdot \frac{(\overline{\rho} D + \delta m) \left(D + \left(1 - \frac{1}{2}\epsilon\right) \frac{\delta m}{\overline{\rho}} \right)}{2} \right] - (\overline{\rho} D + \delta m) \nabla_\perp h \,, \tag{5.68}$$

which, after some algebraic transformation yields

$$\begin{aligned} &\frac{\partial}{\partial t}\Big((\overline{\rho} D + \delta m) \overline{\mathbf{u}} \Big) - \mathscr{F} + g D \nabla_\perp \left[\left(\frac{\rho_*^\bullet}{\overline{\rho^\bullet}} - \frac{1}{2}\epsilon \right) \delta m \right] + g \left(\frac{\rho_*^\bullet}{\overline{\rho^\bullet}} - \frac{1}{2}\epsilon \right) \delta m \nabla_\perp \zeta \\ &\qquad\qquad + g \left(\frac{\rho_*^\bullet}{\overline{\rho^\bullet}} - 1 - \frac{1}{2}\epsilon \right) \delta m \nabla_\perp h \\ &\qquad\qquad + g \nabla_\perp \left[\left(\frac{\rho_*^\bullet}{\overline{\rho^\bullet}} - \frac{5}{6}\epsilon \right) \frac{\delta m^2}{\overline{\rho}} - \frac{1}{6}\epsilon \frac{\delta m^3}{\overline{\rho}^2 D} \right] = \ldots \\ &\frac{\partial}{\partial t} \delta m + \nabla_\perp \Big((\overline{\rho} D + \delta m) \overline{\mathbf{u}} \Big) = \ldots \end{aligned} \tag{5.69}$$

where we have kept terms with all powers of δm, but have dropped all terms with power of ϵ higher than the first, and terms which involve quadratically-small product of ϵ by $(\rho_*^\bullet/\overline{\rho^\bullet} - 1)$.

The entire splitting algorithm is therefore formulated as follows: bottom pressure p_b is considered to be a prognostostic variable, and it evolves in slow time by adding increments $g \cdot \delta m$, which are computed (fast-time averaged) by the barotropic mode. Before starting fast-time stepping of barotropic mode from n to $n+1$ all necessary terms notably the state of free-surface ζ and full vertically integrated PGF terms are precomputed using full 3D algorithms with compressible EOS. Also computed at this stage and kept constant thereafter until the next baroclinic time step are the stiffened density ratios $\rho_*^\bullet/\overline{\rho^\bullet}$ needed by (5.69). After these preparations, the barotropic mode is advanced toward $n+1$,

$$\begin{pmatrix} \delta m = 0 \\ \\ \overline{\mathbf{u}} = \langle \overline{\mathbf{u}} \rangle^n \end{pmatrix} \to \begin{pmatrix} \langle \delta m \rangle^{n+1} \\ \langle (\overline{\rho} D + \delta m) \overline{\mathbf{u}} \rangle^{n+1} \\ \langle\langle (\overline{\rho} D + \delta m) \overline{\mathbf{u}} \rangle\rangle^{n+1/2} \end{pmatrix} \to \begin{pmatrix} \langle p_b \rangle^{n+1} = \langle p_b \rangle^n + g \langle \delta m \rangle^{n+1} \\ \\ \langle \overline{\mathbf{u}} \rangle^{n+1} = \dfrac{\langle (\overline{\rho} D + \delta m) \overline{\mathbf{u}} \rangle^{n+1}}{\langle p_b \rangle^{n+1}/g} \end{pmatrix}, \tag{5.70}$$

where the first column symbolizes setting of initial conditions, the second in time stepping of barotropic mode via (5.69) performing fast-time averaging on the way, and the third column is translation back to slow-time variables [21] .

[21] To prevent the accumulation of roundoff errors it is useful to extract a constant-in-time bulk part from p_b,

$$p_b = p_b^{(0)} + \hat{p}_b \,, \qquad \text{where} \quad p_b^{(0)} = p_b^{(0)}(x,y) = g \rho_0^\bullet \int_{z=-h}^{\zeta=0} r \, \mathrm{d}z \,,$$

and use $\hat{p}_b$ as the prognostic variable in instead of p_b, meaning that the increments $\langle \delta m \rangle^{n+1}$ are added to $\hat{p}_b$ in (5.70), not to p_b. Then, whenever needed, $\langle p_b \rangle^{n+1}$ is computed *afterward* by adding back the bulk part, $\langle p_b \rangle^{n+1} = p_b^{(0)} + \langle \hat{p}_b \rangle^{n+1}$, which can be used everywhere in the code except time differencing and time integra-

The overall structure of (5.69) is similar to its Boussinesq counterpart (5.53) with an obvious one-to-one correspondence between all the terms, with the exception of δm^2- and δm^3-terms in r.h.s. of the first equation (5.69). As expected, (5.69) reverts back to shallow-water equations if $(\rho^\bullet_*/\overline{\rho^\bullet}) \to 1$ and $\epsilon \to 0$. What is essentially new is that in the general case of $\rho^\bullet_*/\overline{\rho^\bullet} \neq 1$ and $\epsilon \neq 0$ linearization of (5.69) around the rest state, $\zeta = \overline{u} = 0$, captures the correct phase speed for the barotropic waves, where *both effects* – slowdown due to stratification (*cf.,* (3.20), also Appendices C and D) and seawater compressibility (*cf.,* (3.21), also Eq. (B.9) from Appendix B.1) – are now accurately represented within the fast mode alone, and the phase speed does not depend on the choice of reference constants such as $\rho^\bullet_0$ – and it should not in non-Boussinesq models. The derivation procedure for (5.69) also illustrates that the contributions due to the two physical effects – baroclinicity and compressibility – cannot be combined into a single effective field: $(\rho^\bullet_*/\overline{\rho^\bullet})$ and ϵ appear in different combinations in r.h.s. of (5.69), so the baroclinic ratio $(\rho^\bullet_*/\overline{\rho^\bullet})$ must be computed from the "stiffened" density field separately from bulk compressibility effect accounted by ϵ. This confirms the assumption made in Sec. 3.2 that the slowdown of barotropic wave speed due to vertical stratification (3.20) can be correctly estimated by the barotropic mode in a Boussinesq model as long as $\overline{\rho}$ and ρ_* in (3.19) are "stiffened". Conversely, using non-stiffened version of them does not yield the correct estimate of influence of compressibility (3.21), not the combination of both effects, resulting in overall incorrect barotropic phase speed.

The case with $\epsilon \equiv 0$ while keeping $\rho^\bullet_*/\overline{\rho^\bullet} \neq 1$ corresponds to "stiffened" non-Boussinesq model. In this case the modification of pressure gradient terms relatively to uniform-density shallow-water equations is controlled entirely by the ratio $\rho^\bullet_*/\overline{\rho^\bullet}$. This is comparable to splitting algorithm of Higdon & de Szoeke (1997); Hallberg (1997), which is also non-Boussinesq, however assuming that all variations of density are solely due to stratification. In terms of complexity and computational cost (while maintaining the same level of mode-splitting errors) this is very similar to the Boussinesq version (5.53): δm and $\delta\zeta$ can be easily related in fast time as $\delta m = \overline{\rho}\,\delta\zeta$, where $\overline{\rho}$ does not change in fast time. This, in principle, makes it possible to express everything directly in the original rather than incremental variables.

Clearly, most of the complexity of (5.69) relative to its Boussinesq counterpart is associated with the bulk compressibility ϵ-terms: because of EOS pressure dependency and, correspondingly, the feedback of the state of free-surface ζ into density distribution, ζ can be accurately computed from bottom pressure p_b only by using full 3D algorithm. Since ζ is needed to compute barotropic-pressure gradient term, a simplified algorithm is needed to express it using 2D variables only during the fast-time stepping. This necessitates approximations which may admit splitting errors. Using incremental variables offers relief: now ζ is computed using full 3D algorithm, but only once per baroclinic time step (at the beginning of fast-time stepping), while it is increment $\delta\zeta$ which is computed using a simplified 2D algorithm [essentially via (5.58) leading to (5.63) and ultimately to (5.69)]. This avoids mode-splitting errors, but brings extra cost associated with the additional terms in (5.69) recomputed at each fast-time step and, an extra 2D field – ϵ – to be computed once and stored. It is essential that EOS compressibility can be split into the bulk and the much smaller residual parts – a property of seawater EOS pointed out by Dukowicz (2001).

---

tion: these must still use $\hat{p}_b$. It can be easily estimated that for typical oceanic conditions $p_b^{(0)}$ is 3 ... 4 orders of magnitude larger than $\hat{p}_b$, while the contrast between $p_b^{(0)}$ and increments $g\langle\delta m\rangle$ is even greater – so the roundoff errors cannot be ignored, even with double precision. However, we emphasize that $\hat{p}_b$ is merely for bookkeeping, and from the mathematical point of view, the splitting algorithm does not rely on the smallness of $\hat{p}_b$ relatively to $p_b^{(0)}$.

5.7 Summary for Boussinesq and non-Boussinesq mode splitting

The preceding analysis shows that the existing non-Boussinesq models essentially rely on the same assumptions as the Boussinesq models, with the relevant smallness parameters estimated as

$$\begin{aligned} \epsilon = \frac{gh}{c^2} &\precsim 0.025\,, & \frac{\Delta\left(c^2\right)}{c^2} &\approx 0.04\,, \\ \frac{\zeta}{h} &\approx 2\times 10^{-4}\ ...\ 0.2\,, & \frac{\rho^{\bullet\prime}}{\rho_0^\bullet} &\approx 0.005\ ...\ 0.01\,, \end{aligned} \tag{5.71}$$

where the extreme parameter values typically do not occur simultaneously which limits the algorithmic error estimates that contain their products. We have assumed a range of values of $c = 1480 - 1540$ since most of this variation is purely due to pressure effect, and therefore can be "absorbed" into r if a nonlinear function of pressure/depth is used. The assumed range of depths varies from mid-ocean to the inner continental shelf. The estimate for $\rho^{\bullet\prime}/\rho_0^\bullet$ (*cf.*, Fig. 1) is significantly smaller than typical values of ρ'/ρ_0 due to stiffening.

The mode-splitting error of the Boussinesq ROMS is estimated as $\mathcal{O}\left((\rho^{\bullet\prime}/\rho_0^\bullet)^2\right)$ with all other parameters (5.71) being irrelevant (see Sec. 3.2). The error increases to the first-order $\mathcal{O}\left(\rho^{\bullet\prime}/\rho_0^\bullet\right)$ if $\overline{\rho}$ and ρ_* in (3.18)-(3.19) are replaced with $\rho_0^\bullet$; and an additional $\mathcal{O}\left(gh/c^2\right)$ error is introduced if a non-stiffened, realistic EOS is used in an *ad hoc* way.

Non-Boussinesq models must use full dynamic pressure in EOS which implies that density (specific volume) within each vertical grid box (or layer in layered model) depends on the state of free surface. At this time we are not aware of any reference where one takes into account the finite compressibility of seawater into the context of mode-splitting – the density field is usually computed using the sate of free surface at the latest available baroclinic step and kept constant during barotropic time stepping from that baroclinic step to the next. This causes mode-splitting errors and, in principle, opens a possibility for the numerical instability either via a mechanism similar to one described in Higdon & Bennett (1996), or in our Sec. 5.2. With some effort, splitting in a non-Boussinesq model can also be made predominantly second-order accurate in sense that the error estimate depends on pair-wise products of parameters (5.71). This can be done in both implementations of non-Boussinesq model – the density extrapolation method of Greatbatch *et al.* (2001) (our Sec. 5.2, following Eq. (5.33)) and if using pressure-based coordinates (Sec. 5.6). The splitting error is essentially avoided by including the $\zeta \rightarrow$ EOS pressure feedback into the fast-time stepping. This is facilitated by factoring EOS in a manner used by Dukowicz (2001), even though it was not originally intended for non-Boussinesq modeling. A complete accounting of all ζ dependencies within the barotropic mode results in a substantial increase in complexity, most likely beyond the point of diminishing return, especially if keeping in mind that a model with stiffened EOS already captures all important physical effects (thermobaricity, and also the steric effect – the principal non-Boussinesq effect), so re-introduction of bulk compressibility brings only minor quantitative changes.

Existing oceanic codes like MOM4p1 use simpler mode-splitting procedures resulting in stronger reliance on the smallness of parameters (5.71), *e.g.*, smallness of ζ relative to total depth and even to the uppermost grid-box if there is strong stratification within the upper portion of the domain. The later is due to vertical redistribution of density by barotropic motions in the case of vertically fixed grid. This can be traced back to the long-standing vision of free-surface pressure as "pressure on the rigid lid", where the Poisson equation was considered primarily as a more efficient replacement for the original stream-function method, and subsequently, the split-explicit free-surface was motivated more by the

ease of implementation in the era of parallel computing (or lack of efficient parallel elliptic solvers at that time) rather than by the interest to the physical phenomena associated with the free surface itself. This view is inherited from the historical de-emphasis of temporal accuracy for barotropic motions (first-order) and the practice of rather heavy-handed temporal filtering of them. In this case conversion to a non-Boussinesq model with new sources of mode-splitting error does not usually lead to an instability because sufficient numerical damping is already present. Since fine-resolution regional modeling gives more interest in barotropic processes (*e.g.,* tides and topographic amplification of tidally-induced motions), the accuracy can be restored by using a more time-scale selective fast-time averaging filter, but this also brings sensitivity to splitting errors. One should note that legacy MOM code does not formally guarantee discrete finite-volume conservation property for tracers, even in their simpler Boussinesq versions (Griffies *et al.*, 2001; Griffies, 2004), and therefore have somewhat less to lose when converting to non-Boussinesq in a simple way (Greatbatch *et al.*, 2001). This situation has been improved with conversion to pressure-based coordinates (with relative ease for z-coordinate model, somewhat more difficult for sigma), but this also commits the model to use hydrostatic approximation and there is no obvious way to overcome this limitation. When considering barotropic mode splitting, the vertical coordinate "integrates out" exposing essentially the original dilemma – density (specific volume) depends on the state of free surface via EOS pressure – which must be dealt with during fast-time stepping or accept additional mode-splitting errors. For hydrostatic models it is still simpler to make a Boussinesq code more self-consistent in its discretized properties than a non-Boussinesq one. Conversely, a more general, nonhydrostatic, non-Boussinesq code for flows with low Mach number (*e.g.,* Gatti-Bono & Colella, 2006) would be more computationally expensive, hence less competitive for realistic, large-scale oceanic simulations.

Another class of hydrostatic oceanic models uses an isopycnic vertical coordinate. As in the case of pressure-based coordinates, these models also avoid the density extrapolation (5.13) by the specific design of their coordinate due to Lagrangian or predominantly Lagrangian movement in the vertical direction. The use of the Montgomery potential in the horizontal pressure-gradient force makes it natural to have a non-Boussinesq formulation. Originally these models were derived using the assumption of incompressible EOS and Lagrangianly conserved (potential) density (Bleck & Boudra, 1981; Bleck & Smith, 1990). When the thermobaric effect was included later by Sun *et al.* (1999), it introduced EOS stiffening for the first time. This also leads to the necessity of using "thermobaric references" to avoid pressure gradient errors of an essentially sigma-type (despite using isopycnic coordinates(!)), resulting in a mechanism for numerical instability and a delicate treatment (Hallberg, 2005). [This approach (along with this particular reason for stiffening) may become obsolete after a recent alternative proposed by Adcroft & Hallberg (2008).] In addition to the above, the mode-slitting algorithm of Higdon & de Szoeke (1997); Hallberg (1997), still used today, was derived assuming incompressible EOS. For these reasons, and because of their practices these models can be classified as "stiffened" non-Boussinesq models.

6 Summary

The desire for a physically correct representation of EOS effects (*e.g.,* thermobaricity) in oceanic modeling requires the use of the nonlinear, realistic seawater EOS. It is often implanted in an "add-on" fashion into a Boussinesq-approximation code. This brings a set of internal inconsistencies with spurious effects (*e.g.,* vertical dependency of acceleration created by a purely barotropic pressure gra-

dient) and interference with barotropic-baroclinic mode-splitting, including potential numerical instability. This paper shows in Secs. 2-4 how a combined approach of Dukowicz (2001) and SM2003 leads to an accurate Boussinesq model with a computationally-practical form of stiffened EOS in the specific context of σ-coordinate modeling. In essence, it comes from the realization that the bulk of the seawater compressibility effect is dynamically passive and can be separated in the EOS from the dynamically relevant parts. Then the constant Boussinesq reference density $\rho_0^\bullet$ is much closer to the varying $\rho^\bullet = \rho^\bullet(\Theta, S, P)$ compared to simply replacing $\rho \to \rho_0$ in the standard Boussinesq approximation. This significantly reduces the Boussinesq errors while retaining all the necessary physical effects outlined in Sec. 3. The output of the EOS routine is not the *in situ* density or its anomaly, but $\rho_1' = \rho_1'(\Theta, S)$ and $q_1' = q_1'(\Theta, S)$. The former one essentially retains its original meaning derived from Jackett & McDougall (1995)), while the latter is now defined by (4.6). The functional form of EOS is modified to include the $\gamma\, z^2$ term in (4.7), which causes a corresponding change in the algorithm for adiabatic differencing (4.8) and a minor revision of the pressure-gradient algorithm.

The limitations of the Boussinesq approximation are widely discussed in the literature, and sometimes its complete abandonment is advocated. In Sec. 5 we show that doing so leads to a more complicated code: the mode-splitting procedure interferes with the density computation via EOS since EOS pressure depends on the state of free-surface field, and consequently EOS can be no longer considered as belonging entirely to the slow mode, resulting in a more complicated splitting algorithm to avoid additional splitting errors and/or extra temporal filtering for the barotropic mode to control numerical instability. This computational aspect of EOS compressibility is usually overlooked in theoretical studies. Remarkably, though originally intended for a Boussinesq code, the factoring of EOS as $\rho = r(P) \cdot \rho^\bullet_{\rm EOS}(\Theta, S, P)$ by Dukowicz (2001) provides a useful framework for designing accurate mode-splitting in a hydrostatic, non-Boussinesq, free-surface model that retains all the compressibility effects in EOS. Removing the bulk compressibility from EOS, but keeping thermobaric part of it (*i.e.,* stiffening) eliminates the need for splitting EOS pressure into fast and slow components, thus simplifying the algorithm, however departure from the fully realistic EOS also means that the model can no longer be considered as a fully non-Boussinesq. Notably, among the existing non-Boussinesq models, modern isopycnic-coordinate models always use stiffened EOS (Sun *et al.,* 1999; Hallberg, 2005). This allows retention of the principal non-Boussinesq effects, notably steric sea-level changes.

Post facto we note a hierarchy of four approximations, all of which are in practical use in hydrostatic oceanic modeling today. They differ only by the treatment of compressibility effects in EOS: full non-Boussinesq $\longrightarrow$ non-Boussinesq with stiffened EOS $\longrightarrow$ Boussinesq with stiffened EOS $\longrightarrow$ standard Boussinesq (ρ_0 in combination with full EOS). We recommend that the last of these be discontinued; *i.e.,* if the Boussinesq approximation is chosen, it should be applied uniformly to the entire code, including EOS. This means stiffening.

Acknowledgments: This research is supported by the Office of Naval Research through grants N00014-05-10293 and N00014-08-10597.

Appendix A: Alternative variants of Boussinesq approximation and Potential Vorticity (PV) equation in a shallow barotropic layer of compressible fluid

McDougall *et al.* (2002, hereafter cited as MGL2002) proposed an alternative version of Boussinesq approximation – their Eqs (27)–(29) – which have exactly the same form as the original Boussinesq equations, with the

exception that velocity $\tilde{\mathbf{u}}$ is not the usual velocity, but is the averaged normalized mass flux per unit area,

$$\tilde{\mathbf{u}} = \overline{\rho \mathbf{u}}^{\rho}/\rho_0 = \overline{\rho \mathbf{u}}/\rho_0\,, \qquad \text{where} \quad \overline{\mathbf{u}}^{\rho} = \overline{\rho \mathbf{u}}/\rho\,, \tag{A.1}$$

see their Eq. (23), where overbar means Reynolds averaging and, for simplicity, we have changed their notation $\overline{\tilde{\mathbf{u}}} \to \tilde{\mathbf{u}}$. Their motivation comes from subgrid-scale parameterization. They noticed that defining mean velocity as density-weighted average $\overline{\mathbf{u}}^{\rho}$ instead of a more conventional Eulerian average $\overline{\mathbf{u}}$, leads to a more physically interpretable turbulent correlation terms. Following these guidelines they derived a set of averaged non-Boussinesq equations – their Eqs. (24)–(26) – to which they applied Boussinesq approximation to derive their alternative Boussinesq. MGL2002 argue, and provide some support for their claim, that their alternative Boussinesq equations are more accurate than the standard – notably, the stationary parts of continuity and tracer equations are equivalent to their non-Boussinesq counterparts, the geostrophic-balance is their momentum equations is equivalent to non-Boussinesq (see their Sec. 5). They also use this claim to dismiss the EOS stiffening approach of Dukowicz (2001) as unnecessary, because their alternative Boussinesq equations already eliminate the non-physical shear in a geostrophically-balanced flow without any need for adjustment in EOS.

Unfortunately the alternative Boussinesq equations of MGL2002 also alter the relationship between the advection and Coriolis terms making it impossible to derive barotropic PV equation, which is possible to derive from non-Boussinesq or stiffened Boussinesq sets.

Consider a layer of non-stratified, but slightly compressible fluid, hydrostatic, non-Boussinesq,

$$\begin{aligned} \partial_t \mathbf{u} + \mathbf{u}\cdot\nabla_\perp \mathbf{u} + w\partial_z \mathbf{u} + f\mathbf{k}\times\mathbf{u} &= -(1/\rho)\nabla_\perp p \\ \partial_t \rho + \nabla_\perp\cdot(\rho\mathbf{u}) + \partial_z(\rho w) &= 0 \\ \partial_z p = -g\rho \qquad &\text{subject to} \quad p\Big|_{z=\zeta} = 0 \\ \rho = \rho_{\rm EOS}(p) \qquad &\text{EOS} \end{aligned} \tag{A.2}$$

along with proper kinematic boundary conditions at free surface $z=\zeta$ and bottom $z=-h$, where $h=h(x,y)$ is bottom topography. Above $\mathbf{u}, w=(u,v,w)$ is 3D velocity vector, $\nabla_\perp$ is horizontal (two-dimensional) gradient or divergence operator. As discussed in Sec. 2 from (2.1) to (2.4), under these circumstances EOS and hydrostatic equations can be solved resulting in self-consistent profiles for density and pressure, $\rho = (1/g)\mathcal{P}'(\zeta - z)$ and $p = \mathcal{P}(\zeta - z)$ (where $\mathcal{P}'$ means derivative of $\mathcal{P}$ with respect to its argument $\zeta - z$), and, as follows from (2.4), the acceleration due to pressure gradient is simply $-g\nabla_\perp\zeta$ and is independent of z regardless of the functional form of $\mathcal{P} = \mathcal{P}(\zeta - z)$. This means that(A.2) admits solutions where horizontal velocities are independent of z,

$$\begin{aligned} \partial_t \mathbf{u} + \mathbf{u}\cdot\nabla_\perp \mathbf{u} + f\mathbf{k}\times\mathbf{u} &= -g\nabla_\perp\zeta \\ \partial_t p_b + \nabla_\perp\cdot(p_b\mathbf{u}) &= 0 \end{aligned} \tag{A.3}$$

where $p_b = g\displaystyle\int_{-h}^{\zeta}\rho\,\mathrm{d}z = \mathcal{P}(\zeta+h)$ is identified as bottom pressure. It is assumed to be invertible, $h+\zeta = [\mathcal{P}]^{-1}(p_b)$. The pressure gradient term $\nabla_\perp\zeta$ can be eliminated by taking horizontal curl of $\mathbf{u}$-equation (A.3),

$$\partial_t[\nabla_\perp\times\mathbf{u}] + \mathbf{u}\cdot\nabla_\perp[\nabla_\perp\times\mathbf{u}] + f\nabla_\perp\cdot\mathbf{u} + [\nabla_\perp\times\mathbf{u}]\nabla_\perp\cdot\mathbf{u} = 0\,, \tag{A.4}$$

or

$$\partial_t\mathcal{A} + \mathbf{u}\cdot\nabla_\perp\mathcal{A} + \mathcal{A}\nabla_\perp\cdot\mathbf{u} = 0\,, \tag{A.5}$$

where $\mathcal{A}$ is absolute vorticity, $\mathcal{A} = f + \nabla_\perp\times\mathbf{u}$. On the other hand, p_b-equation (A.3) can be dressed up as

$$\partial_t p_b + \mathbf{u}\cdot\nabla_\perp p_b + p_b\nabla_\perp\cdot\mathbf{u} = 0\,. \tag{A.6}$$

Multiplying the $\mathcal{A}$-equation by p_b, the latest p_b-equation by $\mathcal{A}$, and subtracting them to cancel the $\nabla_\perp \cdot \mathbf{u}$-terms,

$$p_b \partial_t \mathcal{A} + p_b \mathbf{u} \cdot \nabla_\perp \mathcal{A} - \mathcal{A} \partial_t p_b - \mathcal{A} \mathbf{u} \cdot \nabla_\perp p_b = 0 \tag{A.7}$$

which ultimately leads to PV equation

$$(\partial_t + \mathbf{u} \cdot \nabla_\perp) \frac{f + \nabla_\perp \times \mathbf{u}}{p_b} = 0 \,. \tag{A.8}$$

So the principle dynamics of this compressible, but barotropic fluid is (*i*) vertical uniformity of $\mathbf{u}$ (as a consequence, vertical uniformity of relative vorticity), and (*ii*) Lagrangian conservation of barotropic PV as stated above. The above derivation can be performed for uniform (on an f-plane) or non-uniform Coriolis parameter, and in horizontal orthogonal curvilinear coordinates as well. The fact that fluid is compressible adds almost nothing – one can easily repeat the above with constant-density layer (in this case it does not matter whether it is Boussinesq or non-Boussinesq) the only difference is replacement $p_b \to g\rho_0(h + \zeta)$.

In the case of conventional Boussinesq approximation with pressure-dependent EOS the pressure-gradient term in the first equation (A.2) becomes $-(1/\rho_0)\nabla_\perp p = -g\rho/\rho_0 \nabla_\perp \zeta$, the $g\rho = P'(\zeta - z)$, which is no longer vertically uniform. This precludes the transition from (A.2) to (A.3) and the subsequent derivation of PV equation similar to above. If one considers only the geostrophic balance in Boussinesq version of (A.2), the resultant velocity becomes proportional to (ρ/ρ_0)-profile as well, which is an artifact of Boussinesq approximation.

Excluding dynamic pressure from EOS equation of (A.2) by replacing it with $\rho = \rho_0 + \rho'_{\mathrm{EOS}}(-\rho_0 g z)$ eliminates the vertical dependency,

$$\begin{aligned} -\frac{1}{\rho_0}\nabla_\perp p &= -g\frac{\rho_0 + \rho'\big|_{z=\zeta}}{\rho_0}\nabla_\perp \zeta - \frac{g}{\rho_0}\int_z^\zeta \underbrace{\nabla_\perp \rho'_{\mathrm{EOS}}(-\rho_0 g z)}_{=0}\,\mathrm{d}z' \\ &\approx -g\left(1 - g\,\frac{\partial \rho'_{\mathrm{EOS}}}{\partial p}\bigg|_{z=\zeta} \cdot \zeta\right)\nabla_\perp \zeta \approx -g\nabla_\perp\left(\zeta - \frac{g\zeta^2}{2c^2}\right) , \end{aligned} \tag{A.9}$$

while introducing an insignificant non-physical term due to the artificial assumption that $\rho = \rho_0$ at $z = 0$ instead of free surface $z = \zeta$ (above c is speed of sound, so the associated smallness parameter $g\zeta/c^2 \sim 2 \times 10^{-6}$ assuming $c = 1500m/s$ and $\zeta = 1m$). With this choice made it is possible to derive an analog of (A.8) while using Boussinesq approximation. Note that the extra term in (A.9) does not preclude elimination of pressure gradient term when taking curl of (A.3).

EOS stiffening by Dukowicz (2001) (in this case trivially reverting EOS in (A.2) to constant density, $\rho = \rho_0$, making it insensitive to the choice of which pressure is used in EOS), also eliminates the vertical dependency in $-(1/\rho_0)\nabla_\perp p$, allowing derivation of barotropic PV equation (A.8).

If the alternative Boussinesq system is used – the hydrostatic version of Eqs. (27)–(29) from MGL2002 in combination with EOS using *in situ* pressure, $\rho = \rho_{\mathrm{EOS}}(p)$ as in (A.2) – then it is not the ordinary velocity, but the density-scaled velocity $\overline{\tilde{\mathbf{u}}}$ becomes proportional to (ρ/ρ_0), which means that unscaled velocity is vertically uniform as it should. However, despite the correct geostrophic balance, the modified Boussinesq set of MGL2002 also does not produce a counterpart of (A.8). Inspection of the derivation above shows that there must be proper scaling relationships among all three terms: Coriolis, pressure-gradient, and advection. In the original Boussinesq the scaling between Coriolis and advection is correct, but pressure gradient receives non-physical vertically-dependent multiplier. In the modified case, rescaling of velocity by ρ/ρ_0 corrects the relationship between Coriolis and pressure gradient, but at the expense of sacrificing the relationship between Coriolis and advection – it is "unscaled", rather than density-weighted (hence vertically-dependent) vorticity should be combined with f in order to form absolute vorticity, and then PV. Conversely, the alternative non-Boussinesq set – Eqs. (24)–(26) from MGL2002 – contains the reverse density multiplier ρ_0/ρ in the nonlinear terms, which

makes it possible to derive the PV equation above merely because the alternative set can be transformed back into the original non-Boussinesq written in terms of the non-scaled $\mathbf{u}$.

In contrast, stiffening of EOS by Dukowicz (2001) repairs the relationship between pressure gradient and Coriolis terms without disturbing the already correct mutual relationship between Coriolis and advection.

Appendix B: Surface gravity waves in a compressible barotropic shallow-water layer

B.1 Non-Boussinesq case

Eqs. (2.1)–(2.4) from Sec. 2 show that the horizontal acceleration generated by a free-surface gradient does not depend on the vertical coordinate when vertical variation of density is due only to compressibility and there is hydrostatic balance,

$$\partial_t \mathbf{u} + ... = -g\nabla_\perp \zeta \,. \tag{B.1}$$

This makes it possible to consider motions where $\mathbf{u}$ is vertically uniform. In this case (B.1) integrates vertically in a trivial manner, and together with vertically integrated mass-conservation equation it yields,

$$\partial_t \left(\overline{\rho} D \overline{\mathbf{u}}\right) + ... = -g\overline{\rho} D \nabla_\perp \zeta \qquad \text{and} \qquad \partial_t \left(\overline{\rho} D\right) + \nabla_\perp \cdot \left(\overline{\rho} D \overline{\mathbf{u}}\right) = 0 \,, \tag{B.2}$$

where

$$\overline{\mathbf{u}} = \frac{1}{\overline{\rho} D} \int_{-h}^{\zeta} \rho \mathbf{u} \, \mathrm{d}z = \frac{1}{D} \int_{-h}^{\zeta} \mathbf{u} \, \mathrm{d}z = \mathbf{u} \,, \qquad \overline{\rho} = \frac{1}{D} \int_{-h}^{\zeta} \rho \, \mathrm{d}z \,, \quad \text{and} \quad D = h + \zeta \,. \tag{B.3}$$

Note that the difference between its *density*-weighted and *volume* averaged $\overline{\mathbf{u}}$ disappears because of vertical uniformity of $\mathbf{u}$. Solution of (B.2) implies that the prognostic variable $\overline{\rho} D$ (to be interpreted here as a whole symbol having the meaning of total weight of water column) needs to be translated into ζ in order to close the system. This is done through EOS. For simplicity we assume that EOS has the form of (2.7), *viz.*, $\rho = \rho_1 + P/c^2$ with ρ_1 and c constant. Combined with hydrostatic balance, this leads to the vertical profile $\rho = \rho_1 \exp\left\{g(\zeta - z)/c^2\right\}$, which results in

$$\overline{\rho} = \rho_1 \cdot \frac{e^{g(\zeta+h)/c^2} - 1}{g(\zeta + h)/c^2} = \rho_1 \cdot \frac{e^{gD/c^2} - 1}{gD/c^2} \,, \qquad \text{hence} \quad \overline{\rho} D = \rho_1 \frac{e^{gD/c^2} - 1}{g/c^2} \,. \tag{B.4}$$

This depends on ζ through D.

Now we consider small motions in a compressible fluid layer over a flat bottom. Substituting expression for $\overline{\rho} D$ from (B.4) into the second equation (B.2) with $h = const$ yields

$$\rho_1 e^{gD/c^2} \cdot \left\{ \partial_t \zeta + \overline{\mathbf{u}} \cdot \nabla_\perp \zeta \right\} + \rho_1 \frac{e^{gD/c^2} - 1}{g/c^2} \nabla_\perp \cdot \overline{\mathbf{u}} = 0 \,, \tag{B.5}$$

or

$$\partial_t \zeta + \overline{\mathbf{u}} \cdot \nabla_\perp \zeta + \left(\overline{\rho}/\rho_\mathrm{b}\right) D \, \nabla_\perp \cdot \overline{\mathbf{u}} = 0 \,, \tag{B.6}$$

where we identify $\rho_\mathrm{b} = \rho_1 e^{gD/c^2}$ as the value of the density near the bottom. To derive (B.6) we have used the EOS for the purpose of specific volume, *i.e.*, to express ζ from mass content $\overline{\rho} D$. This situation is common for non-Boussinesq models, and it reverses the role of EOS in a Boussinesq-approximation model. Linearization of (B.1) and (B.6) yields the system,

$$\partial_t \overline{\mathbf{u}} = -g\nabla_\perp \zeta \qquad \text{and} \qquad \partial_t \zeta = -\left(\overline{\rho}/\rho_\mathrm{b}\right) h \, \nabla_\perp \cdot \overline{\mathbf{u}} \,, \tag{B.7}$$

which admits wave solutions with phase speed

$$\widetilde{c} = \sqrt{gh\frac{\overline{\rho}}{\rho_{\rm b}}} = c\cdot\sqrt{1-e^{-gh/c^2}} \quad \begin{array}{ll} \nearrow \sqrt{gh}\,, & gh/c^2 \ll 1 \\ \searrow c\,, & gh/c^2 \gg 1\,. \end{array} \tag{B.8}$$

(Since $gh\overline{\rho} = P_b$ can be identified as bottom pressure, this result coincides with Eq. (29) in Dukowicz (2006) for a non-stratified case, *i.e.,* by there setting $N^2 = 0$.) For typical oceanic conditions of $h = 5500$ m, speed of sound $c = 1500$ m/s, and acceleration of gravity $g = 9.81$ m/s^2, we estimate $\epsilon = gh/c^2 = 0.025 \ll 1$. This means that the inclusion of the compressibility effect leads to a slightly smaller ($\sim 0.6\%$) phase speed than that of a layer of the same thickness filled by an incompressible fluid,

$$\widetilde{c} = \sqrt{gh}\cdot\sqrt{\frac{1-e^{-\epsilon}}{\epsilon}} = \sqrt{gh}\left(1-\frac{\epsilon}{4}+...\right)\,, \qquad \epsilon \ll 1\,. \tag{B.9}$$

The physical explanation for the reduced phase speed comes from the fact change in $\overline{\rho}D$ caused by divergence of vertically-integrated fluxes results in a lesser, by a factor of $\approx 1-\epsilon/2$, change in ζ than in the case of incompressible fluid, while the remaining $\epsilon/2$ fraction of $\overline{\rho}D$ translates into change in density $\overline{\rho}$, which does not contribute to acceleration due to pressure gradient in (B.7).

Eq. (B.8) indicates that the gravity-wave phase speed cannot be larger than the speed of sound. The opposite asymptotic limit, $gh/c^2 \gg 1$, has meaning as well, $\widetilde{c} \to c$. This corresponds to a lowest-vertical-mode wave of compression in an isotropic atmosphere, which does not have a well-defined free surface; rather its density decreases with height, so that the e-folding scale c^2/g plays the role of its effective thickness. The hydrostatic approximation alone excludes acoustic waves without making an assumption of incompressibility or small density variation; in fact, acoustic and gravity waves become indistinguishable in the hydrostatic case.

B.2 Boussinesq case with $\rho = \rho_{\rm EOS}(P)$

As follows from (2.5), the Boussinesq counterpart of (B.1) with pressure-dependent EOS $\rho = \rho_1 + P/c^2$ is

$$\partial_t \mathbf{u} + ... = -\left(g/\rho_0\right)\cdot\rho_1 e^{g(\zeta-z)/c^2}\cdot\nabla_\perp\zeta\,, \tag{B.10}$$

where $\mathbf{u}$ can no longer be vertically uniform. However it is still possible to derive an analog of (B.7) by substituting $\mathbf{u} = \tilde{\mathbf{u}}\cdot e^{g(\zeta-z)/c^2}$, hence

$$e^{g(\zeta-z)/c^2}\cdot\partial_t\tilde{\mathbf{u}} + \tilde{\mathbf{u}}\cdot\left(g/c^2\right)\cdot e^{g(\zeta-z)/c^2}\cdot\partial_t\zeta + ... = -\left(g/\rho_0\right)\cdot\rho_1 e^{g(\zeta-z)/c^2}\cdot\nabla_\perp\zeta\,, \tag{B.11}$$

or

$$\partial_t\tilde{\mathbf{u}} + \tilde{\mathbf{u}}\left(g/c^2\right)\partial_t\zeta + ... = -g\left(\rho_1/\rho_0\right)\cdot\nabla_\perp\zeta\,, \tag{B.12}$$

which admits solutions with $\tilde{\mathbf{u}}$ independent of z as long as the nonlinear terms (denoted as dots) are vanishingly small. Equation for free surface becomes

$$\partial_t\zeta = -\nabla_\perp\cdot\int_{-h}^{\zeta}\tilde{\mathbf{u}}e^{g(\zeta-z')/c^2}\,{\rm d}z' = -\nabla_\perp\cdot\left(\tilde{\mathbf{u}}\frac{e^{gD/c^2}-1}{g/c^2}\right) \tag{B.13}$$

Linearization of (B.12) and (B.13) assuming $h = const$, yields

$$\partial_t\tilde{\mathbf{u}} = -g\left(\rho_1/\rho_0\right)\cdot\nabla_\perp\zeta \qquad \text{and} \qquad \partial_t\zeta + h\left[\left(e^\epsilon-1\right)/\epsilon\right]\nabla_\perp\cdot\tilde{\mathbf{u}}\,, \tag{B.14}$$

where, once again, $\epsilon = gh/c^2$. The resultant phase speed of barotropic waves is

$$\widetilde{c} = \sqrt{gh\left(\rho_1/\rho_0\right)\cdot\left(e^\epsilon-1\right)/\epsilon} \tag{B.15}$$

where it is worth to note, *cf.,* (B.4), that $\rho_1\left(e^\epsilon-1\right)/\epsilon = \overline{\rho}$, hence $\widetilde{c} = \sqrt{gh\cdot\overline{\rho}/\rho_0}$. The choice of Boussinesq reference density $\rho_0 = \overline{\rho}$ makes $\widetilde{c} = \sqrt{gh}$, however it should be noted that in the case of non-uniform topography this choice cannot be made universal because $\overline{\rho}$ depends on h. The effect of slowdown of barotropic waves by compressibility is lost.

B.3 Boussinesq with reference pressure in EOS

Everything is the same as in the previous case, except that EOS pressure is computed assuming $\zeta \equiv 0$, and is not allowed to change with ζ. Then $\rho = \rho_1 \exp\left\{-gz/c^2\right\}$, so the counterpart of (B.1) becomes

$$\partial_t \mathbf{u} + ... = -\frac{1}{\rho_0}\nabla_\perp \int_z^\zeta g\rho_1 e^{-gz'/c^2}\mathrm{d}z' = -\frac{g}{\rho_0}\rho\Big|_{z=\zeta}\nabla_\perp\zeta - \frac{g}{\rho_0}\int_z^\zeta \underbrace{\nabla_\perp\left(\rho_1 e^{-gz'/c^2}\right)}_{=0}\mathrm{d}z' \tag{B.16}$$

or $\partial_t \mathbf{u} + ... = -\dfrac{g\rho_1}{\rho_0}e^{-g\zeta/c^2}\nabla_\perp\zeta \approx -\dfrac{g\rho_1}{\rho_0}\nabla_\perp\zeta$ which permits solutions with vertically uniform $\mathbf{u}$, and we note that $-g\zeta/c^2 \sim 5\times 10^{-6}$ assuming $c = 1500m/s$. The analog of the linearized system (B.7) becomes

$$\partial_t \mathbf{u} = -g\left(\rho_1/\rho_0\right)\cdot\nabla_\perp\zeta \qquad \text{and} \qquad \partial_t\zeta = -h\nabla_\perp\cdot\mathbf{u}\,. \tag{B.17}$$

which yields phase speed

$$\widetilde{c} = \sqrt{gh\cdot\rho_1/\rho_0}\,. \tag{B.18}$$

For the choice of $\rho_0 = \overline{\rho} = \rho_1\left(e^\epsilon - 1\right)/\epsilon \approx \rho_1\left(1+\epsilon/2\right)$, where $\epsilon = gh/c^2 \ll 1$, the above turns into $\widetilde{c} \approx \sqrt{gh}\cdot(1-\epsilon/4)$, which is similar to (B.9). This result is merely a coincidence: the Boussinesq system (B.17) does not provide a proper physical mechanism for phase speed reduction due to compressibility effects (note that in comparison with (B.7) the density multiplier appears in front of pressure gradient term, rather than in free-surface equation). This result also suggests that using the near-surface value of density to compute pressure gradient term in barotropic mode is an optimal choice for a simple mode-splitting algorithm (simple means that it does not take into account the influence of stratification onto barotropic phase speed) in a Boussinesq model with reference EOS pressure *cf.*, Griffies (2004, see Secs. 12.3-12.4 there); Griffies (2009, see Sec. 7.7.3, Eq. (7.129)).

Appendix C: Surface gravity waves in a stratified two-layer fluid

C.1 Incompressible case

The simplest system with both barotropic and baroclinic modes is a two-layer model. It is also the simplest way to illustrate the influence of stratification on the phase speed of surface gravity waves. For small oscillations around the resting state, the two-layer model has a set linear equations:

$$\begin{aligned} \partial_t u_1 &= -g\cdot\nabla_x\zeta\,; & \partial_t(\zeta-\eta) + H_1\cdot\nabla_x u_1 &= 0 \\ \partial_t u_2 &= -g\frac{\rho_1}{\rho_2}\cdot\nabla_x\zeta - g\left(1-\frac{\rho_1}{\rho_2}\right)\cdot\nabla_x\eta\,; & \partial_t\eta + H_2\cdot\nabla_x u_2 &= 0\,, \end{aligned} \tag{C.1}$$

where u_k, ρ_k, and H_k are velocities, densities, and unperturbed thicknesses of the top ($k=1$) and the bottom ($k=2$) layers; ζ is free-surface elevation; η is interface elevation (both are relative to their unperturbed states, $z=0$ and $z=-H_1$). This system assumes hydrostatic balance for an incompressible fluid, but it does not use the Boussinesq approximation.

Fourier analysis: Let $\left(u_1,\zeta,u_2,\eta\right) = \left(\widehat{u}_1,\widehat{\zeta},\widehat{u}_2,\widehat{\eta}\right)\cdot e^{kx-i\omega t}$, then (C.1) becomes

$$\begin{aligned} -i\omega\cdot\widehat{u}_1 &= -ik\cdot g\widehat{\zeta}\,; & -i\omega\cdot\widehat{\zeta} + i\omega\cdot\widehat{\eta} &= -ik\cdot H_1\widehat{u}_1\,; \\ -i\omega\cdot\widehat{u}_2 &= -ik\cdot g\cdot\frac{\rho_1}{\rho_2}\cdot\widehat{\zeta} - ik\cdot g\left(1-\frac{\rho_1}{\rho_2}\right)\cdot\widehat{\eta}\,; & -i\omega\cdot\widehat{\eta} &= -ik\cdot H_2\widehat{u}_2\,. \end{aligned} \tag{C.2}$$

The right pair of equations can be used to exclude $\widehat{u}_1$ and $\widehat{u}_2$ from the left pair:

$$\begin{aligned} \left(\widetilde{c}^2 - gH_1\right)\widehat{\zeta} &= \widetilde{c}^2\widehat{\eta} \\ \left(\widetilde{c}^2 - gH_2\frac{\rho_2-\rho_1}{\rho_2}\right)\widehat{\eta} &= gH_2\frac{\rho_1}{\rho_2}\widehat{\zeta}\,, \end{aligned} \tag{C.3}$$

where we have introduced $\widetilde{c} = \omega/k$ which is identified as phase speed for the vertical modes, external or internal [22] . This has non-trivial solutions if

$$\left(\widetilde{c}^2 - gH_1\right)\cdot\left(\widetilde{c}^2 - gH_2\frac{\rho_2-\rho_1}{\rho_2}\right) = \widetilde{c}^2 gH_2\frac{\rho_1}{\rho_2}\,. \tag{C.4}$$

It can be rewritten as

$$\widetilde{c}^4 - \widetilde{c}^2\widetilde{c}_0^2 + \widetilde{c}_0^2\hat{c}_1^2 = 0\,, \tag{C.5}$$

where

$$\widetilde{c}_0^2 = g\left(H_1+H_2\right) \qquad \text{and} \qquad \hat{c}_1^2 = g\frac{H_1H_2}{H_1+H_2}\cdot\frac{\rho_2-\rho_1}{\rho_2}\,. \tag{C.6}$$

Equation (C.5) has two solutions,

$$\widetilde{c}_\pm^2 = \frac{\widetilde{c}_0^2}{2} \pm \sqrt{\frac{\widetilde{c}_0^4}{4} - \widetilde{c}_0^2\hat{c}_1^2} = \frac{\widetilde{c}_0^2}{2} \pm \frac{\widetilde{c}_0^2}{2}\sqrt{1-4\hat{c}_1^2/\widetilde{c}_0^2} \approx \frac{\widetilde{c}_0^2}{2} \pm \frac{\widetilde{c}_0^2}{2} \mp \hat{c}_1^2\,, \qquad \text{as long as} \quad \hat{c}_1^2 \ll \widetilde{c}_0^2\,, \tag{C.7}$$

where $\widetilde{c}_+^2 = \widetilde{c}_0^2 - \hat{c}_1^2$ is associated with the barotropic mode, and $\widetilde{c}_-^2 = \hat{c}_1^2$ with the baroclinic. This indicates that the presence of stratification reduces the square of phase speed of the barotropic mode relative to that of a constant-density layer of the same thickness, $H_1 + H_2$, by the square of the baroclinic phase speed. This conclusion is true even beyond the assumption of a small density difference, $\rho_2 - \rho_1 \ll \rho_2$: (C.5) has the property that the sum of its two roots is always $\widetilde{c}_0^2$.

Structure of the barotropic mode: $\widehat{\zeta}$ and $\widehat{\eta}$ are moving in proportion,

$$\frac{\widehat{\eta}}{\widehat{\zeta}} = 1 - \frac{gH_1}{c^2} = \frac{H_2 - \dfrac{H_1H_2}{H_1+H_2}\cdot\dfrac{\rho_2-\rho_1}{\rho_2}}{H_1+H_2-\dfrac{H_1H_2}{H_1+H_2}\cdot\dfrac{\rho_2-\rho_1}{\rho_2}} \approx \frac{H_2}{H_1+H_2}\left[1-\frac{H_1^2}{(H_1+H_2)^2}\left(1-\frac{\rho_1}{\rho_2}\right)\right]\,, \tag{C.8}$$

which is slightly smaller than the fraction of the distance from the bottom to the interface between the two layers relative to the total depth. Correspondingly,

$$\frac{\widehat{u}_2}{\widehat{u}_1} = 1 - \frac{\hat{c}_1^2}{gH_2} \approx 1 - \frac{H_1}{H_1+H_2}\left(1-\frac{\rho_1}{\rho_2}\right)\,, \tag{C.9}$$

indicating that the bottom layer moves slower than the top.

Direct splitting: Equations (C.8) and (C.9) indicate that neither the volume- nor density-weighted vertically averaged velocity,

$$\overline{u} = \frac{H_1u_1+H_2u_2}{H_1+H_2}\,, \qquad \text{or} \qquad \overline{u} = \frac{\rho_1H_1u_1+\rho_2H_2u_2}{\rho_1H_1+\rho_2H_2}\,, \tag{C.10}$$

[22] Because later in this appendix we will consider the case of compressible fluid with a finite speed of sound, to avoid potential conflict in notation, we denote the phase speed of gravity waves as $\widetilde{c}$ or $\hat{c}$, using $\widetilde{c}$ for both modes, if they appear together, or for barotropic, if separately, while $\hat{c}$ is used for baroclinic only if it appears separately. Plain c (without any symbol on top) is reserved for speed of sound.

can be identified as a depth-independent barotropic flow. However, the proportionality property of perturbations, $\widehat{\eta}$ *vs.* $\widehat{\zeta}$ and $\widehat{u}_2$ *vs.* $\widehat{u}_1$, provides a path for splitting (C.1) into independent barotropic and baroclinic subsystems. To do this multiply the upper-left equation (C.1) by H_1 and the lower-left by βH_2 and combine the layers; similarly, multiply the lower-right by β and combine it with the upper-right:

$$\begin{aligned} \partial_t \left(H_1 u_1 + \beta H_2 u_2 \right) &= -\nabla_x \left[g \left(H_1 + \beta H_2 \frac{\rho_1}{\rho_2} \right) \zeta + \beta g H_2 \frac{\rho_2 - \rho_1}{\rho_1} \eta \right] \\ \partial_t \left[\zeta + (\beta - 1) \eta \right] &= -\nabla_x \left(H_1 u_1 + \beta H_2 u_2 \right) , \end{aligned} \tag{C.11}$$

where β is yet to be determined. Note that u_1 and u_2 already appear in identical combinations under ∂_t and ∇_x in the first and the second equations, and the goal is to achieve the same for ζ and η. This leads to the proportionality condition,

$$\frac{g \left(H_1 + \beta H_2 \frac{\rho_1}{\rho_2} \right)}{1} = \frac{\beta g H_2 \frac{\rho_2 - \rho_1}{\rho_1}}{\beta - 1} , \tag{C.12}$$

and the selection of β as a root of the quadratic equation $\beta^2 - \frac{\rho_2}{\rho_1} \left(1 - \frac{H_1}{H_2} \right) \beta - \frac{\rho_2}{\rho_1} \cdot \frac{H_1}{H_2} = 0$ or,

$$\beta = \frac{1}{2} \cdot \frac{\rho_2}{\rho_1} \left\{ 1 - \frac{H_1}{H_2} \pm \left[\left(1 + \frac{H_1}{H_2} \right)^2 - \frac{4 H_1}{H_2} \cdot \left(1 - \frac{\rho_1}{\rho_2} \right) \right]^{1/2} \right\} . \tag{C.13}$$

Assuming that $1 - \rho_1 / \rho_2 \ll 1$, this leads to

$$\beta_+ = 1 + \frac{H_2}{H_1 + H_2} \left(\frac{\rho_2}{\rho_1} - 1 \right) \qquad \text{and} \qquad \beta_- = -\frac{H_1}{H_2} \cdot \left[1 - \frac{H_2}{H_1 + H_2} \left(\frac{\rho_2}{\rho_1} - 1 \right) \right] , \tag{C.14}$$

which corresponds to the barotropic and baroclinic modes respectively. Once β is known, (C.11) can be turned into two independent systems (choosing either $+$ or $-$ sign index below),

$$\begin{aligned} \partial_t U_\pm &= -\widetilde{c}_\pm^2 \nabla_x \zeta_\pm \\ \partial_t \zeta_\pm &= -g \, \nabla_x U_\pm \end{aligned} \qquad \text{where} \qquad \begin{cases} \zeta_\pm = \zeta + (\beta_\pm - 1) \eta \\ U_\pm = H_1 u_1 + \beta_\pm H_2 u_2 \left(\rho_1 / \rho_2 \right) \\ \widetilde{c}_\pm^2 = g \left[H_1 + \beta_\pm H_2 \left(\rho_1 / \rho_2 \right) \right] . \end{cases} \tag{C.15}$$

It can be shown that the phase speeds $\widetilde{c}_\pm^2$ for each mode are the same as (C.7) for $\beta = \beta_\pm$ respectively. One can also verify that (C.8) and (C.9) can be obtained from the conditions,

$$\zeta + (\beta_- - 1) \eta = 0 \qquad \text{and} \qquad H_1 u_1 + \beta_- \cdot H_2 u_2 \left(\rho_1 / \rho_2 \right) = 0 , \tag{C.16}$$

that have the meaning of non-excitation of baroclinic degrees of freedom by purely barotropic motions. Since

$$1 < \beta_+ < \rho_2 / \rho_1 , \tag{C.17}$$

the weighting of u_1 and u_2 for the barotropic mode is within the bounds of set by (C.10). It leans toward ρ_2 / ρ_1 when the top layer is shallow relative to the bottom layer, $H_1 \ll H_2$.

C.2 Compressible two-layer non-Boussinesq case

Consider a two-layer fluid with densities in the upper and lower layers dependent on pressure,

$$\rho = \rho_1 - P / c_1^2 \qquad \text{and} \qquad \rho = \rho_2 - P / c_2^2 , \tag{C.18}$$

with $\rho_1 \neq \rho_2$ due to stratification and speeds of sound $c_1 \neq c_2$ to simulate the dependencies on temperature, salinity, and pressure.

Using the hydrostatic balance the above leads to self-consistent profiles of density and pressure in the top, $-H_1+\eta < z < \zeta$, and bottom, $-H_1-H_2 < z < -H_1+\eta$, layers :

$$\rho = \begin{cases} \rho_1 e^{g(\zeta-z)/c_1^2} \\ \left(\rho_2 + P_1/c_2^2\right) e^{g(\eta-H_1-z)/c_2^2} \end{cases} \qquad P = \begin{cases} \rho_1 c_1^2 \left[e^{g(\zeta-z)/c_1^2}-1\right] & \text{top} \\ P_1 + \left(P_1+\rho_2 c_2^2\right)\left[e^{g(\eta-H_1-z)/c_2^2}-1\right] & \text{bottom}\,, \end{cases} \tag{C.19}$$

where $P_1 = \rho_1 c_1^2 \left[e^{g(\zeta-\eta+H_1)/c_1^2}-1\right]$ is pressure at the interface between the layers, $z=-H_1+\eta$. Equation (C.19) yields continuity of pressure P across the interface. Similar to (2.4), the acceleration due to PGF $(-1/\rho)\nabla_x P$ is independent of the vertical coordinate within each layer and equal to

$$-\frac{1}{\rho}\nabla_x P = -g\nabla_x\zeta \qquad \text{and} \qquad -\frac{1}{\rho}\nabla_x P = -\frac{\rho_1 g\left(\nabla_x\zeta-\nabla_x\eta\right)e^{g(\zeta-\eta+H_1)/c_1^2}}{\rho_2+\rho_1\left(c_1^2/c_2^2\right)\left[e^{g(\zeta-\eta+H_1)/c_1^2}-1\right]} - g\nabla_x\eta \tag{C.20}$$

for the top and bottom layer, respectively. This leads to the momentum equations,

$$\begin{aligned} \partial_t u_1 &= -g\nabla_x\zeta \\ \partial_t u_2 &= -g\nabla_x\zeta - g\left[\left(1-\frac{\rho_1}{\rho_2}\right)-\frac{\rho_1}{\rho_2}\cdot\frac{gH_1}{c_1^2}\cdot\left(1-\frac{\rho_1 c_1^2}{\rho_2 c_2^2}\right)\right]\cdot\left(\nabla_x\eta-\nabla_x\zeta\right)\,, \end{aligned} \tag{C.21}$$

where we have expanded (C.20) in a Taylor series for $gH_1/c_1^2 \ll 1$ and retained only the leading-order terms. The equations are linearized assuming $\zeta, \eta \ll H_1, H_2$ and neglecting the advection terms. As expected, the second equation (C.21) reverts to (C.1) if $c_1 \to \infty$, while the ratio c_1/c_2 remains finite. Furthermore, the additional terms due to compressibility vanish if gH_1/c_1^2 remains finite, but $\rho_1 c_1 = \rho_2 c_2$, indicating their baroclinic and thermobaric nature.

The top-layer thickness equation is derived following the path of transition from (B.2) to (B.6) in Appendix B. This leads to

$$\partial_t(\zeta-\eta) = -H_1\left(1-\frac{1}{2}\frac{gH_1}{c_1^2}\right)\nabla_x u_1\,, \tag{C.22}$$

which is linearized, and only leading-order corrections due to finite compressibility are retained. The bottom-layer thickness equation stems from mass conservation,

$$\partial_t\big(\overline{\rho}_2(H_2+\eta)\big)+\nabla_x\big(\overline{\rho}_2(H_2+\eta)u_2\big)=0\,, \tag{C.23}$$

or

$$\left(\partial_t+u_2\cdot\nabla_x\right)\big(\overline{\rho}_2(H_2+\eta)\big)+\overline{\rho}_2(H_2+\eta)\nabla_x u_2=0\,, \tag{C.24}$$

where, as follows from (C.19), the vertically averaged density within the bottom layer is

$$\overline{\rho}_2 = \left(\rho_2+\frac{P_1}{c_2^2}\right)\frac{e^{g(H_2+\eta)/c_2^2}-1}{g/c_2^2}\,. \tag{C.25}$$

Since the interface pressure P_1 depends on the thickness of the top layer, $\overline{\rho}_2$ depends on it as well. This leads to the participation of ζ in the bottom thickness equation. Substitution of the expression for P_1 just after (C.19) into (C.25), with subsequent substitution into (C.24) leads to

$$\partial_t\eta - \frac{\rho_1}{\rho_2}\frac{gH_2}{c_2^2}\cdot\partial_t(\zeta-\eta)+H_2\left(1-\frac{1}{2}\frac{gH_2}{c_2^2}\right)\nabla_x u_2=0\,, \tag{C.26}$$

where we retain only leading-order compressibility corrections. The above reverts to the corresponding equation in (C.1) in the incompressible limit, $gH_2/c_2 \to 0$.

Equations (C.21), (C.22), and (C.26) comprise a closed system that describes small oscillations in a compressible two-layer fluid. Its Fourier analysis similar to the transition from (C.1) to (C.2) yields

$$\begin{aligned} -i\omega\cdot\widehat{u}_1 &= -ik\cdot g\widehat{\zeta}\,; & -i\omega\cdot\widehat{\zeta}+i\omega\cdot\widehat{\eta} &= -ik\cdot H_1'\widehat{u}_1\,; \\ -i\omega\cdot\widehat{u}_2 &= -ik\,g\left(1-\delta'\right)\cdot\widehat{\zeta}-ik\,g\delta'\cdot\widehat{\eta}\,; & -i\omega\,(1-\epsilon)\cdot\widehat{\eta}-i\omega\,\epsilon\cdot\widehat{\zeta} &= -ik\cdot H_2'\widehat{u}_2\,, \end{aligned} \tag{C.27}$$

where we define

$$\begin{aligned} \delta' &= \left(1-\frac{\rho_1}{\rho_2}\right)-\frac{\rho_1}{\rho_2}\cdot\frac{gH_1}{c_1^2}\left(1-\frac{\rho_1 c_1^2}{\rho_2 c_2^2}\right) & H_1' &= H_1\left(1-\frac{1}{2}\frac{gH_1}{c_1^2}\right) \\ \epsilon &= \frac{\rho_1}{\rho_2}\cdot\frac{gH_2}{c_2^2} & H_2' &= H_2\left(1-\frac{1}{2}\frac{gH_2}{c_2^2}\right), \end{aligned} \tag{C.28}$$

and expect that δ', ϵ are sufficiently small and H_1', H_2' deviate only slightly from H_1, H_2. This leads to the characteristic equation,

$$\widetilde{c}^4 - g\left[H_2'+H_1'(1-\epsilon)\right]\widetilde{c}^2 + g^2\delta'\,H_1'H_2' = 0\,, \tag{C.29}$$

where $\widetilde{c}=\omega/k$. This essentially repeats (C.5)–(C.6), but with a modified set of coefficients. The resulting phase speeds for the barotropic and first baroclinic modes are

$$\widetilde{c}_+^2 = g\left[H_2'+H_1'(1-\epsilon)\right] - \frac{g\delta'\,H_1'H_2'}{H_2'+H_1'(1-\epsilon)} \qquad \hat{c}_-^2 = \frac{g\delta'\,H_1'H_2'}{H_2'+H_1'(1-\epsilon)}\,, \tag{C.30}$$

where, similar to (C.7), we keep only leading-order corrections arising from stratification and here compressibility.

When $gH_1/c_1^2 \to 0$ and $gH_2/c_2^2 \to 0$, both phase speeds revert to their incompressible limits in (C.7). On the other hand, for a compressible fluid without stratification, $\rho_1 = \rho_2$, and the speed of sound is the same in both layers ($c_1 = c_2$); hence, the barotropic phase speed from c_+ from (C.30) becomes

$$\widetilde{c}_+^2 = g(H_1+H_2)\left[1-\frac{1}{2}\cdot\frac{g(H_1+H_2)}{c^2}+\ldots\right], \tag{C.31}$$

where the dots denote higher-order terms with respect to $g(H_1+H_2)/c^2 \ll 1$. This coincides with (B.9) where $h = H_1 + H_2$.

In the general case with both stratification and compressibility effects, as follows from (C.30), the stratification still causes the reduction of phase speed of the barotropic mode relative to the non-stratified case in the same manner as in (C.7), *i.e.*, the square of barotropic phase speed is reduced by the square of the first baroclinic mode speed. In addition, both are reduced by the compressibility (finite speeds of sound), due to the replacement of layer thicknesses H_1, H_2 with their primed counterparts H_1', H_2'. The baroclinic mode speed is also affected by the second term in δ', which involves the ratio of $\rho_1 c_1^2/\rho_2 c_2^2$. In principle, this admits the existence of internal waves even if $\rho_1 = \rho_2$, but the speed of sound in the upper layer is greater than in the lower to yield a positive $\delta' > 0$. For typical oceanographic conditions we expect the ratio of phase speeds for the first baroclinic and the barotropic modes to be within the range of 20 - 100, which leads to an estimate of $\hat{c}_-^2/\widetilde{c}_+^2 \sim 10^{-3}$. This causes a substantially smaller reduction of the barotropic wave speed than the influence of bulk compressibility (B.9) and makes stratification less of a concern as the source of mode-splitting error.

C.3 Boussinesq case

The Boussinesq version of (C.1) is

$$\begin{aligned} \partial_t u_1 &= -g\,(\rho_1/\rho_0)\,\nabla_x\zeta\,; & \partial_t(\zeta-\eta) + H_1\cdot\nabla_x u_1 &= 0 \\ \partial_t u_2 &= -g\,(\rho_1/\rho_0)\,\nabla_x\zeta - g\frac{\rho_2-\rho_1}{\rho_0}\nabla_x\eta\,; & \partial_t\eta + H_2\cdot\nabla_x u_2 &= 0\,. \end{aligned} \tag{C.32}$$

So the counterparts of (C.12) and the left side (C.14) become

$$\beta^2 - \left(\frac{\rho_2}{\rho_1} - \frac{H_1}{H_2}\right)\beta - \frac{H_1}{H_2} = 0 \qquad\qquad \beta_+ = 1 + \frac{\rho_2 H_2}{\rho_1 H_1 + \rho_2 H_2}\left(\frac{\rho_2}{\rho_1} - 1\right)\,. \tag{C.33}$$

This indicates, once again, that the velocity weighting parameter β_+ corresponding to the barotropic mode is neither 1 (volume weighting) nor ρ_2/ρ_1 (density weighting).

Appendix D: Surface gravity waves in a stratified shallow-water layer

Consider a Boussinesq fluid layer, where, for simplicity, we restrict our attention to a two-dimensional case in an x–z plane without Coriolis force:

$$\begin{aligned} \partial_t u + ... &= -(1/\rho_0)\partial_x P \\ \partial_t\rho + u\partial_x\rho + w\partial_z\rho &= 0 \\ \partial_z P &= -g\rho \\ \partial_x u + \partial_z w &= 0\,. \end{aligned} \tag{D.1}$$

We rewrite this with a σ-coordinate that follows ζ:

$$\sigma = \frac{z-\zeta}{h+\zeta}\ \begin{matrix}\nearrow 0\,, & z\to\zeta \\ \searrow -1\,, & z\to -h\end{matrix} \qquad \text{conversely,} \quad z = \zeta + \sigma(h+\zeta)\ \begin{matrix}\nearrow \zeta\,, & \sigma\to 0 \\ \searrow -h\,, & \sigma\to -1\,.\end{matrix} \tag{D.2}$$

We assume bottom topography is flat, $h = const$, so that the only distinction between $\partial_x\big|_z$ and $\partial_x\big|_\sigma$ is due to $\zeta \neq 0$. Thus,

$$\left.\frac{\partial P}{\partial x}\right|_z = \left.\frac{\partial P}{\partial x}\right|_\sigma - \left.\frac{\partial z}{\partial x}\right|_\sigma \cdot \frac{\partial P}{\partial z} = \left.\frac{\partial P}{\partial x}\right|_\sigma - (1+\sigma)\frac{\partial\zeta}{\partial x}\cdot\frac{\partial P}{\partial z}\,. \tag{D.3}$$

Since $P = g\displaystyle\int_z^\zeta \rho\,\mathrm{d}z = g(h+\zeta)\int_\sigma^0 \rho\,\mathrm{d}\sigma'$, we can further transform this into

$$\left.\frac{\partial P}{\partial x}\right|_z = g\left\{\rho(1+\sigma) + \int_\sigma^0 \rho\,\mathrm{d}\sigma'\right\}\cdot\frac{\partial\zeta}{\partial x} + g(h+\zeta)\int_\sigma^0 \left.\frac{\partial\rho}{\partial x}\right|_\sigma \mathrm{d}\sigma'\,. \tag{D.4}$$

The density equation in σ-coordinates is

$$\partial_t\big|_\sigma\rho + u\cdot\partial_x\big|_\sigma\rho + \big(\mathscr{W}/(h+\zeta)\big)\cdot\partial_\sigma\rho = 0\,, \tag{D.5}$$

where $\partial_t\big|_\sigma\rho$ is the time tendency relative to the moving σ-surface. The vertical velocity in σ-coordinates $\mathscr{W}$ is related to its Eulerian counterpart as $\mathscr{W} = w - (1+\sigma)\cdot\left[\dfrac{\partial\zeta}{\partial t} + u\cdot\dfrac{\partial\zeta}{\partial x}\right]$, which automatically satisfies the

no-flux boundary condition $\mathscr{W}\big|_{\sigma=0} = 0$ at the free surface as a consequence of the Eulerian kinematic surface boundary condition, $w = \partial_t\zeta + u\partial_x\zeta$. The non-divergent continuity equation is

$$\partial_t\zeta + \partial_x\big|_\sigma\big((h+\zeta)u\big) + \partial_\sigma\mathscr{W} = 0\,, \tag{D.6}$$

which leads to equations for ζ,

$$\partial_t\zeta + \partial_x\big((h+\zeta)\overline{u}\big) = 0\,, \qquad \text{where} \quad \overline{u} = \int_{-1}^{0} u\,\mathrm{d}\sigma\,, \tag{D.7}$$

and for $\mathscr{W}$

$$\partial_x\big|_\sigma\big((h+\zeta)(u-\overline{u})\big) + \partial_\sigma\mathscr{W} = 0\,. \tag{D.8}$$

The first equation in (D.1) with its PGF expressed by (D.4), along with (D.7), and (D.8), comprise a closed system which describes evolution of a layer of stratified fluid with a free surface. Since we are interested in small oscillations around the mean resting state, $\zeta \equiv u \equiv \mathscr{W} \equiv 0$ and $\rho = \underline{\boldsymbol{\rho}}(\sigma)$, and we linearize the system using the variables,

$$\zeta = \zeta' \qquad u = \overline{u} + u' \qquad \mathscr{W} = \mathscr{W}' \qquad \rho = \underline{\boldsymbol{\rho}}(\sigma) + \rho'\,, \tag{D.9}$$

where all except $\underline{\boldsymbol{\rho}}(\sigma)$ are considered as small perturbations. Note that splitting of horizontal velocity into $\overline{u}$ and u', such that $\displaystyle\int_{-1}^{0} u'\,\mathrm{d}\sigma \equiv 0$, is a matter of convenience, rather than an assumption that the second (primed) term is smaller than the first. The system becomes

$$\frac{\partial}{\partial t}\left(\overline{u} + u'\right) = -\frac{g}{\rho_0}\cdot\left\{(1+\sigma)\underline{\boldsymbol{\rho}}(\sigma) + \int_\sigma^0 \underline{\boldsymbol{\rho}}(\sigma')\mathrm{d}\sigma'\right\}\cdot\frac{\partial\zeta'}{\partial x} - \frac{gh}{\rho_0}\int_\sigma^0 \left.\frac{\partial\rho'}{\partial x}\right|_\sigma \mathrm{d}\sigma'\,; \tag{D.10}$$

$$\frac{\partial\zeta'}{\partial t} + h\cdot\frac{\partial\overline{u}}{\partial x} = 0\,; \qquad \frac{\partial\rho'}{\partial t} + \frac{\mathscr{W}'}{h}\cdot\frac{d\underline{\boldsymbol{\rho}}(\sigma)}{d\sigma} = 0\,; \qquad \left.\frac{\partial u'}{\partial x}\right|_\sigma + \frac{1}{h}\cdot\frac{\partial\mathscr{W}'}{\partial\sigma} = 0\,, \tag{D.11}$$

where the first equation can be split into separate ones for $\overline{u}$, obtained by vertical integration of (D.10),

$$\frac{\partial\overline{u}}{\partial t} = -\frac{g}{\rho_0}\cdot\frac{\partial\zeta'}{\partial x}\cdot\int_{-1}^{0}\left\{(1+\sigma)\underline{\boldsymbol{\rho}}(\sigma) + \int_\sigma^0 \underline{\boldsymbol{\rho}}(\sigma')\mathrm{d}\sigma'\right\}\mathrm{d}\sigma - \frac{gh}{\rho_0}\int_{-1}^{0}\int_\sigma^0 \left.\frac{\partial\rho'}{\partial x}\right|_\sigma \mathrm{d}\sigma'\,\mathrm{d}\sigma\,, \tag{D.12}$$

and for u', the residual of (D.10) after subtraction of (D.12). With

$$\mathscr{P}(\sigma) = \int_\sigma^0 \underline{\boldsymbol{\rho}}(\sigma')\mathrm{d}\sigma'\,, \tag{D.13}$$

integration of the first term inside the left integral in the r.h.s. of (D.12) yields

$$\int_{-1}^{0}(1+\sigma)\underline{\boldsymbol{\rho}}(\sigma)\mathrm{d}\sigma = \int_{-1}^{0}(1+\sigma)\left(-\frac{d\mathscr{P}}{d\sigma}\right)\mathrm{d}\sigma = -\underbrace{(1+\sigma)\mathscr{P}(\sigma)\Big|_{-1}^{0}}_{=0} + \int_{-1}^{0}\mathscr{P}(\sigma)\,\mathrm{d}\sigma\,. \tag{D.14}$$

Then the entire (D.12) an be rewritten as

$$\frac{\partial\overline{u}}{\partial t} = -\frac{g\rho_*}{\rho_0}\cdot\frac{\partial\zeta'}{\partial x} - \frac{gh}{\rho_0}\int_{-1}^{0}\int_\sigma^0 \left.\frac{\partial\rho'}{\partial x}\right|_\sigma \mathrm{d}\sigma'\,\mathrm{d}\sigma\,, \tag{D.15}$$

where we have identified

$$\rho_* = 2\int_{-1}^{0}\int_\sigma^0 \underline{\boldsymbol{\rho}}(\sigma')\,\mathrm{d}\sigma'\mathrm{d}\sigma\,, \tag{D.16}$$

which coincides with (3.19) from Sec. 3.2.

Let

$$\left(\zeta',\, \overline{u},\, u',\, \mathscr{W}',\, \rho'\right) = \left(\widehat{\zeta},\, \widehat{\overline{u}},\, \widehat{u}',\, \widehat{\mathscr{W}},\, \widehat{\rho}\right) \cdot e^{ikx-i\omega t}\,, \tag{D.17}$$

where the last three, $\widehat{u}$, $\widehat{\mathscr{W}}$, $\widehat{\rho}$ are functions of σ. Substitution into (D.10) leads to

$$-ik\cdot\left\{\frac{\omega^2}{k^2}-\frac{gh}{\rho_0}\left[(1+\sigma)\underline{\boldsymbol{\rho}}(\sigma)+\int_\sigma^0 \underline{\boldsymbol{\rho}}(s')\,\mathrm{d}\sigma'\right]\right\}\widehat{\zeta} = -\frac{\omega}{k}\cdot\frac{\partial\widehat{\mathscr{W}}}{\partial\sigma}-\frac{k}{\omega}\cdot\frac{gh}{\rho_0}\int_\sigma^0 \widehat{\mathscr{W}}\cdot\frac{d\underline{\boldsymbol{\rho}}(\sigma')}{d\sigma}\,\mathrm{d}\sigma'\,, \tag{D.18}$$

where we have eliminated all variables except $\widehat{\zeta}$ and $\widehat{\mathscr{W}}$ using a Fourier-transform of (D.11), *viz.*,

$$\widehat{\overline{u}} = \frac{\omega}{k}\cdot\frac{\widehat{\zeta}}{h}\,, \qquad \widehat{\rho}' = \frac{1}{i\omega}\cdot\frac{\widehat{\mathscr{W}}}{h}\cdot\frac{d\underline{\boldsymbol{\rho}}(\sigma)}{d\sigma}\,, \quad \text{and} \quad \widehat{u}' = -\frac{1}{ikh}\cdot\frac{\partial\widehat{\mathscr{W}}}{\partial\sigma}\,. \tag{D.19}$$

Eq. (D.18) comprises a Sturm–Liouville problem with unknowns ω (playing the role of an eigenvalue), $\widehat{\zeta}$ (an arbitrary non-trivial Fourier amplitude), and $\widehat{\mathscr{W}} = \widehat{\mathscr{W}}(\sigma)$ (a vertical profile multiplied by an arbitrary non-zero constant). The profile is subject to a pair of boundary conditions ,$\widehat{\mathscr{W}}\big|_{\sigma=0} = 0$ and $\widehat{\mathscr{W}}\big|_{\sigma=-1} = 0$. A property of (D.18) is that for $\underline{\boldsymbol{\rho}}(\sigma) = \mathrm{const}$, the only possible non-trivial solution is $\widehat{\zeta} \neq 0$, as allowed by $\omega^2 = k^2\cdot gh\cdot\underline{\boldsymbol{\rho}}/\rho_0$, and $\widehat{\mathscr{W}} \equiv 0$. This corresponds to familiar barotropic gravity waves. It also makes $\rho_0 = \underline{\boldsymbol{\rho}}$ the natural choice for the Boussinesq reference density, resulting in a correct phase speed $\omega/k = \sqrt{gh}$. Conversely, assuming $\widehat{\zeta} \equiv 0$ but $d\underline{\boldsymbol{\rho}}(\sigma)/d\sigma < 0$ results in a Sturm–Liouville problem for $\widehat{\mathscr{W}}$ alone, which leads to a set of baroclinic modes.

In the general case a dilemma is that the expression inside $\{.[...]\}$ in l.h.s. of (D.18) depends on σ, while $\widehat{\zeta}$ does not. To resolve this, as in the case of (D.15), vertical integration of (D.18) yields

$$-ik\cdot\left\{\frac{\omega^2}{k^2}-gh\frac{\rho_*}{\rho_0}\right\}\widehat{\zeta} = -\frac{k}{\omega}\cdot\frac{gh}{\rho_0}\int_{-1}^0\int_\sigma^0 \widehat{\mathscr{W}}\cdot\frac{d\underline{\boldsymbol{\rho}}(\sigma')}{d\sigma}\,\mathrm{d}\sigma'\,\mathrm{d}\sigma\,, \tag{D.20}$$

where the expression inside $\{...\}$ no longer depends on s. Setting $\omega/k = \sqrt{gh\cdot\rho_*/\rho_0}$ allows for a non-trivial $\widehat{\zeta}$, provided that $\widehat{\mathscr{W}} = 0$, however, substitution of this ω/k back into (D.18) results there in non-vanishing expression $\{.[...]\}$ and ultimately leads to a nontrivial profile of $\widehat{\mathscr{W}} = \widehat{\mathscr{W}}(\sigma)$, which is proportional, and in fact, is driven by $\widehat{\zeta}$.

This dilemma has two consequences. First, it suggests an iterative method for finding ω/k for the barotropic mode: use $\omega^2 = k^2\cdot gh\cdot\rho_*/\rho_0$ as the initial guess and substitute it into

$$ik\cdot\frac{gh}{\rho_0}\cdot\sigma\cdot\frac{d\underline{\boldsymbol{\rho}}(\sigma)}{d\sigma}\cdot\widehat{\zeta} = -\frac{\omega}{k}\cdot\frac{\partial^2\widehat{\mathscr{W}}}{\partial\sigma^2}+\frac{k}{\omega}\cdot\frac{gh}{\rho_0}\cdot\widehat{\mathscr{W}}\cdot\frac{d\underline{\boldsymbol{\rho}}(\sigma)}{d\sigma}\,, \tag{D.21}$$

which is the vertical derivative of (D.18). Then the l.h.s. of (D.21) can be treated as known. This leads to a problem for $\widehat{\mathscr{W}}$ alone. This problem is well posed, because this value of ω/k is far away from the eigenvalues of the operator in the r.h.s. of (D.21) (*i.e.*, its eigenvalues are associated with internal modes and have much lower frequencies). The solution results in a profile, $\widehat{\mathscr{W}} = \widehat{\mathscr{W}}(\sigma)$, proportional to $\widehat{\zeta}$. Substitute it into the r.h.s. of (D.20) and recompute ω/k, after which the iterative cycle is repeated. Convergence is guaranteed because (D.21) can be rewritten as

$$i\omega\epsilon^2 s\cdot\widehat{\zeta} = \frac{\partial^2\widehat{\mathscr{W}}}{\partial\sigma^2}+\epsilon^2\widehat{\mathscr{W}}\,, \tag{D.22}$$

where $\epsilon^2 = \dfrac{k^2}{\omega^2}\cdot h^2N^2 = \dfrac{k^2}{\omega^2}\cdot gh\cdot\left(-\dfrac{1}{\rho_0}\cdot\dfrac{d\underline{\boldsymbol{\rho}}(\sigma)}{d\sigma}\right)$ is of the same order as the square of the ratio of the first-baroclinic and barotropic mode phase speeds, hence $\epsilon^2 \ll 1$. The scaling of $\widehat{\mathscr{W}}$ relative to $\widehat{\zeta}$ is estimated as

$\widehat{\mathscr{W}} \sim i\omega\epsilon^2\widehat{\zeta}$, and the scaling of the mismatch between this l.h.s. and r.h.s. of (D.20) is estimated as

$$ik\left\{\frac{\omega^2}{k^2} - gh\frac{\rho_*}{\rho_0}\right\} \quad \text{vs.} \quad i\omega\cdot\frac{\omega}{k}\cdot\epsilon^4\,, \tag{D.23}$$

which implies that the corrections are indeed sufficiently small.

The second consequence is that, even though the system is linear, it did not split into two independent subsystems: barotropic and baroclinic. This does not mean that the it is not splittable in principle, but rather that the actual structure of the barotropic mode cannot be represented by a vertically uniform velocity: it has a non-constant profile that depends on stratification $\underline{\boldsymbol{\rho}}(\sigma)$. Similarly, the presence of a non-trivial $\widehat{\mathscr{W}}$ slaved to $\widehat{\zeta}$ indicates than vertical density profile is not "frozen" in σ-coordinates in purely barotropic motions, but it changes following ζ. This indicates that the ideal stretching of the σ-coordinate by ζ should not just be proportional to the distance from the bottom,

$$z = z^{(0)} + \zeta\cdot\left(z^{(0)}+h\right)/h\,, \tag{D.24}$$

but should depend on the density profile as well to cancel $\mathscr{W}$ associated with barotropic motions, and thus cancel changes of density. This determines the level of error in the mode-splitting algorithm of SM2005 because the mismatch in (D.20) indicates that the phase speed of the barotropic mode is different between the 2D and 3D parts of the code. The 2D part sees it as just $\omega/k = \sqrt{gh\cdot\rho_*/\rho_0}$, and the 3D part sees it as the complete solution of (D.20)–(D.21). This is a mode-splitting error, because there are contributions in the vertically-integrated r.h.s. of the 3D momentum equations that depend on ζ and have a hyperbolic character, yet are frozen during the barotropic time-stepping, hence are computed using effectively a forward-in-time Euler algorithm.

References:

Adcroft, A. and J.-M. Campin, 2004: Rescaled height coordinates for accurate representation of free-surface flows in ocean circulation models. *Ocean Modeling*, **7**, 269-284. doi:10.1016/j.ocemod.2003.09.003

Adcroft, A., R. Hallberg, and M. Harrison, 2008: A finite volume discretization of the pressure gradient force using analytic integration. *Ocean Modeling*, **22**, 106-113. doi:10.1016/j.ocemod.2008.02.001

Antonov, J. I., R. A. Locarnini, T. P. Boyer, A. V. Mishonov, and H. E. Garcia, 2006: *World Ocean Atlas 2005, Vol. 2: Salinity*. S. Levitus, Ed. NOAA Atlas NESDIS 62, U.S. Government Printing Office, Washington, D.C., 182 pp.

Berntsen, H., Z. Kowalik, S. Sælid, and K. Sørli, 1981: Efficient numerical simulation of ocean hydrodynamics by splitting procedure. *Modeling, Identification and Control*, **2**, 181-199.

Bleck, R. and D. B. Boudra, 1981: Initial testing of a numerical ocean circulation model using a hybrid (quasi-isopycnic) vertical coordinate. *J. Phys. Ocean.*, **11**, 755-770.

Bleck, R. and L. T. Smith, 1990: A wind-driven isopycnic coordinate model of the north and equatorial Atlantic Ocean: 1. Model development and supporting experiments. *J. Geophys. Res.*, **95C**, 3273-3285.

Blumberg, A. F. and G. L. Mellor, 1987: A description of a three-dimensional coastal ocean circulation model. In: *Three-Dimensional Coastal Ocean Models*, N. S. Heaps (Ed.), pp. 1-16, Pub. AGU, Washington, DC.

Boussinesq, J. 1903: Thórie analytique de la chaleur. Tome II. (Analytic theory of heat. Vol. 2) *Gauthier-Villars*, Paris. 625pp. http://gallica.bnf.fr/ark:/12148/bpt6k61635r

Brydon, D., S. Sun, and R. Bleck, 1999: A new approximation of the equation of state for seawater, suitable for numerical ocean models. *J. Geophys. Res.*, **104**, 1537-1540.

Campin, J.-M., A. Adcroft, C. Hill, J. Marshall, 2004: Conservation of properties in a free-surface model. *Ocean Modeling*, **6**, 221-244. doi:10.1016/S1463-5003(03)00009-X

Casulli, V. and R. T. Cheng, 1992: Semi-implicit finite-difference methods for 3-dimensional shallow-water flow. *Int. J. of Num. Meth. in Fluids*, **15**, 629-648.

Dewar, W. K., Y. Hsueh, T. J. McDougall, and D. I. Yuan, 1998: Calculation of pressure in ocean simulations. *J. Phys. Ocean.*, **28**, 577-588.

Dukowicz J. K., 1997: Steric sea level in the Los Alamos POP code – Non-Boussinesq effects. *Numerical Methods in Atmospheric and Oceanic Modeling: The Andre Robert Memorial Volume*, C. Lin, R. Laprise, and H. Ritchie, Eds., NRC Research Press, 533546.

Dukowicz, J. K., 2001: Reduction of density and pressure gradient errors in ocean simulations. *J. Phys. Ocean.*, **31**, 1915-1921.

Dukowicz, J. K., 2006: Structure of the barotropic mode in layered ocean models. *Ocean Modeling,* **11**, 49-68. doi:10.1016/j.ocemod.2004.11.005

Gatti-Bono, C. and P. Colella, 2006: An anelastic allspeed projection method for gravitationally stratified flows. *J. Comp. Phys.*, **216**, 589-615. doi:10.1016/j.jcp.2005.12.017

Greatbatch, R. J., 1994, A note on the representation of steric sea level in models that conserve volume rather than mass, *J. Geophys. Res.*, **99**, 12,76712,771.

Greatbatch, R. J., Y. Lu, and Y. Cai, 2001: Relaxing the Boussinesq approximation in ocean circulation models. *J. Atmos. Oceanic Technology*, **18**, 1911-1923. doi:10.1175/1520-0426(2001)018<1911:RTBAIO>2.0.CO;2

Greatbatch, R. J. and T. J. McDougall, 2003: The non-Boussinesq temporal residual mean. *J. Phys. Ocean.*, **33**, 1231-1239.

Griffies, S. M., A. Gnanadesikan, R. C. Pacanowski, V. D. Larichev, J. K. Dukowicz, and R. D. Smith, 1998: Isoneutral diffusion in a z-coordinate ocean model. *J. Phys. Ocean.*, **28**, 805-830

Griffies, S. M., R. C. Pacanowski, M. Schmidt, and V. Balaji, 2001: Tracer conservation with an explicit free surface method for z-coordinate ocean models. *Monthly Weather Review*, **5**, 1081-1098.

Griffies, S. M., 2004: Fundamentals of ocean climate models. *Princeton University Press*, 496 pp. ISBN-13 #09780691118925

Griffies, S. M. and A. J. Adcroft, 2008: Formulating the equations of ocean models. In *Ocean Modeling in an Eddying Regime*, Geophysical Monograph 177, M. W. Hecht, and H. Hasumi, eds., Washington, DC, American Geophysical Union, 281-318.

Griffies, S. M., 2009: Elements of MOM4p1. *GFDL Ocean Group Technical report No. 6. NOAA/GFDL*, April 21, 2009, 444 pp.

Hallberg, 1997: Stable split time stepping schemes for large-scale ocean modeling. *J. Comp. Phys.*, **135**, 54-65.

Hallberg, 2005: A thermobaric instability of Lagrangian vertical coordinate ocean models. *Ocean Modeling*, **8**, 279-300. doi:10.1016/j.ocemod.2004.01.001

Higdon, R. L. and A. F. Bennett, 1996: Stability analysis of operator splitting for large-scale ocean modelling. *J. Comp. Phys.*, **123**, 311-329.

Higdon, R. L. and R. A. de Szoeke, 1997: Barotropic-baroclinic time splitting for ocean circullation modeling. *J. Comp. Phys.*, **135**, 31-53.

Huang, R. X. and H. Z. Jin, 2002: Sea surface elevation and bottom pressure anomalies due to thermohaline forcing. Part I: Isolated perturbations. *J. Phys. Ocean.*, **32**, 2131-2150

Ingersoll, A. P., 2005: Boussinesq and anelastic approximations revisited: Potential energy release during thermobaric instability. *J. Phys. Ocean.*, **35**, 1359-1369. doi:10.1175/JPO2756.1

Jackett, D. R. and T. J. McDougall, 1995: Minimal adjustment of hydrostatic profiles to achieve static stability. *J. Atmos. Oceanic Technology*, **12**, 381-389.

Jackett, D. R. and T. J. McDougall, 1997: A neutral density variable for the world's oceans. *J. Phys. Ocean.*, **27**, 237-263.

Jackett, D. R., T. J. McDougall, R. Feistel, D. G. Wright, and S. M. Griffies, 2006: Algorithms for density, potential temperature, conservative temperature, and the freezing temperature of seawater. *J. Atmos. Oceanic Technology*, **23**, 1709-1728.

Kanarska, Y., Shchepetkin, A. F., and J. C. McWilliams, 2007: Algorithm for Non-Hydrostatic Dynamics in ROMS. *Ocean Modeling,* **18**, 143-174. doi:10.1016/j.ocemod.2007.04.001.

Killworth, P. D., D. Stainforth, D. J. Webb and S. M. Paterson, 1991: The development of a free-surface Bryan-Cox-Semtner ocean model. *J. Phys. Ocean.*, **21**, 1333-1348.

Locarnini, R. A., A. V. Mishonov, J. I. Antonov, T. P. Boyer, and H. E. Garcia, 2006: *World Ocean Atlas 2005, Vol. 1: Temperature*. S. Levitus, Ed. NOAA Atlas NESDIS 61, U.S. Gov. Printing Office, Washington, D.C., 182 pp.

Losch, M., A. Adcroft, and J.-M. Campin, 2004: How sensitive are coarse general circulation models to fundamental approximations in the equations of motion? *J. Phys. Ocean.*, **34**, 306-319. doi:10.1175/1520-0485(2004)034<0306:HSACGC>2.0.CO;2

Lu, Y., 2001: Including non-Boussinesq effect in Boussinesq ocean circulation models. *J. Phys. Ocean.*, **31**, 1616-1622.

Marshall, J., A. Adcroft, J.-M. Campin, C. Hill, and A. White, 2004: Atmosphere-ocean modeling exploiting fluid isomorphisms. *Monthly Weather Review*, **132**, 2882-2894. doi:10.1175/MWR2835.1

McPhee, M. G., 2000: Marginal thermobaric stability in the ice-covered upper ocean over Maud Rise. *J. Phys. Ocean.*, **30**, 27102722. doi:10.1175/1520-0485(2000)030<2710:MTSITI>2.0.CO;2

McDougall, T. J. and C. J. R. Garrett, 1992: Scalar conservation equations in a turbulent ocean. *Deep-Sea Res.*, **39**, 1953-1966.

McDougall, T. J., R. J. Greatbatch, and Y. Lu., 2002: On conservation equations in oceanography: How accurate are Boussinesq ocean models? *J. Phys. Ocean.*, **32**, 1574-1584. doi:10.1175/1520-0485(2002)032<1574:OCEIOH>2.0.CO;2

McDougall, T. J., D. J. Jackett, D. G. Wright, and R. Feistel, 2003: Accurate and computationally efficient algorithms for potential temperature and density and of seawater. *J. Atmos. Oceanic Technology*, **20**, 730-741.

McDougall, T. J. and D. R. Jackett, 2007: The thinness of the ocean in $S - \Theta - p$ space and the implications for mean diapycnal advection. *J. Phys. Ocean.*, **37**, 1714-1732. doi:10.1175/JPO3114.1.

Mellor, G. L., 1991: An Equation of State for numerical modeling of oceans and estuaries. *J. Atmos. Oceanic Technology*, **1991**, 609-611.

Mellor, G. L. and Ezer, 1995: Sea level variations induced by heating and cooling: An evaluation of the Boussinesq approximation in ocean models. *J. Geophys. Res.*, **100**, 20,565-20,577.

Mihaljan, J. M., 1962: A Rigorous exposition of the Boussinesq approximations applicable to a thin layer of fluid. *Astrophys. J.*, **136**, 1126-1133. doi:10.1086/147463.

Oberbeck, A. 1879: Ueber die Wärmeleitung der Flss̈igkeiten bei Berc̈ksichtigung der Strm̈ungen infolge von Temperaturdifferenzen. *Annalen der Physik* **243**, 271–292. doi:10.1002/andp.18792430606.

Oberbeck, A. 1888: On the phenomena of motion in the atmosphere (first comm). In *The Mechanics of the Earth's Atmosphere*, transl. by Cleveland Abbe. publ. Smithsonian Inst., Washington, 1891. pp. 176-187. http://books.google.com/books?id=kGBDAAAAIAAJ

Paluszkiewicz, T., R. W. Garwood, and D. W. Denbo, 1994: Deep convective plumes in the ocean. *Oceanography*, **7**, 3744.

Robertson, R., L. Padman, and M. D. Levine, 2001: A correction to the baroclinic pressure gradient term in the Princeton ocean model. *J. Atmos. Oceanic Technology*, **18**, 1068-1075.

Rueda, F. J., E. Sanmiguel-Rojas, and B. R. Hodges, 2007: Baroclinic stability for a family of two-level, semi-implicit numerical methods for the 3D shallow water equations. *Int. J. of Num. Meth. in Fluids*, **54**, 237-268. doi:10.1002/fld.1391

Shchepetkin, A. F. and J. C. McWilliams, 2003: A method for computing horizontal pressure-gradient force in an oceanic model with a non-aligned vertical coordinate. *J. Geophys. Res.*, **108**, 3090-3124. doi:10.1029/2001JC001047.

Shchepetkin, A. F. and J. C. McWilliams, 2005: The regional oceanic modeling system (ROMS): A split-explicit, free-surface, topography-following-coordinate oceanic model. *Ocean Modeling*, **9**, 347-404. doi:10.1016/j.ocemod.2004.08.002.

Shchepetkin, A. F. and J. C. McWilliams, 2008: Computational kernel algorithms for fine-scale, multi-process, long-term oceanic simulations. In: *Handbook of Numerical Analysis, Vol. XIV: Computational Methods for*

the Ocean and the Atmosphere, P. G. Ciarlet, editor, R. Temam & J. Tribbia, guest eds., *Elsevier Science*, pp. 121-183, doi:10.1016/S1570-8659(08)01202-0.

Spiegel, E. A. and G. Veronis, 1960: On the Boussinesq approximation for a compressible fluid. *Astrophys. J.*, **131**, 442–447.

Stacey, M. W., S. Pond, and Z. P. Nowak, 1995: A numerical model of the circulation in knight inlet, British Columbia, Canada. *J. Phys. Ocean.*, **25**, 10371062.

Sun, S., R. Bleck, C. Rooth, J. Dukowicz, E. Chassignet, and P. Killworth, 1999: Inclusion of thermobaricity in isopycnis-coordinate ocean models. *J. Phys. Ocean.*, **29**, 2719-2729. doi:10.1175/1520-0485(1999)029<2719:IOTIIC>2.0.CO;2

de Szoeke, R. A. and R. M. Samelson, 2002: The duality between the Boussinesq and non-Boussinesq hydrostatic equations of motion. *J. Phys. Ocean.*, **32**, 2194-2203. doi:10.1175/1520-0485(2002)032<2194:TDBTBA>2.0.CO;2

Tailleux, R., 2009: On the energetics of stratified turbulent mixing, irreversible thermodynamics, Boussinesq models and the ocean heat engine controversy. *J. Fluid Mech.*, **638**, 339-382. doi:10.1017/S002211200999111X.

Tailleux, R., 2010: Identifying and quantifying nonconservative energy production/destruction terms in hydrostatic Boussinesq primitive equation models. *Ocean Modeling*, **34**, 125-136. doi:10.1016/j.ocemod.2010.05.003.

Wright, D. G., 1997: An equation of state for use in ocean models: Eckart's formula revisited. *J. Phys. Ocean.*, **14**, 735-741.

Young, W. R., 2010: Dynamic enthalpy, conservative temperature, and the seawater Boussinesq Approximation *J. Phys. Ocean.*, **40**, 394-400. doi:10.1175/2009JPO4294.1.

Zeytounian, R. Kh., 2003: Joseph Boussinesq and his approximation: a contemporal view. *C/ R. Mecanique*, **331**, 575-586. doi:10.1016/S1631-0721(03)00120-7.

Zahariev, K. and C. Garrett, 1997: An apparent surface buoyancy flux associated with the nonlinearity of the equation of state. *J. Phys. Ocean.*, **27**, 362-368. doi:10.1175/1520-0485(1997)027<0362:AASBFA>2.0.CO;2